LINKING MOLECULAR MICROBIOLOGY AND GEOCHEMISTRY TO BETTER UNDERSTAND MICROBIAL ECOLOGY IN COASTAL MARINE SEDIMENTS

A Dissertation

by

BRANDI KIEL REESE

Submitted to the Office of Graduate Studies of
Texas A&M University
in partial fulfillment of the requirements for the degree of

DOCTOR OF PHILOSOPHY

December 2011

Major Subject: Oceanography

Linking Molecular Microbiology and Geochemistry to Better Understand Microbial Ecology in Coastal Marine Sediments

LINKING MOLECULAR MICROBIOLOGY AND GEOCHEMISTRY TO BETTER UNDERSTAND MICROBIAL ECOLOGY IN COASTAL MARINE SEDIMENTS

A Dissertation

by

BRANDI KIEL REESE

Submitted to the Office of Graduate Studies of
Texas A&M University
in partial fulfillment of the requirements for the degree of

DOCTOR OF PHILOSOPHY

Approved by:

Co-Chairs of Committee,	Heath J. Mills
	John W. Morse
Committee Members,	Thomas Bianchi
	Terry Gentry
	Peter Santschi
Head of Department,	Piers Chapman

December 2011

Major Subject: Oceanography

ABSTRACT

Linking Molecular Microbiology and Geochemistry to Better Understand Microbial Ecology in Coastal Marine Sediments. (December 2011)

Brandi Kiel Reese, B.S., Southern Methodist University;

M.S., University of California, Riverside

Co-Chairs of Advisory Committee: Dr. Heath J. Mills
Dr. John W. Morse

The overall objective of the research presented here was to combine multiple geochemical parameters and molecular characterizations to provide a novel view of active microbial community ecology of sediments in a large-river deltaic estuary. In coastal and estuarine environments, a large portion of benthic respiration has been attributed to sulfate reduction and implicated as an important mechanism in hypoxia formation. The use of high-resolution sampling of individual sediment cores and high throughput nucleic acid extraction techniques, combined with 454 FLX sequencing, provided a robust understanding of the metabolically active benthic microbial community within coastal sediments. This was used to provide further understanding and show the importance of simultaneously analyzing the connectivity of sulfur and iron cycling to the structure and function of the microbial population. Although aqueous sulfide did not accumulate in the sediments of the northern Gulf of Mexico, active sulfate reduction was observed in all locations sampled. Microbial recycling and

sequestration as iron sulfides prevented the release of sulfide from the sediment. Prominent differences were observed between the sample locations and with depth into the sediment column. This study emphasized the importance of combining novel molecular techniques with simultaneous traditional geochemical measurements to show the interdependence of microbiology and geochemistry. In addition, this study highlights the need to consider microbial community biogeography along with small-scale variations in geochemistry and biology that impact the overall cycling of redox elements when constructing biogeochemical models in marine sediments.

DEDICATION

This dissertation is dedicated to the memory of John W. Morse. He was a pioneer in the fields of sedimentary sulfur cycling and pyrite formation. He would later become a leader in biogeochemical research, fixated on the wholistic approach of scientific research. My memories of John extended beyond the scientific discussions and laboratory work. His long-winded meals at his favorite restaurants showed he cared for his students, loud blues music from his office next door provided countless laughs, and he always defended what was true and honest in everything he did. John provided me confidence and independence as a researcher, and for that I am grateful to have been mentored by him in his final years. I would also like to dedicate this to my co-advisor, Heath Mills, for the seemless transition he made into being my primary mentor and his unending support throughout my dissertation. He is staunch in his beliefs, but never suppresses a good scientific debate. I will always appreciate the loyalty he shows toward his students and the patient consideration he gives to each one.

I also dedicate this work to my Grandmother, Mary Bynum Cobb Wilson, who instilled in me the value of education. She often said, “Nobody can ever take your education from you.” She was brilliant and tenacious and encouraged the same from me. She was an inspiration in life as she is in her passing, and it is because of her that I am the woman that I am today.

ACKNOWLEDGEMENTS

I would like to acknowledge the many contributions of my co-advisors, John Morse and Heath Mills, as well as those of my committee members, Tom Bianchi, Terry Gentry, and Peter Santschi. Each one has molded this research with their helpful comments and advice.

It takes a villiage to complete any research, and I could not have done this without the help of many individuals. I want to thank Steve DiMarco, Wayne Gardner, Scot Dowd, Gary Williams, and Angela Witmer for their help in sample collection and data analysis. I would also like to thank the numerous undergraduate and graduate students in both the Morse and Mills labs who have assisted along the way. In addition, I am grateful for the support of the scientific party and crew of the *R/V Pelican*.

We would not have the ability to do great research without the support of funding. This research was supported by the Louis and Elizabeth Scherck Endowed Chair in Oceanography (Morse), Big XII Grant (Mills), and the Center for Sponsored Coastal Ocean Research (CSCOR) of National Oceanic and Atmospheric Administration (NOAA) (grant # NA06N0S4780198). Tuition, assistantship, and travel funding were provided through the Texas A&M University Diversity Fellowship, Philanthropic Education Organization (PEO) Scholar Fellowship, Lighthouse Scholarship Award, Pipes Merit Award, and Center for Dark Energy Biosphere Investigations (C-DEBI).

Last, but certainly not least, I would like to acknowledge my family and friends for their encouragement when I needed it most. The love and devotion of my husband,

A.J. Reese, has been critical to completing this research, and I will always be indebted. He has been through the ups and the downs that any doctoral student inevitably experiences and has stood by me always patient, lending a hand and a smile. “Thank you” does not begin to express my gratitude.

NOMENCLATURE

DNA	Deoxyribonucleic acid
DOP	Degree of pyritization
dsrA	Dissimilatory sulfite reductase subunit A
FeOB	Iron oxidizing bacteria
FeRB	Iron reducing bacteria
MDR	Mixed diamine reagent
NGoM	Northern Gulf of Mexico
OTU	Operational taxonomic unit
PCR	Polymerase chain reaction
RNA	Ribonucleic acid
SOB	Sulfide oxidizing bacteria
SRB	Sulfate reducting bacteria
SRR	Sulfate reduction rate
SSU	Small subunit
TRS	Total reducible sulfide
TC	Total carbon
TOC	Total organic carbon

TABLE OF CONTENTS

CHAPTER Page

CHAPTER Page

CHAPTER Page

LIST OF FIGURES

Page

LIST OF TABLES

Page

CHAPTER I

INTRODUCTION

Hypoxia

The existence of coastal and estuarine hypoxia (dissolved oxygen less than 63 μmol L^{-1}) has been known for centuries and the numerous effects from such a phenomenon have been well studied (Diaz and Rosenberg 2008). The exact causes and their relative significance, however, are often debated as they are derived from a variety of sources. Traditionally, it is believed that coastal hypoxia begins with eutrophication enhancing biomass growth and therefore production of labile organic matter. This is followed by microbial growth and respiration, which increases the demand for dissolved oxygen. This rather predictable cycle of events is further complicated by stratification from salinity or temperature variations. If hypoxia is severe or persistent over many years, nutrients and organic matter accumulate in the sediments and an additional source of hypoxia is introduced. This sequence has been documented internationally in areas such as Chesapeake Bay (Zhang et al. 2010), Baltic Sea (Middelburg and Levin 2009), Yangtze River (Zhang et al. 2010) and the Gulf of Mexico (Bianchi et al. 2010).

The Gulf of Mexico hypoxic zone has had an average annual size greater than 15,600 km^2 since 1993 (Rabalais and Turner 2001), making it the largest in the United States and second largest in the world. The hypoxic zone spans a horizontal region along

---

This dissertation follows the style of Geomicrobiology Journal.

the inner continental shelf from the Mississippi River to west of the Atchafalaya River, a distance of nearly 390 km. The mechanisms controlling hypoxia in the northern Gulf of Mexico have been debated over the past decade (Bianchi et al. 2010; Hetland and DiMarco 2008; Rabalais and Turner 2001; Rabalais et al. 2007).

The influence of both the Mississippi and Atchafalaya rivers has lead researchers to hypothesize regional causes of hypoxia formation beyond the traditional eutrophication cycle described above. The general consensus for hypoxia formation in all regions has been shallow water depths, weak summer convective mixing and density-driven stratification from Mississippi and Atchafalaya fresh water river inputs. Additionally, researchers have proposed distinctly different mechanisms that influence the hypoxic zone in various regions, including differing contributions of physical mixing, and biological and chemical reactions within the sediment and water column, (Green et al. 2006; Rowe and Chapman 2002).

Oxygen concentrations below the pycnocline may be reduced by both biological and chemical mechanisms, each contributing to the water column hypoxia (Bianchi et al. 2010; Morse and Eldridge 2007; Rowe et al. 2002). The biological contribution in the form of prokaryotic respiration is well recognized as the primary mechanism for reducing the oxygen concentrations due to faster oxygen consumption rates than that of chemical oxidation (Plas et al. 1992). The chemical oxidation of reduced compounds in the sediment (e.g., NH_4^+, Fe(II), Mn(II), H_2S) removes molecular oxygen from the overlying water upon diffusion (Tuttle et al. 1987) thus providing an additional important but slower mechanism for hypoxia formation.

Inorganic sulfur cycle

The formation of sulfide ($\Sigma H_2S_{aq} = H_2S_{aq} + HS^- + S^{2-}$), along with other reduced compounds, has been implicated in hypoxic or anoxic water column formation within lakes (Reese et al. 2008), wetlands (Luther and Church 1988), and marine coastal environments (Jorgensen 1977; Roden and Tuttle 1992). Sulfide is produced within the sediments through dissimilatory sulfate reduction when bacteria use oxidized forms of sulfur (i.e., SO_4^{2-}, SO_3^-) as the terminal electron acceptor in the remineralization of organic matter. A basic reduction reaction is as follows:

$$SO_4^{2-} + 2(CH_2O) \rightarrow HCO_3^- + HS^- + CO_2 + H_2O \qquad \text{(Eq. 1.1)}$$

where organic matter (CH_2O) is oxidized and alkalinity (HCO_3^-) and sulfide (HS^-) are produced. The reaction rate is dependent on several chemical factors including sulfate concentration, availability and quality of organic matter and other nutrients, and biological factors including population density and composition. The reduction of sulfate is the terminal microbial respiration process in anaerobic sediments when sulfate (SO_4^{2-}) is not limiting (Capone and Kiene 1988).

Previous studies have shown that sulfate reduction, and likewise sulfide accumulation, in the sediments is controlled by sulfate availability, bioturbation, dissolved oxygen concentration in the water column, rate of sulfide reoxidation, and availability of reactive iron (Marvin-DiPasquale and Capone 1998). In marine environments where the terminal electron acceptor (sulfate) is abundant, the primary regulator in sulfate reduction is the availability of degradable organic matter and

secondarily by the sedimentation rate as it impacts the total carbon flux (Canfield 1991; Holmkvist et al. 2011).

A significant fraction of the sulfides formed as a result of sulfate reduction are chemically and biologically reoxidized to SO_4^{2-} and a less significant fraction reacts with reactive iron compounds to form insoluble minerals. The rate of biological reoxidation as been shown to exceed the rate of chemical oxidation (Luther et al. 2011). Jorgensen (1982) showed that as much as 90% of the sulfide produced in the upper sediment layers can be oxidized and reduced in more than one oxidation-reduction cycle. The products of sulfate reduction can be divided into acid-volatile (i.e., S^{2-}, HS^-, H_2S, and FeS) and non-acid-volatile (elemental S and FeS_2) fractions. Metal sulfides, such as pyrite (FeS_2), are the primary sequestration product of sulfate and iron diagenesis, although acid volatile sulfide (AVS) may be produced under some conditions. Therefore, these precipitation reactions are an important contribution to maintaining low concentrations of dissolved sulfide, which is highly toxic to a variety of organisms.

Pyrite formation proceeds via the reaction of ΣH_2S_{aq} with detrital iron minerals, also termed reactive iron (Canfield 1989). A model of pyritization in sediments is shown by the reaction between dissolved sulfide and iron oxide as magnetite (Fe_3O_4) or as goethite (FeOOH) (Canfield 1989; Lord and Church 1983):

$$FeOOH + 3/2\ HS^- + 1/16\ S_8 + 3/2\ H^+ = FeS_2 + 2H_2O \qquad \text{(Eq. 1.2)}$$

Reactive iron is the form of iron that readily reacts with sulfide to form iron sulfides and may include Fe(III) oxyhydroxides (e.g., ferrihydrite and goethite), Fe oxides (e.g., hematite and magnetite) and Fe sheet silicates (Canfield and Berner 1987).

Additionally, the microbial metabolism of particulate organic-Fe contributes to the availability of dissolved iron to the environment. The dissolved reduced iron can contribute to the potential sequestration of dissolved sulfides in the sediment.

Microbial ecology

A diverse group of microorganisms are responsible for the reduction and oxidation of sulfur. Organisms from both prokaryote domains, *Archaea* and *Bacteria*, are capable of sulfate reduction. Most known sulfate reducing bacteria (SRB) are classified in 23 genera of *Deltaproteobacteria*; however, more than 140 species belonging to 35 genera have been discovered. Located within the *Archaea* is a single genus of sulfate reducers *Archaeoglobus* (Canfield et al. 2005; Stackebrandt et al. 1995). The main steps in the sulfate reduction pathway by these organisms involve the transport of sulfate across the cell membrane with the use of the proton motive force (Equation 1.3). ATP sulfurylase activates the sulfate to APS, which is then reduced to sulfite with the enzyme APS reductase. Sulfide produced as a result of this reaction is quickly transported out of the cell:

$$SO_4^{2-} \;\vdots\!\!\longrightarrow\; SO_4^{2-} \xrightarrow{ATP} APS + PPi \xrightarrow{e^-} SO_3^{2-} \xrightarrow{e^-} HS^- \qquad \text{(Eq. 1.3)}$$

Outside Inside

The dissimilatory sulfite reductase subunit A gene (*dsrA*) encodes a key enzyme in the sulfate reduction pathway that catalyzes the reduction of sulfite. Conserved regions within the gene and the gene transcript have been used previously as a molecular target to determine potential and active sulfate reduction.

Similarly, dissimilatory Fe(III) iron-reducing bacteria (FeRB) in the sediment are phylogenetically diverse and are observed throughout both the *Bacteria* and *Archaea* domains (Kashefi and Lovley 2003). They include a large phylogenetically-cohesive group, the *Geobacteraceae*, which oxidize acetate to CO_2 with Fe(III) serving as the electron acceptor (Lonergan et al. 1996), as well as the H_2-oxidizing Fe(III) reducers like *Shewanellaceae* (Orcutt et al. 2011). Previous studies have shown that the Fe(III) reducers have the capability to not only reduce Fe(III) oxyhydroxides, but were also able to reduce Fe(III) sheet silicates and magnetite (Kostka and Nealson 1995). Many of the Fe(III) reducing organisms are closely phylogenetically related to sulfate reducing bacteria (i.e., *Desulfuromonadaceae*) and some species of the *Geobacteracea* reduce S(0) (Pereira et al. 2007). The iron-reducers and sulfate-reducers may be part of a tight ecology; the FeRB may use acetate, which is a common product of SRB metabolism. The iron in the oxic and transition zones in the sediment is therefore likely to be considerably affected by these organisms. The amount of Fe(III) reacting directly with ΣH_2S_{aq} and the amount that is reduced by FeRB and reacting with the Fe(II) produced has been shown to depend on the relative rates of the pyritization and bacterial reduction reactions. It will also depend on the time the Fe(III) spends in the bacterial iron-reducing sub-environment before being exposed ΣH_2S_{aq} (Rickard and Morse 2005).

Microbial community characterization

The key to linking geochemical observation to microbial function is being able to quantitatively and qualitatively analyze functional gene transcripts. Molecular analysis

of a microbial community focuses on the identification and comparison of nucleic acids. The specific nucleic acid targeted (i.e., DNA, ribosomal RNA, or messenger RNA) is dependent upon the information needed. Studies based on DNA may describe the taxa and metabolic pathways from the total microbial community present in the sediment, whether the cells sampled were metabolically active, quiescent or dead (Fegatella et al. 1998). In environments that vary geochemically, a DNA-based approach would not provide evidence for short-term changes in community structure or function. In contrast, techniques based on either small subunit ribosomal RNA (SSU rRNA; also referred to as 16S rRNA) or messenger RNA (mRNA) are more informative regarding changes in the metabolically active fraction of the microbial community and specific metabolic processes within a dynamic environment. The metabolically active taxa within the total population can be identified by isolation and characterization of SSU rRNA. The concentration of ribosomes, and thus copies of SSU rRNA within a cell, is linearly correlated to cellular metabolic activity (Delong et al. 1989; Kerkhof and Ward 1993). Therefore, the detection and characterization of a gene transcript from an environmental sample can be directly linked to an active population (rRNA) or process (mRNA). The extraction and amplification of environmental RNA is widely recognized as much more difficult than the isolation of DNA, yet it is required to determine linkages between sediment geochemistry and microbiology.

Molecular characterization of a microbial community avoids culture biases, allowing a more robust overall analysis. Technical limitations have inhibited molecular characterization of microbial communities when cell densities were less than 10^5 cells

cm^{-3}. Specialized extraction techniques have been developed to isolate and characterize both DNA and RNA targets in shallow subsurface sediments with cell densities of approximately 10^4 cells cm^{-3} (Akob et al. 2008; Akob et al. 2007). Traditional molecular techniques allow the targeting and subsequent sequence analysis of specific lineages or metabolic processes, without the host organism being cultured.

The **overall objective** of the research presented here was to combine multiple geochemical parameters and molecular analyses to provide a novel characterization of the metabolically active microbial community ecology of sediments in a large-river deltaic estuary. The **long-term goal** of this research is to provide greater understanding of the benthic microbial community to incorporate into general models of iron and sulfur geochemical cycling and local models determining mechanisms controlling hypoxia. *The **central hypothesis** was that production of reduced iron and sulfide in the sediment contributes to the overlying water column hypoxia in the Northern Gulf of Mexico.* In addition, I also hypothesized that both geochemical and microbiological analyses are required to fully characterize benthic processes and therefore make conclusions regarding their potential to impact an environment.

CHAPTER II

EXAMINATION AND REFINEMENT OF THE DETERMINATION OF AQUEOUS HYDROGEN SULFIDE BY THE METHYLENE BLUE METHOD*

Overview

The accurate and precise measurement of total sulfide has been of major interest for well over a century. The most commonly used method involves the formation of a methylene blue-sulfide complex and spectrophotometric measurement of its concentration. The study presented herein compares the two most commonly used methods as outlined in *Standard Methods for the Examination of Water and Wastewater* (APHA 1960) and by Cline (1969). In addition, this study clarifies the existing confusion of Cline's reagent preparation procedure, as it is apparent that various interpretations exist among research groups regarding reagent preparation. After evaluating both methods with respect to precision and accuracy, detection limit, sample storage time, and ease of use, the method outlined in Cline was determined to be superior. Furthermore, we suggest that the reagent concentration has to be optimized depending on the range of sulfide concentrations to increase the accuracy and precision of the method.

---

* Reprinted with permission from Reese, B.K., Finneran, D.W., Mills, H.J., Zhu, M.-X., Morse, J.W. 2011. Examination and refinement of the determination of aqueous hydrogen sulfide by the methylene blue method. Aquatic Geochemistry 17(4):567-582. Copyright 2011 by Springer

Introduction

Aqueous hydrogen sulfide ($\Sigma H_2S_{aq} = H_2S_{aq} + HS^- + S^{2-}$ (trace) + ΣS(-II) ion complexes, clusters, nanoparticles and colloids) is commonly found in natural and waste waters, and sediments, usually under reducing conditions. Even at relatively low (μmolar) concentrations, it can be potentially toxic to organisms. It also plays a major role in the sedimentary sulfur cycle and can influence the toxicity of a variety of trace metals because of the low solubility of many metal sulfide minerals.

The accurate and precise measurement of ΣH_2S_{aq} has consequently been of major interest for well over a hundred years (Fischer 1883). A number of methods and techniques are in use for measuring ΣH_2S_{aq} including chromatography, specific ion electrodes, voltammetery, and coulometery (Lawrence et al. 2000). However, the most commonly used methods involve the formation of the methylene blue-sulfide complex and spectrophotometric measurement of its concentration.

The objectives of this paper are 1) to briefly review the history and development of the methylene blue method for determination of ΣH_2S_{aq}, 2) to compare the major currently used different techniques and the variations in their procedures, and 3) to establish their precision and accuracy over concentration ranges. Based on the results, a detailed procedure will be presented that we deem has an optimal combination of analytical reliability and ease of use for general applications. Using the principles of the method documented here, the general procedure may then be further optimized by the individual researcher based on laboratory-specific requirements.

Background

The reaction between N,N-dimethyl-*p*-phenylene diamine (*N*,*N*-dimethylbenzene-1,4-diamine) and ΣH_2S_{aq}, under acidic conditions in the presence of an oxidizing agent (usually ferric iron), results in the formation of methylene blue, an intense blue colored dye soluble in water seen in Equation 2.1 below (modified from Mecklenburg and Rosenkranzer 1914).

(Eq. 2.1)

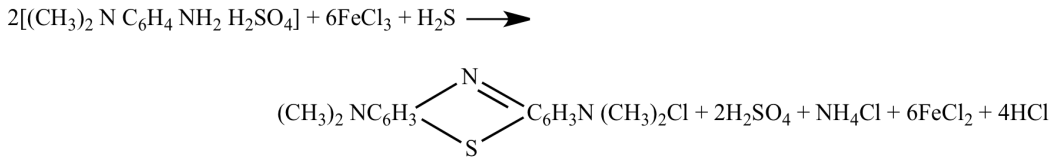

Emil Fischer (Fischer 1883) suggested more than a century ago that the methylene blue reaction could be used to determine hydrogen sulfide concentration. Lindsay (1901) used this method to quantitatively estimate the amount of sulfur in pig iron by visual comparison to standards. For those with trouble distinguishing different shades of blue, Lindsay suggested the use of other diamines to produce different colors and specifically noted that the use of p-phenylene diamine (1,4-benzenediamine) in the reaction would produce Lauth's violet, also referred to as thionin. It should be noted that Lauth's violet ($C_{12}H_{10}N_3SCl$) is NOT methylene blue ($C_{16}H_{18}N_3SCl$), as there are no methyl groups on the terminal nitrogen. In 1929, the first substantial changes to the procedure included substituting sulfuric acid and ferric ammonium sulfate for hydrochloric acid and ferric chloride, respectively, which results in the reduction of the yellow ferric chloride color (St. Lorant 1929). This allows for the addition of excess

ferric iron, thus decreasing the reaction time for full color development to only ten minutes rather than two hours (although a wait time of one hour was still recommended).

Arguably, the first thorough investigation of the methylene blue method called for the addition of excess ferric chloride to obtain full color development in one minute followed by the addition of phosphate or phosphoric acid (specifically, diammonium phosphate). Phosphate was added to remove the ferric chloride color due to the reaction of phosphate and iron to form unionized ferric phosphate (Pomeroy 1936), which is relatively insoluble at room temperature based on K_{sp}. However, the author noted that the presence of phosphate in the sample inhibits full color development. More than 20,000 tests later, Pomeroy further clarified this method (Pomeroy 1941), which was later incorporated into *Standard Methods for the Examination of Water and Wastewater* (hereafter referred to as *Standard Methods*) (APHA 1960) and has remained, with one modification to be described later, as the accepted method for the determination of hydrogen sulfide.

Subsequent studies investigated the effect of temperature on the reaction showing that the maximum yield of the reaction (i.e., greatest color formation) occurs at 24°C with side reactions playing a larger role at lower temperatures leading to lower relative percent yield of methylene blue color (Fogo and Popowsky 1949). This study also noted the effect of pH on the reaction, which was hypothesized to affect the absorbance of the methylene blue product and not the overall yield of the reaction. Sands et al. (1949) found that although color development was more rapid with the use of the hydrocholoric salt of the diamine in comparison to the sulfate salt, the color faded more rapidly as well,

and therefore suggested the use of the sulfate salt. Additionally, this study suggested an importance of the diamine to sulfide molar ratio as they found the absorbance increased with an increase in diamine concentration until a critical ratio was reached (which appears to be approximately 20). To prevent erroneously low concentration estimates, Budd and Bewick (1952) suggested that the diamine reagent be mixed with the sulfide solution prior to the addition of the ferric chloride. Additionally, this study suggests that errors (up to +10%) may be introduced if a curve is used in which the standards were not likewise aliquoted and diluted after color formation.

In 1965, Nusbaum (1965) suggested that the oxalate salt of the diamine be used because it is more stable than the free base as well as hydrochloride and sulfate salts. This recommendation was subsequently incorporated into *Standard Methods*. The United States Environmental Protection Agency (EPA) adopted the *Standard Method* as an approved sulfide test method; however, the method was later withdrawn as a part of the EPA Method Update Rule effective July 2007. The EPA currently has no recommended method for the measurement of dissolved sulfide.

In 1969, Cline published the most widely cited (>1200 citations at this writing) methylene blue method (hereafter referred to as *Cline Method*). Cline was the first investigator to specifically mix the N,N-dimethyl-*p*-phenylenediamine sulfate (hereafter referred to as diamine) and ferric reagents prior to addition to the sample. In doing so, the loss of sulfide due to volatilization at higher temperatures is minimized. Additionally, Cline found by using a mixed reagent the apparent molar absorption coefficient remained relatively constant in the temperature range of 5°C to 30°C,

contrary to the results found by Fogo and Popowsky (1949). Cline was also the first investigator to note the importance of the final molar ratio of diamine to sulfide, as he observed departures from Beer's law when this molar ratio was less than seven.

Kloster and King (1977) proposed the use of N,N-diethyl-*p*-phenylene diamine sulfate in place of the N,N-dimethyl-*p*-phenylene diamine oxalate in the standard methylene blue sulfide test based on an observed doubling of the sensitivity. Their use of dichromate alleviated the need to add phosphate to the reaction mixture as well. However, *Standard Methods* (APHA 1960) continues utilizing the method of Pomeroy (1941) with the use of the oxalate salt as suggested by Nusbaum (1965). Lindsay and Baedecker (1988) provided another modification to that of Cline methodology ensuring that the final molar ratio of diamine to sulfide was never less than 20. Also, contrary to the procedure of Kloster and King (1977), they found results for the diethyl derivative to be less sensitive than the dimethyl diamine.

From the previous discussion, it is evident that many modifications have been made to the methylene blue method. Multiple applications of the methylene blue procedure are reported in the literature and the continued appearance of new modifications indicates both that it has reliability yet lacks perfection (Patterson 1978). The main variations that exist on the theme include Pomeroy (*Standard Methods*) and Cline (*Cline Method*), which are the most widely used and, consequently, will be the focus of comparison in this study.

Furthermore, in our examination of the *Cline Method*, we intend to clarify the existing confusion of this procedure, as it is apparent that various interpretations exist

among research groups regarding reagent preparation. Based on these comparisons, a final method will also be presented that future researchers may employ with greater confidence.

Experimental section

General: All spectrophotometric measurements were carried out on Shimadzu UV-1601 (Columbia, MD) using 1 cm polystyrene disposable cuvettes, unless otherwise noted. All chemicals and reagents used in this work were of analytical grade. Sulfide standard solutions were prepared immediately before use from sodium sulfide crystals ($Na_2S \cdot 9H_20$) (EMD Chemicals, Gibbstown, NJ) dissolved in 18.2 mΩ-cm deionized (DI) water that was deoxygenated by sparging with ultra high purity N_2 gas for a minimum of one hour. All crystals were rinsed with deoxygenated water and wiped dry with a lint-free tissue prior to use to remove oxidation products from the surface. The sulfide solutions were standardized using a 25 mmol L^{-1} iodine solution (Mallinckrodt Baker, Phillipsburg, NJ) and a 25 ± 0.01 mmol L^{-1} sodium thiosulfate ($Na_2S_2O_3$) (Ricca Chemical, Arlington, TX) secondary standard, certified traceable to potassium dichromate ($K_2Cr_2O_7$) (APHA 1960; Cline 1969; Lindsay and Baedecker 1988). Concentrations of the working sulfide standards were between 1 μmol L^{-1} and 1000 μmol L^{-1}.

All statistical analyses were performed in Microsoft Office Excel 2003 and the variations reported here are standard errors or standard deviations of the mean, unless otherwise noted.

A total of four procedures are described below. Procedures 1-3 were developed as a result of the various interpretations of the *Cline Method* (Cline 1969). The interpretations differ primarily in the reagent preparation, as Cline's Table 1 and the associated explanation in the original study is unclear. Procedure 4 follows *Standard Methods* (APHA 1960).

For procedures 1 through 3, a 0.4 mL aliquot of the mixed diamine reagent (MDR, preparation described below) was added to 5 mL of the sulfide standard and promptly capped in an appropriate-sized glass test tube to minimize the amount of headspace in order to reduce oxygenation or volatilization of hydrogen sulfide. The blanks were prepared in the same manner, but using deoxygenated DI water in place of the sulfide standard. In each of the procedures tested, the color was allowed to develop for 20 to 30 minutes prior to measuring the absorbance. A spectra of the absorbances was obtained for wavelengths 400 nm to 900 nm for all the procedures. The molar absorption coefficients were calculated from the slope of the standard curves at the 99% confidence limit and for a path length of 1 cm, unless otherwise stated.

Procedure 1: This procedure was evaluated by the researchers in this current study as the most common interpretation of the *Cline Method*.

Three reagents were prepared for sulfide concentration ranges of 1 - 40 μmol L^{-1}, 40 - 250 μmol L^{-1}, and 250 - 1,000 μmol L^{-1} using N,N-dimethyl-*p*-phenylenediamine sulfate (Alpha Aesar, Ward Hill, MA) (hereafter referred to as diamine) and ferric chloride ($FeCl_3 \cdot 6H_20$) (Fisher Scientific, Waltham, MA). The appropriate amounts

(indicated in Table 2.1) of diamine and ferric chloride were dissolved into a single solution of 500 mL of room temperature 6 mol L^{-1} (50% v/v) reagent-grade HCl (EMD Chemicals, Gibbstown, NJ), hereafter referred to as mixed diamine reagent (MDR). All reagents were stored in dark bottles at 4°C and allowed to equilibrate to room temperature prior to use. The shelf life and stability of MDR solutions were tested during this study by using MDR solutions made approximately 3, 6 and 12 months prior and were used in a standard assay as described below.

The higher sulfide concentrations formed a dark blue color; therefore, dilutions for concentrations 40 – 250 μmol L^{-1} and 250 – 1,000 μmol L^{-1} were made following color development in Procedure 1. Cline indicates that the lower concentration range requires a dilution of 1:1, which can be interpreted as one part standard/sample solution to one part dilutant (i.e., 50% dilution) or as one part solution to one part total (i.e., no dilution). If interpreted as the former, the methylene blue color at the lowest concentrations was diluted to the point of no detectable absorbance. The sensitivity is decreased significantly at the 50% dilution. Therefore, the correct interpretation was no dilution is required at the lower concentration range and could be measured directly. A dilution factor of 2:25 (2 parts solution added to 23 parts dilutant) was used for the concentration range 40 – 250 μmol L^{-1} and a dilution factor of 1:50 (1 part solution added to 49 parts dilutant) was used for the concentration range 250 – 1,000 μmol L^{-1}.

The feasibility of using this procedure in a micro volume spectrophotometer was also tested. A NanoDrop ND-1000 Spectrophotometer (ThermoFisher, Wilmington, DE) was used to test the potential of applying Procedure 1 to a small sample volume (µl). A

volume of 1 μl was measured across a 1 mm path length with absorption recorded at a wavelength of 667 nm. Dilutions were not required as no absorbance exceeded 1. Standard curves were produced from the mean value of duplicate measurements at each standard concentration for both aged MDR and the NanoDrop samples. The molar absorption coefficients were calculated as described above; however, a path length of 1 mm was used for the NanoDrop assay.

All samples from procedures 1 through 3 were measured against a blank solution, which was prepared using deoxygenated DI water in place of the sodium sulfide solution.

Table 2.1: Amount of N,N-dimethyl-*p*-phenylenediamine sulfate and ferric chloride ($FeCl_3$) to be dissolved into 6 mol L^{-1} HCl for each procedure and the ratios of solutions to be mixed for Procedures 2 and 3

Sulfide concentration range (μmol L^{-1})	**Procedure 1** Amount dissolved into single 500 mL solution of 50% HCl		**Procedures 2 and 3** Amount dissolved into separate 500 mL solutions of 50% HCl		**Procedure 2**	**Procedure 3**
	Diamine	$FeCl_3$	Diamine	$FeCl_3$	Ratio of diamine and ferric solutions to be mixed	Ratio of diamine and ferric solutions to be mixed
1 - 40	2 g (10.8 mM)	3 g (37.0 mM)	2 g (10.8 mM)	3 g (37.0 mM)	1:1 (5.4 mM; 18.5 mM)	1:1 (5.4 mM; 18.5 mM)
40 - 250	8 g (43.2 mM)	12 g (148.0 mM)	8 g (43.2 mM)	12 g (148.0 mM)	2:23 (3.5 mM; 136.1 mM)	1:1 (21.6 mM; 74.0 mM)
250 - 1,000	20 g (108.0 mM)	30 g (370.0 mM)	20 g (108.0 mM)	30 g (370.0 mM)	1:49 (2.2 mM; 362.5 mM)	1:1 (54.0 mM; 185.1 mM)

Procedure 2: This procedure followed that of Parsons et al. (1984), which interprets the dilution factor in Cline's Table 2 (Cline 1969) as the amount of each reagent to be mixed.

Three reagents were prepared for the concentration ranges listed previously. However, the appropriate amounts of diamine and $FeCl_3$ were first dissolved separately, each in a 500 mL solution of room temperature 6 mol L^{-1} reagent-grade HCl. Following dissolution in independent containers, the diamine reagent and the $FeCl_3$ solutions were mixed into a single dark bottle (Table 2.1) and stored at 4°C. For the lower sulfide concentration range (1 – 40 μmol L^{-1}), the solutions were mixed 1 part diamine to 1 part $FeCl_3$; for the 40 – 250 μmol L^{-1} sulfide concentration range, 2 parts diamine were combined with 23 parts $FeCl_3$; and for the 250 – 1,000 μmol L^{-1} concentration range, 1 part diamine was combined with 49 parts $FeCl_3$. Any necessary dilutions were carried out following color development resulting from combining the mixed reagent and the sample. The dilution factor used was calculated to bring the concentration into the 1 – 40 μmol L^{-1} range.

Procedure 3: This procedure was developed as yet another interpretation of the reagent preparation and subsequent dilutions.

Reagents were prepared for each concentration range and, as in Procedure 2, the diamine solution and the $FeCl_3$ solutions were prepared separately in 500 mL of room temperature 6 mol L^{-1} HCl. The two solutions were mixed equally (1:1 ratio) into a 1 L dark bottle for each concentration range. The mixed reagent was then diluted by the

dilution factor indicated in Table 2.1. Any necessary dilutions of the standard solution occurred after the addition of the reagent and the color development, which follows Procedure 2.

Procedure 4: This procedure follows that of *Standard Methods* (APHA 1960). The primary differences of the *Standard Method* from that of *Cline Method* include: preparation of reagents (i.e., the diamine and the $FeCl_3$ reagents are prepared and added separately in *Standard Methods*), the acidic medium for the diamine reagent (i.e., H_2SO_4 is used in *Standard Methods* and HCl is used in *Cline*), and a single set of reagents for all concentration ranges.

An amino-sulfuric acid stock solution (0.74 mol L^{-1}) was prepared by dissolving 27 g N,N-dimethyl-p-phenylenediamine oxalate (Alpha Aesar, Ward Hill, MA) into a solution of 50 mL reagent-grade sulfuric acid (H_2SO_4) (Sigma Aldrich, St. Louis, MO) and 20 mL 18.2 mΩ-cm DI water. Following dissolution, this solution was diluted to a final volume of 100 mL with DI water. An amino-sulfuric acid reagent was made by diluting 25 mL of the amino-sulfuric acid stock solution with 9 mol L^{-1} (50% v/v) H_2SO_4 to a final volume of 1,000 mL (0.018 mol L^{-1} final concentration). A separate $FeCl_3$ solution was prepared from 100 g $FeCl_3 \cdot 6H_2O$ in 40 mL DI water. A diammonium hydrogen phosphate solution was prepared by dissolving 400 g $(NH_4)_2HPO_4$ (Sigma Aldrich, St. Louis, MO) into 800 mL DI water. A sulfide sample volume of 7.5 mL was transferred to a glass test tube, to which 0.5 mL of amino-sulfuric acid reagent and 0.15 mL $FeCl_3$ solution were quickly added and capped. A blank solution was prepared by

adding 0.5 mL of 9 mol L^{-1} H_2SO_4 and 0.15 mL $FeCl_3$ solution to 7.5 mL of the sulfide sample. After waiting 5 minutes for color development, 1.6 mL of diammonium hydrogen phosphate solution was added to both. The color was allowed to develop for 5 more minutes before measuring the absorbance. Samples with absorbance greater than 1 were diluted prior to adding reagents and any color development, which is consistent with the reported methodology. A spectra of the absorbance was obtained for wavelengths 400 nm to 900 nm.

Results and discussion

Procedure 2 was determined to not contain enough diamine in the final mixed reagent for the reaction to proceed and for methylene blue color to develop (discussed below). As such, this procedure was quickly ruled out as a reasonable interpretation of the method. Furthermore, the higher two concentration ranges would result in a large amount of waste of the diamine reagent (i.e., if only 1 part of diamine was used to 50 parts of $FeCl_3$). A brief literature search revealed more than 20 references directly following the method as described in Parsons et al. (1984).

Procedure 3 was determined to be an unlikely interpretation of the *Cline Method* due to the large dilution of the mixed reagent required. If this interpretation were correct, the method would begin with a lesser amount of diamine or $FeCl_3$ or with a weaker acid concentration if the end goal were to dilute the mixture. Furthermore, as in Procedure 2, the amount of diamine present in the final reagent mixture was inadequate for the full

methylene blue color development at the higher concentration ranges (i.e., greater than 40 μM).

Procedure 4 (*Standard Method*) produced a linear standard curve (19,900±100 L $mole^{-1}$ cm^{-1}; r^2=0.9992) for the average of two replicates for five concentrations (5 μmol L^{-1} to 31 μmol L^{-1}). For samples with an absorbance greater than one (Fischer 1883), dilution was required according to the method. A linear calibration curve was still present when the absorbance was corrected for the dilution factor (r^2=0.9997).

For comparison, the *Standard Method* procedure was evaluated using two sets of prepared blank solutions. One set of blank solutions was prepared according to the methodology provided using the sample combined with 9 mol L^{-1} sulfuric acid, such that no color develops. A second set was prepared using DI water in place of the sodium sulfide solution and treating it the same as a sample. No change was observed in the molar absorption coefficient of the calibration curve, thus we concluded that the method of preparing the blank solution does not matter.

As a note, dilution AFTER color development is not possible with the *Standard Method* procedure due to the formation of a precipitate (i.e., ferric phosphate) following addition of DI water. This reaction is the result of an increase in pH and sulfide interaction with the diammonium hydrogen phosphate solution. Therefore, the sulfide concentration range of the sample must be anticipated and diluted accordingly prior to the addition of any reagents, which is not always feasible in field conditions. Adding the diamine reagent initially followed by the $FeCl_3$ reagent risks the loss of sulfide due to

volatilization. Using three separate reagents as opposed to one makes the use of the *Standard Method* procedure more difficult, particularly in field conditions.

The accuracy of the *Standard Method* procedure was determined by comparisons to iodimetric titrations of a sodium sulfide solution and the precision was determined using 10 replicates. The accuracy was determined to be ± 10%, which is consistent with previously reported values. Precisions of 1% and 5% were obtained with 25 μmol L^{-1} and 370 μmol L^{-1}, respectively. The detection limit was determined using 1 cm cells and was calculated at two times the blank concentration, to be approximately 3.1 μmol L^{-1}. Using the spectra obtained from 400 nm to 900 nm wavelengths, the peak absorbance for the *Standard Method* procedure was determined to be at 667 nm, not 625 nm as indicated in the method.

Procedure 1 (*Cline Method*) also produced a linear standard curve for the average of three replicates for each of the three concentration ranges, 1 to 40 μmol L^{-1} (r^2=0.9994), 40 to 250 μmol L^{-1} (r^2=0.9997) and 250 to 1,000 μmol L^{-1} (r^2=0.9932) (Figures 2.1a, 2.1b, and 2.1c, respectively). A standard deviation for each concentration was calculated but was too low (< 1%) to be adequately visualized, thus they were

omitted and will remain as data not shown. Using the spectra obtained from 400 nm to 900 nm wavelengths, we observed the peak absorbance at 666 or 667 nm, close to the 670 nm as previously published (Cline 1969). For each concentration range (1-40, 40-250, and 250-1000 µmol sulfide L^{-1}), molar absorption coefficients (MAC; 27,200±100, 33,800±300, and 34,500±400 L $mole^{-1}$ cm^{-1}, respectively) were calculated at the 99% confidence limit from the slope of the standard curve, path length and dilution, which

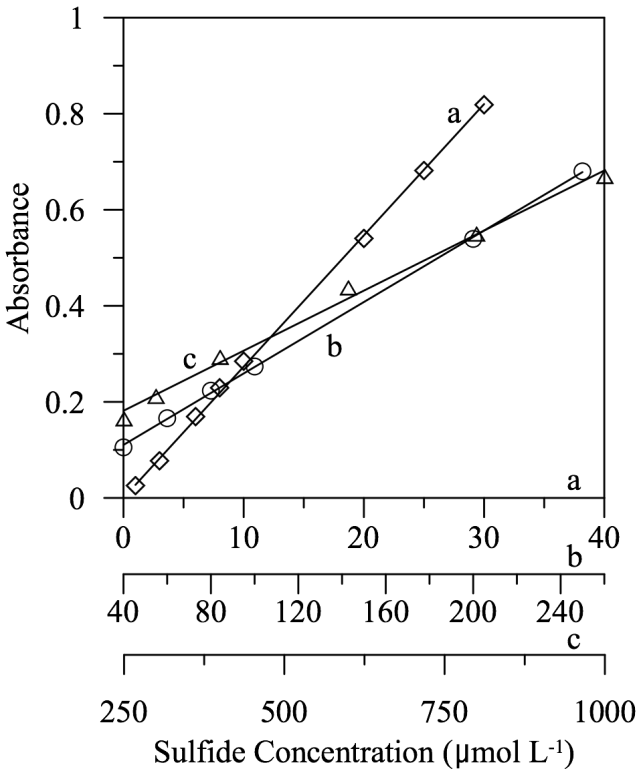

Figure 2.1. Standard calibration curve using the method outlined in Procedure 1 (*Cline Method*). The concentration ranges include: a) 1–40 µmol L^{-1}, b) 40–250 µmol L^{-1}, and c) 250–1000 µmol L^{-1}.

were in agreement with Cline (1969). It is interesting to note that the lower range (1-40 μmol sulfide L^{-1}) has a lower molar absorptivity indicating reduced solution interference. The mid and high range sulfide standards have coefficients in close agreement to each other.

According to the method, samples with an absorbance greater than 1, a dilution was required following color development (Fischer 1883). However, the method (as originally written) is not clear regarding the optimal dilutant (e.g., DI water or blank solution). Regardless of the dilutant utilized, a linear calibration curve for the corrected absorbance was observed (Figure 2.2). This linearity illustrated in Figure 2.2 is significant because it demonstrates a relationship between all concentrations tested (i.e., 3 – 1000 μM) across all three MDR ranges if the absorbances are corrected for the dilutions used (e.g., 3-40 μM MDR – no dilution required, absorbance plotted as listed; 40-250 μM MDR – 2:25 dilution factor, absorbance multiplied by 12.5; 250-1000 μM MDR – 1:50 dilution factor, absorbance multiplied by 50). Standard representation of the data would typically require three individual lines for each MDR with three different MAC. Therefore, a single MAC can represent the total data set, simplifying the data processing required when sulfide concentrations detected cross between MDRs. For example, the standards diluted with pure water can be represented with a single curve (r^2=0.9995; MAC=30,934).

The precision and the accuracy were determined for the *Cline Method* in the same manner as previously described for the *Standard Method*. The accuracy was determined to be ± 5.5%. The precision at 25 μmol L^{-1} was determined to have a relative

standard deviation of ± 1%, which is consistent with previously reported values. The precision at a higher concentration of 370 μmol L^{-1} was determined to be ± 4.3%. A detection limit of approximately 1.13 μmol L^{-1} (p<0.01) was determined at two times the blank concentration using 1 cm cells. Lower detection limits can be obtained using a 5 or 10 cm cell; however, larger sample volumes would be necessary and may not be realistically obtainable from media such as groundwater or sediment porewater.

The amount of time that the samples could be reliably archived was evaluated for Procedures 1 and 4 only, as these interpretations produced good color development at all concentration ranges. The samples were stored in an airtight test tube after color development for one month and measured every other day to determine the optimal maximum storage time. Results suggest that the optimal hold time for the *Cline Method* is not more than one week for samples at the higher concentration range (>250 μmol L^{-1}). Samples with concentrations less than 40 μmol L^{-1} can be reliably held for the entire one month period as no loss of absorbance was experienced. Sample storage at 4°C was most favorable, as opposed to in the dark at room temperature or sitting on the bench top under natural or artificial light. Samples stored on the bench top experience

photodegradation from artificial and natural light resulting in 2% loss per day. Similarly, the results observed for the *Standard Method* procedure indicated that the optimal hold time for samples less than 40 μmol L^{-1} was approximately two days, whereas the higher concentrated samples did not experience any significant loss in peak absorbance after one month. Similar to the *Cline Method*, the optimal storage method for an extended period of time (>1 day) required refrigeration (4°C). According to this study, holding the samples in their undiluted form, then diluting just prior to analysis was shown to be more favorable than holding the sample in its diluted state (data not shown). Furthermore, it is recommended that the headspace be limited and the preserved samples be stored in an airtight container for any length of time to prevent volatilization and evaporation.

Reagent stability: The mixed diamine reagent (MDR), made according to Procedure 1, was evaluated for its long-term stability. The MDR was prepared for each of the concentration ranges and stored in a dark container for 3 months, 6 months, and 1 year. An additional MDR was prepared fresh and standard curves were compared to test the stability of the reagents. All reagents were also stored in the refrigerator to increase stability and avoid degradation of the organic compounds. The MDR prepared fresh for the 40 – 250 μmol sulfide L^{-1} and the 250 – 1000 μmol sulfide L^{-1} showed a calibration curve that was significantly different (p>0.05) than the MDRs that stored for 6 months and one year.

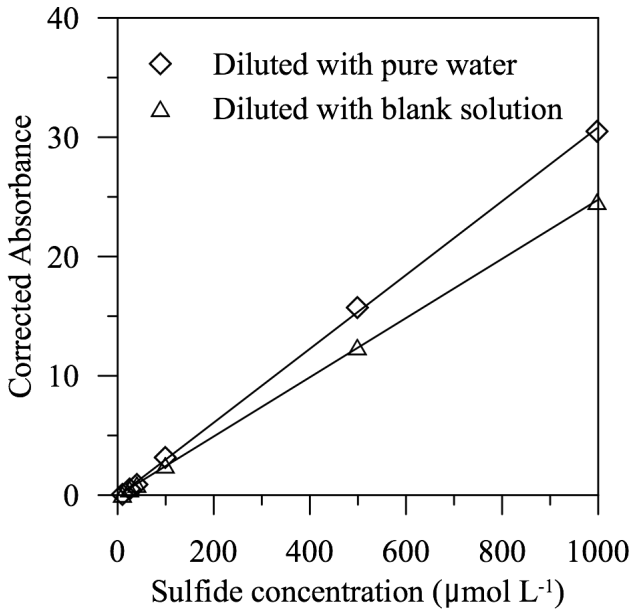

	Measured Absorbance								
MDR Concentration Range	3 - 40 µM			40 - 250 µM			250 - 1000 µM		
Standard Concentrations (µM)	9.9	24.9	40.0	40.0	99.1	250.0	250.0	498.7	997.4
Diluted with Pure Water	0.090	0.550	0.934	0.064	0.250	0.700	0.150	0.324	0.611
Diluted with Blank Solution	0.090	0.550	0.934	0.070	0.201	0.715	0.158	0.249	0.494
	Corrected Absorbance								
MDR Concentration Range	3 - 40 µM			40 - 250 µM			250 - 1000 µM		
Standard Concentrations (µM)	9.9	24.9	40.0	40.0	99.1	250.0	250.0	498.7	997.4
Diluted with Pure Water	0.090	0.550	0.934	0.800	3.125	8.750	7.500	16.200	30.550
Diluted with Blank Solution	0.090	0.550	0.934	0.875	2.513	8.938	7.900	12.450	24.700

Figure 2.2. Standard calibration curves of Procedure 1, in which one set of sulfide standards was diluted with deionized water (open squares) and a second set was diluted with the blank solution (open triangles). Measured and corrected absorbances are listed in the two tables. Corrected absorbances were calculated by multiplying the measured absorbance with the dilution factor as follows: 3-40 µM mixed diamine reagent (MDR) – no dilution required, no correction required; 40-250 µM MDR – 2:25 dilution factor, absorbance multiplied by 12.5; 250-1000 µM MDR – 1:50 dilution factor, absorbance multiplied by 50. Calibration curves were plotted from corrected absorbances to illustrate linear relationship between all standard concentrations.

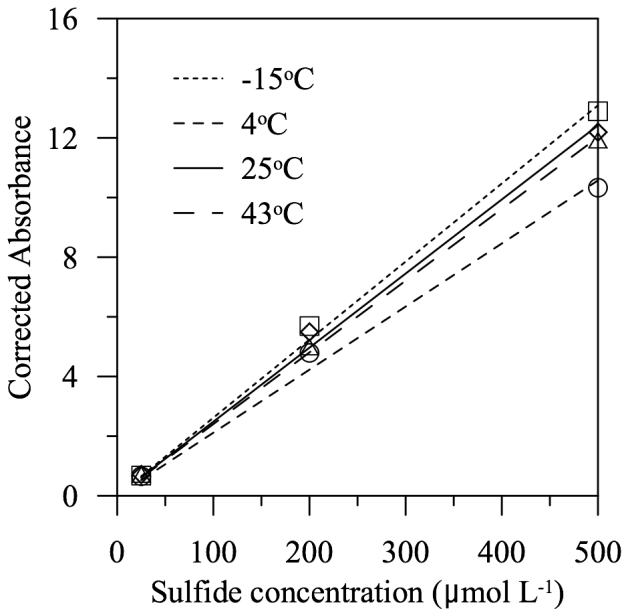

		Measured Absorbance			
Experiment Temperature		-15°C	4°C	25°C	43°C
Standard Concentrations (µM)	25.0	0.687	0.665	0.721	0.727
	200.1	0.458	0.391	0.440	0.408
	500.0	0.258	0.207	0.244	0.239
		Corrected Absorbance			
Experiment Temperature		-15°C	4°C	25°C	43°C
Standard Concentrations (µM)	25.0	0.687	0.665	0.721	0.727
	200.1	5.720	4.888	5.500	5.100
	500.0	12.900	10.340	12.200	11.940

Figure 2.3. Calibration curves of Procedure 1, in which temperature was varied and the absorbance was corrected for the dilution factor. The molar absorption coefficient for each curve are as follows: -15°C = 26,300 L mole^{-1} cm^{-1}; 4°C = 21,800 L mole^{-1} cm^{-1}; 25°C = 25,000 L mole^{-1} cm^{-1}; 43°C = 24,500 L mole^{-1} cm^{-1}. Calibration curves were plotted with absorbances corrected for the dilution factor as follows: 3-40 µM mixed diamine reagent (MDR) – no dilution required, absorbance plotted as listed; 40-250 µM MDR – 2:25 dilution factor, absorbance multiplied by 12.5; 250-1000 µM MDR – 1:50 dilution factor, absorbance multiplied by 50.

Although the calibration curves were significantly different statistically and the molar absorption coefficient has shifted, each curve still showed good linearity (r^2>0.99). The MDR stored for 3 months had a standard curve that was similar to the fresh MDR. The MDR prepared for the lower concentration range (1 – 40 μmol sulfide L^{-1}) showed no significant difference (p<0.05) up to one year from the MDR prepared fresh before use. It is important to note that although the reagents may stable for months, it is recommended that the same MDR is used for the analysis of the samples and the standards and that an old standard curve is not used to interpret newer or later measurements.

Temperature dependency: Procedures 1 and 4 were also evaluated for their dependency on temperature by preparing standard sulfide solutions (25 μmol L^{-1}, 200 μmol L^{-1}, and 500 μmol L^{-1}) on ice (approximately -15°C), 4°C, room temperature (approximately 25°C), and approximately 43°C. This was immediately followed by storage at their respective temperatures during color development. The color development for both methods was fastest in the 4°C samples, followed by the samples which remained at room temperature. All absorbance were then analyzed on the spectrophotometer at room temperature. It is interesting to note that while temperature does affect the reaction rate, the highest temperatures do not produce the fastest reactions. Each temperature produced a linear standard curve (r^2>0.99), however the slopes of each curve varied slightly (Figure 2.3). Note that the same rationale and method for calculation of corrected absorbance described for Figure 2.2 was applied to data presented in Figure 2.3. The

absorbance of the samples measured at the original temperature (-15°C and 4°C) was significantly (p>0.05) different than the absorbance of the same sample that was warmed to room temperature. Such observations indicate the importance of preparing and preserving standards at a similar temperature compared to the in situ conditions from which the samples were collected, prepared and preserved.

Sample acidity: The pH of the sample to be analyzed is an important factor to consider when using either of the methylene blue methods. The *Cline Method* and *Standard Method* are optimal when the sample pH is near-neutral. Solutions with a high basic pH will form a precipitate upon the addition of the mixed diamine reagent or the amino-sulfuric acid reagent and produce a distinctive pinkish-purple color. The precipitate is likely ferric sulfate and/or ferric phosphate. According to experiments in this study, the precipitate and color change make determining sulfide concentrations in high basic solutions using this method impossible. Manipulating the pH with the addition of a strong acid after color development can dissolve the precipitate; however, the amount of acid added can be variable and subjective, resulting in a non-precise dilution of the sample.

Several common methods of sulfide preservation take advantage of precipitate formation or trapping in a high pH solution. For example, acid-volatile sulfides (AVS) and total reducible sulfides (TRS) are analyzed by trapping extracted sulfide in a high pH solution of zinc acetate and/or sodium hydroxide, forming a zinc sulfide complex or the ionized form of sulfide (i.e., HS^- or S^{2-}), respectively (Canfield et al. 1986; Morse et

al. 1987). This precipitate that is produced following the addition of the color developing reagent may be avoided by first decreasing the pH of the sample to be analyzed through drop-wise addition of HCl. The researcher must take care to minimize the volatilization and loss of H_2S that occurs while decreasing the pH to near-neutral.

Variances in ionic strength: Previous studies have investigated the effect of ionic strength of the sample on the methylene blue color development: therefore, this study did not address this experimentally. Reese et al. (2008) showed that Procedure 1, based on the *Cline Method*, had no salting out effect in a hypersaline lake with a salinity of 60. Based on the results of this study and numerous studies citing Cline (1969), Procedure 1 can be reliably applied to samples with a salinity range of 0-60.

Assay scalability: In an effort to demonstrate that this method can be adapted to smaller sample volumes, a set of standards were run on a NanoDrop ND-1000 Spectrophotometer (ThermoFisher, Wilmington, DE) using 1 μl of sample. In contrast to the large volume (1 ml) assays in a standard spectrophotometer, no dilutions were required for these measurements as no absorbance was greater than 1.0. The two lower MDR standard solutions (i.e., 1 - 40 and 40 - 250 μmol L^{-1}) produced linear standard curves with calculated molar absorption coefficients of 21,900±100 L $mole^{-1}$ cm^{-1} (r^2=0.9894) and 17,700±200 L $mole^{-1}$ cm^{-1} (r^2=0.9759). These molar absorptivity values are lower with weaker r^2 values than reported above for a 1 ml cuvette and standard spectrophotometer. The highest MDR range failed to produce a linear standard curve

(r^2<0.5) with a complete failure to accurately read concentrations above 500 μmol L^{-1}. Despite the upper range limitation, a small volume spectrophotometer based procedure would prove to be beneficial in some field applications when the volume of sample is limited. Similar results would be expected from a 96 well microtiter plate analysis, providing scalability to this overall assay.

Diamine and iron ratios: We further investigated the sensitivity of the method as a function of the concentration ratio of diamine reagent to the sulfide solution as well as the iron chloride reagent to sulfide present using the Cline's methodology for a concentration of 25 μmol L^{-1} sulfide. According to the stoichiometry of the reaction, 2 moles of diamine and 6 moles of $FeCl_3$ are required for every mole of sulfide for the reaction to proceed to methylene blue. Thus, stoichiometry of the reaction indicates the amount of diamine is limiting in the reaction. Cline noted, however, that departures from Beer's law were observed when the diamine to sulfide molar ratio was less than 7. Additionally, Lindsay and Baedeker (1988) reported a departure from Beer's Law when the diamine to sulfide molar ratio was less than 20. Results from the current study also observed departures from Beer's law when the molar ratio deviated from the optimal stoichiometry (Figures 2.4a and 2.4b). The absorbance increased until a diamine to sulfide ratio of 10 was reached and began to decline again after a ratio of 25. Therefore, we suggest an optimal window of absorbance exists when the diamine to sulfide molar ratio is approximately 10 to 25 (Figure 2.4b). Likewise, an optimal absorbance was also

observed when the $FeCl_3$ to sulfide molar ratio was approximately 12 to 80 (Figure 2.4a).

These data support the conclusion that the amount of diamine and $FeCl_3$ utilized during Procedure 2 and Procedure 3 is inadequate. Additionally, the *Standard Methods* procedure was found to underestimate the amount of diamine and $FeCl_3$ reagents necessary for full color development at the higher concentration range (>250 μmol L^{-1}). This also explains why the linearity of the calibration curve decreases and no longer obeys Beer's law at higher concentrations (data not shown).

Based on the range of diamine to sulfide ratio on the optimal absorbance, a

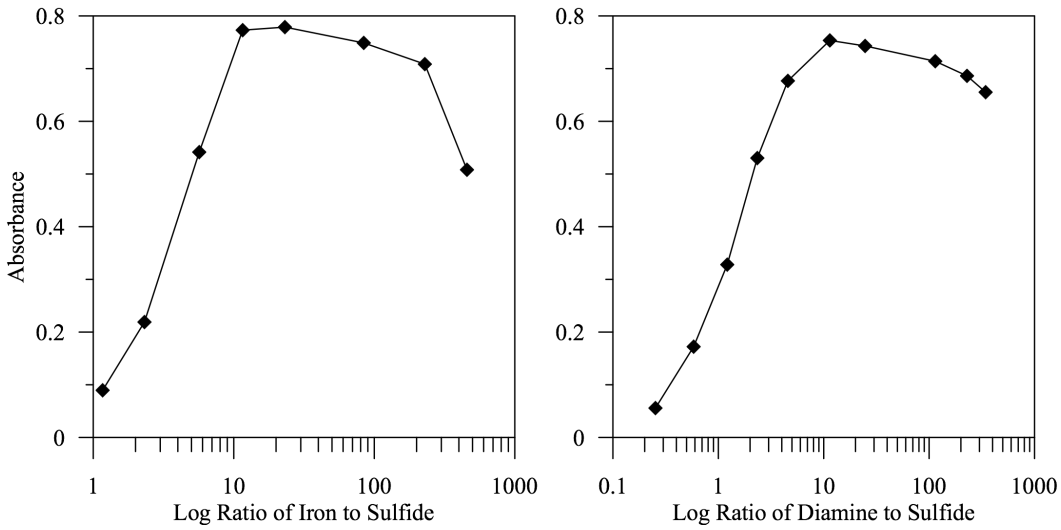

Figure 2.4. Molar ratio of a) iron to sulfide and b) diamine to sulfide. The ratio between the iron and sulfide (a) and the diamine and sulfide (b) were varied to determine the optimal reaction ranges. In experiment (a) the diamine was maintained at approximately 10 mM while the iron concentration varied and in experiment (b) the iron concentration was maintained at approximately 37 mM while the diamine varied.

reagent should be made that is specific to the concentration range the researcher anticipates for their study. The optimal amount of diamine used for the high end of the sulfide concentration is given by

$$[\text{diamine}] = 10 \times [\text{sulfide}]_{\text{high}} \quad \text{(Eq. 2.2)}$$

where the concentration units of diamine and sulfide are equal. Likewise, the amount of diamine for the lower end of the sulfide concentration is given by

$$[\text{diamine}] = 25 \times [\text{sulfide}]_{\text{low}} \quad \text{(Eq. 2.3)}$$

Furthermore, the amount of $FeCl_3$ added to the mixed reagent is calculated by

$$[FeCl_3] = 12 \times [\text{sulfide}]_{\text{high}} \quad \text{(Eq. 2.4)}$$

$$[FeCl_3] = 80 \times [\text{sulfide}]_{\text{low}} \quad \text{(Eq. 2.5)}$$

After evaluating both the *Standard Method* and *Cline Method* with respect to precision and accuracy, detection limit, sample storage time, and ease of use, we determined that the *Cline Method* (specifically, Procedure 1) was optimal. The detection limit of Procedure 1 was calculated to be approximately three times less than that of the *Standard Method*. Furthermore, the optimal storage time of this method was nearly a week longer for samples with concentrations less than 40 μmol L^{-1}. The method described in Procedure 1 requires the use of only one mixed diamine reagent, whereas the *Standard Method* requires three reagents. The use of multiple reagents allows for the volatilization of sulfide as well as adds difficulty for the researcher to transport and use in a field situation. Furthermore, the *Standard Method* requires the dilution of samples prior to the addition of reagents, which further risks the loss of sulfide via volatilization.

When using the *Cline Method* on samples of unknown concentration, it is recommended that the researcher use the reagent mixtures outlined in Procedure 1 and Table 1 (Cline 1969). This allows the researcher to determine the concentration range and refine the method by making a mixed diamine reagent to suit the situation. Once the concentration range is known, the researcher may follow equations 2.2 through 2.5 to calculate the appropriate diamine and $FeCl_3$ amounts to be added to the mixed diamine reagent. It is prudent to remember that the MDR must not be prepared for a concentration range that is too broad as the diamine or the $FeCl_3$ may then be in excess or insufficient for the optimal reaction to occur.

CHAPTER III

FACTORS AFFECTING MOLECULAR AND GEOCHEMICAL CHARACTERIZATION OF SULFUR CYCLING WITHIN AN ESTUARINE SYSTEM

Overview

Sulfate reduction has long been considered the predominant terminal electron-accepting process under anoxic conditions in shallow marine environments. However, recent investigations suggest that Fe(III) respiration may successfully compete with sulfate reduction to comprise a large percentage of carbon oxidation, especially in low salinity environments. Along the southern Texas coastline, the Nueces River empties into the Corpus Christi and Nueces Bays, providing a unique opportunity to study a range of salinities (0.9 – 45) where sediment microbial metabolic processes are limited by either low sulfate or iron concentrations. Benthic microbial terminal electron-accepting processes and populations were characterized at 2 cm intervals over the top 20 cm of sediment in the Nueces River and Nueces Bay to provide varying salinity as well as varying concentrations of iron and sulfate. Sulfate reduction rates were determined using standard ^{35}S incubation assays. Sulfate and iron reducing bacteria community structure was determined using 454 FLX pyrosequencing of SSU rRNA transcripts. An overlap of porewater Fe(II) and H_2S was measured within the samples, suggesting possible overlapping communities (i.e., iron reducing populations capable of sulfate reduction). Qualitative and semi-quantitative characterization provided a link between

observed geochemical processes and microbial activity at in situ conditions. As predicted, a combined geochemical and molecular approach was required to identify benthic environments that were influenced by sulfur or iron terminal electron-accepting processes.

Introduction

Dissimilatory sulfate reduction is an important biogeochemical process influencing the sulfur, iron and carbon cycles in estuarine systems. In coastal and estuarine environments, a large portion of benthic respiration may be attributed to sulfate reduction (Canfield 1989; Chambers et al. 1994; Jorgensen 1982). Although the sulfur cycle is often overlooked in freshwater portions of an estuary, sulfate reducing bacteria may contribute significantly to organic matter degradation due to the rapid turnover of reduced sulfur to sulfate (Luther et al. 2011; Pallud and Van Cappellen 2006).

Sulfate reduction rates are most commonly measured using slurry experiments or whole sediment core incubations with ^{35}S tracer. The influences of sediment macro- and meiofauna, benthic flora, bacterial mats, sediment heterogeneity and microenvironments, and non-steady state conditions further complicate the interpretation of classical ^{35}S measurements. Furthermore, intact core incubations are not typically well adapted for determining the functional dependencies of rates on environmental variables despite their widespread use (Pallud and Van Cappellen 2006). The experimental conditions during incubation, although readily quantifiable, may select for organisms that are not necessarily the most ecologically relevant members of the bacterial community.

Sulfate reducing bacteria (SRB) responsible for the reduction of sulfate have traditionally been viewed as obligate anaerobic heterotrophs that have been relegated to purely anoxic environments. The dogma that SRB are intolerant of oxygen derived from 1) the idea that SRB are poisoned because of the sensitivity of pyrophosphatase (enzyme involved in sulfate reduction) to oxygen and 2) the thermodynamic theory that aerobic heterotrophy is more energetically favorable and thus SRB are out competed (Baumgartner et al. 2006). However, both culture and in situ studies show SRB tolerance to oxygen (Cypionka et al. 1985; Laier et al. 1992). Sediment zonation is a mosaic of microenvironments with different redox conditions and with different bacterial populations. Changes observed with depth are not one-dimensional, as it is typically presented (Boudreau and Jorgensen 2000). SRB should then be characterized throughout the sediment column for both presence and activity. In addition, the range of metabolically active sulfur oxidizing bacteria (SOB) should be better examined as this group may have equal importance to the SRB with a counter geochemical effect.

To observe changes in the microbial community as it relates to the geochemical environment, it is necessary to examine the active portion of the community using RNA transcripts. Studies based on DNA may describe the taxa and metabolic pathways from the total microbial community present in the sediment, whether the cells sampled were metabolically active, quiescent or dead. Therefore, taxa and metabolic pathways identified within the microbial community may not be relevant to observed changes in the geochemistry. Techniques based on either small subunit ribosomal RNA (SSU rRNA) or messenger RNA (mRNA) are more informative regarding changes in the

metabolically active fraction of the microbial community and specific metabolic processes within a dynamic environment, respectively, such as an estuary or river where large geochemical fluctuations can occur over small time scales (Poretsky et al. 2005; Poulsen et al. 1993; Wawer et al. 1997).

The metabolically active taxa within the total population can be identified by isolation and characterization of SSU rRNA. The concentration of ribosomes, and thus copies of SSU rRNA within a cell, is linearly correlated to cellular metabolic activity (Delong et al. 1989; Kerkhof and Ward 1993), with quiescent and dead cells having few to no ribosomes present (Fegatella et al. 1998). Therefore, cells potentially significant to the biogeochemistry of the environment due to high metabolic activity but representing a small fraction of the total microbial population may be below detection limits using DNA-based techniques but detectable by RNA-based techniques (Moeseneder et al. 2005). However, ribosomal RNA analysis is limited to only phylogenetic description of lineages. The processes active within a cell may remain unknown.

Functional gene transcripts (i.e., mRNA) provide a molecular target to determine metabolic processes occurring at the time of sampling; mRNA have short half-lives within a cell, from 30 sec to 13 min, and are rapidly degraded extracellularly (Belasco 1993; Hartig and Zumft 1999). Previous studies have shown correlations between transcript abundance and metabolic activity by comparing functional gene transcript concentrations (Chin et al. 2004; Fleming et al. 1993; Jeffrey et al. 1996; Nazaret et al. 1994). However, the abundance of some metabolic transcripts would then depend on electron donor or acceptor limitations. Therefore, quantifying gene transcripts would

serve as a monitor of metabolic activity at a process level and complement the geochemical characterization of the ecosystem.

The objective of this study was to examine factors affecting the rates of sulfate reduction and the resulting geochemical signatures across a salinity and seasonal gradient. Most studies to date have examined biogeochemical processes from either a chemical or a biological viewpoint and make inferences about the missing half. The research presented herein will combine both disciplines by characterizing the sulfate reducing bacterial population through novel high throughput pyrosequencing and the corresponding sulfate reduction rate. The classic geochemical signature of sulfate reduction within sediments (i.e., loss of sulfate and accumulation of sulfide) is challenged at two locations on the Texas coast (Nueces Bay and Nueces River) during the spring and fall seasons. This study highlights the need to understand both the geochemistry and the microbiology to fully assess the in situ biogeochemical setting and presents a framework for co-analyzing two distinct data sets.

Materials and methods

Site description and sample collection: Nueces Bay is located along the South Texas coast and is a secondary bay linked to the Gulf of Mexico via the Corpus Christi Bay to the east. The major fluvial source is the Nueces River to the west. Tidal forcing is generally minor in the bay, making freshwater inflow a major determinant of salinity patterns within the bay (Mannino and Montagna 1997).

Sediment samples from the Nueces estuary were collected in April during pre-hypoxia conditions and September 2009 during hypoxia conditions. Samples were collected from two locations: Nueces River (27.8604^{o}N, 97.5561^{o}W) and Nueces Bay (27.8424^{o}N, 97.4104^{o}W), each in 2 to 3 m water depth. Five sediment cores were collected at each site, which included duplicate cores for geochemical analysis and triplicate cores for molecular analysis in 7 cm diameter polystyrene core liners using a pole corer (construction of corer described in Gardner et al. 2011). Sediment for geochemical analysis was immediately frozen intact at -20^{o}C and transported to Texas A&M University on dry ice. Additional cores were collected by hand for sulfate reduction rate measurements in 3.5 cm internal diameter translucent polyvinylchloride (PVC) core liners by hand. These cores and the cores for molecular analysis were immediately transported, with minimal disturbance, to the nearby TAMU Agricultural Experiment Station (Beeville, TX) to be processed for sulfate reduction rates or sectioned and preserved for molecular microbiological analysis. All microbiological samples were frozen immediately in liquid nitrogen and transported on dry ice. All incubations for sulfate reduction rate measurements occurred at the experimental station and were initiated less than two hours after sediment collection.

Sulfate reduction rates: Sediment for sulfate reduction rates (SRR) was collected in acrylic core liners containing 1to 2 mm ports every 2 cm along the vertical axis. Ports were sealed with silicon cement before sampling. A small volume (5 μL) of radiolabeled sulfate (0.4 μCi mL^{-1} $Na_2{}^{35}SO_4$) was directly injected via syringe into the sediment

through ports at 2 cm intervals starting 1 cm below the sediment surface. A set of cores was incubated in duplicate for 6 hours and a second set was incubated in duplicate for 12 hours in the dark at in situ temperatures (25^{o}C). All incubations began within 2 hours of sample collection. After incubation, cores were immediately frozen at -20^{o}C to stop activity and were transported to Texas A&M University for further processing. Additional cores were collected as control blanks in which no isotope was injected before being incubated for the same length of time as the test cores. The controls were immediately frozen after incubation.

Frozen cores for sulfate reduction rate analysis were sectioned into 2 cm sections, but every other sediment slice was extracted for SRR measurements. Radioactive sulfide ($H_2{}^{35}S$) was extracted using the single-step method of Fossing and Jorgensen (1989) and the evolved $H_2{}^{35}S$ was trapped in 1 mol L^{-1} zinc acetate. The radioisotope was measured on a 1209 RackBeta liquid scintillation counter (PerkinElmer, Beltsville, MD). The SRR was calculated per unit sediment volume and time as given in Equation 3.1 where [SO_4^{2-}] is the sulfate concentration in nmol cm^{-3} of sediment, $^{35}S\text{-}SO_4^{2-}$ and $^{35}S\text{-}H_2S$ are the total sulfate and sulfide radioactivity, *t* is the incubation time measured in days, and α is a correction factor (1.06) for the expected isotope fractionation against ^{35}S-sulfate versus the bulk ^{32}S-sulfate by the sulfate reducing bacteria.

$$\text{SRR} = \frac{[SO_4{}^{2-}] \times ({}^{35}S - H_2S) \times \alpha}{({}^{35}S - SO_4{}^{2-}) \times t} \quad \text{nmol } SO_4^{2-}\ cm^{-3}\ d^{-1} \qquad \text{(Eq. 3.1)}$$

Sediment and porewater geochemistry: Cores were sectioned (2 cm resolution) within an anaerobic chamber. Porewater was extracted via squeezing (Reeburgh 1967) and

collected in gas-tight syringes. Total sulfide and dissolved iron were determined immediately using the methylene blue and ferrozine colorimetric methods, respectively (Reese et al. 2011a; Viollier et al. 2000). Additional porewater was filtered using a 0.2 μm syringe filter and immediately frozen at -20^{o}C for later sulfate and chloride analysis. Dissolved sulfate and chloride were determined by ion chromatography with an IonPac ASII high capacity anion-exchange column (Dionex, Sunnyvale, CA) after dilution to 200:1. The silt and clay fractions (wt% < 63 μm) were measured by wet sieving. Porosity was determined by drying the sediment in an ~80°C oven and calculating the ratio of percent solid to percent water. Total organic carbon (TOC) and total carbon (TC) were determined on unacidified and acidified oven-dried sediment, respectively, through coulometry using a UIC Model CM-5012 CO_2 coulometer attached to a modified version of the CM-5120 combustion furnace (UIC Inc, Joliet, IL) (Lyle et al. 2000).

Nucleic acid extraction: Total nucleic acids were extracted from 0.5 to 0.6 g sediment (wet weight), sampled from every other 2 cm sediment section (Mills et al. 2008). DNase enzyme was added to the nucleic acid extracts to remove deoxyribonucleic acid (DNA) before reverse amplification of ribonucleic acid (RNA) targets. Controls during polymerase chain reaction (PCR) confirmed no contaminating nucleic acids during the extraction process and no residual DNA remained in RNA extracts (data not shown). Small subunit (SSU) ribosomal RNA (rRNA) was reverse transcribed to complementary DNA (cDNA) using moloney murine leukemia virus (MMLV) reverse transcriptase (Promega, Madison, WI) during a 30 min incubation at 37^{o}C with reverse primer 518R

(5'-CGT ATT ACC GCG GCT GCT GG-3') (Nogales et al. 1999). The reverse transcribed SSU rRNA cDNA was PCR-amplified using NEB Taq DNA Polymerase (New England Biolabs, Ipswich, MA) and the *Bacteria* domain-specific SSU rRNA gene primers 27F (5'-AGR GTT TGA TCM TGG CTC AG-3') (Giovannoni et al. 1991) and 518R on an Applied Biosystems Veriti 96 well (ABI Inc., Foster City, CA). The following protocol was used: initial incubation at 95^{o}C for 5 min; followed by 35 cycles of 95^{o}C for 1 min, 50^{o}C for 1 min, and 72^{o}C for 1 min; with a final extension step at 72^{o}C for 10 min. Amplicons were visualized and size verified with gel electrophoresis using a 0.7% agarose gel.

Pyrosequencing: Primers 28F (5'-GAG TTT GAT CNT GGC TCA G-3') and 519R (5'-GTN TTA CNG CGG CKG CTG-3') produced amplicons from cDNA that spanned three hypervariable regions, V1 through V3 (Handl et al. 2011). Amplicons from each sample were first labeled with a 10-base unique multiplex identifier (MID) sequence to allow all samples to be sequenced on a single run of a Roche 454 FLX (454 Life Sciences, Branford, CT). PCR amplicons from each of the 20 sediment samples were sequenced at the Research and Testing Laboratory in Lubbock, Texas. Downstream sequence analysis parsed the individual sequences into sample-specific libraries. Resulting libraries were screened for reads less than 200 bases, reads lacking a Roche-designed four base key sequence, and non-bacterial reads lacking specific 28F primer recognition site. All sequences passing quality control were deposited in the National

Center for Biotechnology Information (NCBI) database using Sequence Read Archive (SRA).

Phylogenetic and statistical analysis: All sequences passing quality control were denoised, assembled into clusters and taxonomically classified (percent of total length query sequence which aligns with a given database sequence) using the NCBI Basic Local Alignment Search Tool (BLASTn) .NET algorithm (accessed January 2011) (Dowd et al. 2005). Sequences with identity scores, to known or well characterized 16S sequences, greater than 97% identity (< 3% divergence) were resolved at the species level, between 95% and 97% at the genus level, between 90% and 95% at the family and between 85% and 90% at the order level, 80 and 85% at the class and 77% to 80% at phyla. Only sequences meeting the genus taxonomic classification were incorporated into statistical analyses. The percentage of sequences identified to each lineage was analyzed for each sample individually providing relative abundance information within and among the samples based upon reads per sample. Sequences were further clustered into operational taxonomic units (OTU) using the Ribosome Database Project (RDP; University of Michigan; Lansing, MI) and a 95% sequence similarity cutoff (corresponding to a genus level classification). A Sorensen similarity index calculated using RDP was used to characterize microbial communities based on season or location. A dendrogram was constructed from the similarity index using the Phylip draw tree program (Felsenstein 1989) with graphic interface (http://www.phylip.com). Resulting

tree outfile was visualized and formatted using NJ Plot v2.2 (Perriere and Gouy 1996) and TreeView v0.5.0 (http://darwin.zoology.gla.ac.uk/~rpage/treeviewx/).

Diversity analyses including evenness, Shannon diversity index, species richness and rarefaction analysis were computed in RDP. Student T-tests examined the null hypotheses of no differences ($\alpha = 0.05$) in the biological composition or geochemistry between sites and seasons. Differences between sites, depths and seasons by OTU, functional groups, and geochemical composition were evaluated through one-way ANOVA. A post-hoc LSD test was performed when significant differences were identified. Correlation analysis was conducted to identify strength of relatedness in geochemical and physical variables. Statistical analyses were performed using Microsoft Excel 2008 and SPSS v. 16.0. Cluster analysis using Ward's linkages was performed to examine relationship of site depth through geochemistry and functional groups using JMP v. 9.0 (SAS Analytics, Cary, NC). Related dendrograms were created using Phylip (http://www.phylip.com), NJ Plot (Perriere and Gouy 1996) and TreeView (http://taxonomy.zoology.gla.ac.uk/rod/treeview.html).

Quantitative reverse transcription PCR: Gene transcripts were quantified using reverse transcription real time PCR. Total RNA was extracted and DNA removed as described above. The *dsrA* gene transcripts were reverse transcribed to cDNA using the DSR2QR primer (5'-GTT GAY ACG CAT GGT RTG-3') (Chin et al. 2008) and the moloney murine leukemia virus (MMLV) reverse transcriptase (Promega, Madison, WI) incubated at 43^{o}C for 60 minutes. An aliquot of the resulting cDNA was quantified using

a 96-well Applied Biosystems StepOne Plus Real-Time PCR system using StepOne Plus Real-Time PCR System Sequence Detection Software (Version 1.3.1). The reaction mix included primers DSR1F (5'-ACS CAC TGG AAG CAC G-3') and DSR2QR (Chin et al. 2008) and used Quantitect SYBR Green PCR kit (Qiagen, Foster City, CA) according to manufacturer's recommendation. Reaction conditions followed manufacturer's recommendations with 45 cycles followed by a standard melt curve. Standards were prepared from amplified *dsrA* genes purified by gel elution (Qiaquick Gel Elution; Qiagen, Foster City, CA) and quantified using a Nanodrop ND-1000 spectrophotometer (ThermoFisher, Wilmington, DE). The *dsrA* standards were diluted over five orders of magnitude and amplified with four replicates at each dilution ($r^2 = 0.996$). Sensitivity was calculated with precision to 10^0 target molecules per reaction. The standard curve was used to quantify the unknown samples. The melt curve was used to verify single product amplification. All controls were performed as customary for qPCR.

Results

Geochemical characterization: During the spring sample collection, the salinity in the river location was elevated because of recent wind activity forcing water from the bay to the river; however, this temporary saltwater intrusion was not reflected in the sediment geochemistry. The salinity in the river during the fall sampling period was 0.5 at the surface and 30 at the bottom of the water column. The salinity in the bay was 35 during both the spring and fall sample collection.

All geochemical measurements reported herein are the average of triplicate sampling. The porosity did not vary greatly with site location or season, but it decreased with depth in each sediment core from an average of 0.86 to 0.81. Grain size analysis was used to classify locations as mostly sandy (% < 63 μm < 25), intermediate (25 < % < 63 μm < 75), or mostly fine-grained (% < 63 μm > 75). The bay location sediment was on average 23% < 63 μm in size and therefore classified as sandy. The river location sediment had an average of 66% < 63 μm and was considered intermediate to fine-grained.

Total organic carbon (TOC) is the fraction of the total carbon (TC) that is typically derived from the decomposition of plants and animals but excludes the inorganic fraction (i.e., carbonates). TOC and TC concentrations in the river were significantly ($p < 0.05$) greater than in the bay (Figure 3.1e-h). The average TOC in the bay was relatively low at 0.51% g dry weight (gdw) during the fall and 0.53% gdw during spring sampling dates. The average TOC in the river during the fall was as much as 1.2% gdw. In the bay location, TOC concentrations changed relatively little with depth into the sediment, but the river location had increased TOC concentrations with depth during both sampling dates. Both TOC and TC showed a significant correlation ($p < 0.05$) with seasonality; the carbon concentrations were 52% - 78% higher during the fall than the spring. Interestingly, TOC correlated significantly ($p < 0.05$) with iron oxidizing bacteria (FeOB) and sulfur oxidizing bacteria (SOB) as well as porosity, including all samples analyzed.

Total iron concentrations were determined for every sample. Based on the pH (7.1) and redox conditions of the sediment, the iron speciation was determined to be Fe(II) and is reported as such in this study. Iron concentrations in the bay (average 5.0 μmol L^{-1}) were 2.5 times greater than in the river (average 2.0 μmol L^{-1}). Overall, iron concentrations were greatest in the surface and decreased significantly ($p < 0.05$) to below the detection limit at depths below approximately 10 cm (Figure 3.1e-h), with the exception being the fall river core. The iron concentrations were measurable throughout all depths. (Figure 3.1f) Iron concentrations also showed significant ($p < 0.05$) correlations to sulfide and to seasonality.

Dissolved total sulfide ($\Sigma H_2S_{aq} = H_2S_{aq} + HS^- + S^{2-}$) concentrations in the river were as much as three orders of magnitude greater than those in the bay during both sampling periods. The bay concentrations were below the detection limit (1 μmol L^{-1}) at every depth, whereas the concentrations in the river increased with depth from 4.7 to 318.3 μmol L^{-1} and from 7.8 to 211.2 μmol L^{-1} during the spring and fall, respectively (Figure 3.1a-d). Porewater SO_4^{2-} and Cl^- concentrations were converted to a ratio (SO_4^{2-}:Cl^-) to normalize the sulfate concentration. The SO_4^{2-}:Cl^- was higher in the bay (0.05) than the river (0.01) and decreased with depth into the sediment in both locations. Sulfate concentrations in the bay did not change with the seasons, but the river sediment showed higher sulfate in the spring than the fall.

A similarity index calculated the percent similarity of the geochemical parameters such as sulfate, sulfide, dissolved iron, sulfate reduction rates, porosity, TOC, and TC. Pairwise comparison between samples resulted in the formation of a similarity

matrix and the construction of a dendrogam using a neighbor-joining algorithm (Figure 3.2). Clade formation within the dendrogram indicated the two sample locations had distinctly different geochemical characteristics (Figure 3.2). Additionally, dendrogram topology showed that the geochemical environment within the river location differed seasonally, whereas no seasonal trends could be determined with the bay sites. Clade formation also showed trends based on depth within the sediment with deeper (> 10 cm) sediment grouping with greater similarity and shallower sediment grouping together.

Sulfate reduction rates: The rate of active sulfate reduction within the sediment column was determined using standard radiotracer geochemical assays. The down-core average sulfate reduction rate (SRR) over the 6-hour incubation was slightly higher during the spring whereas the 12-hour incubation was slightly higher during the fall sampling (Table 3.1). An exception to the spring trend was noted at the 10-12 cm depth at both sites as the SRR increased at the 12-hour time point. Despite these overall variations between the 6-hour and the 12-hour incubations, Student's T-tests showed no significant difference for the 6-hour or the 12-hour incubations. The SRR in both the Nueces River and Nueces Bay were highly variable with depth and no discernable pattern was observed down the sediment core. However, seasonal differences were observed.

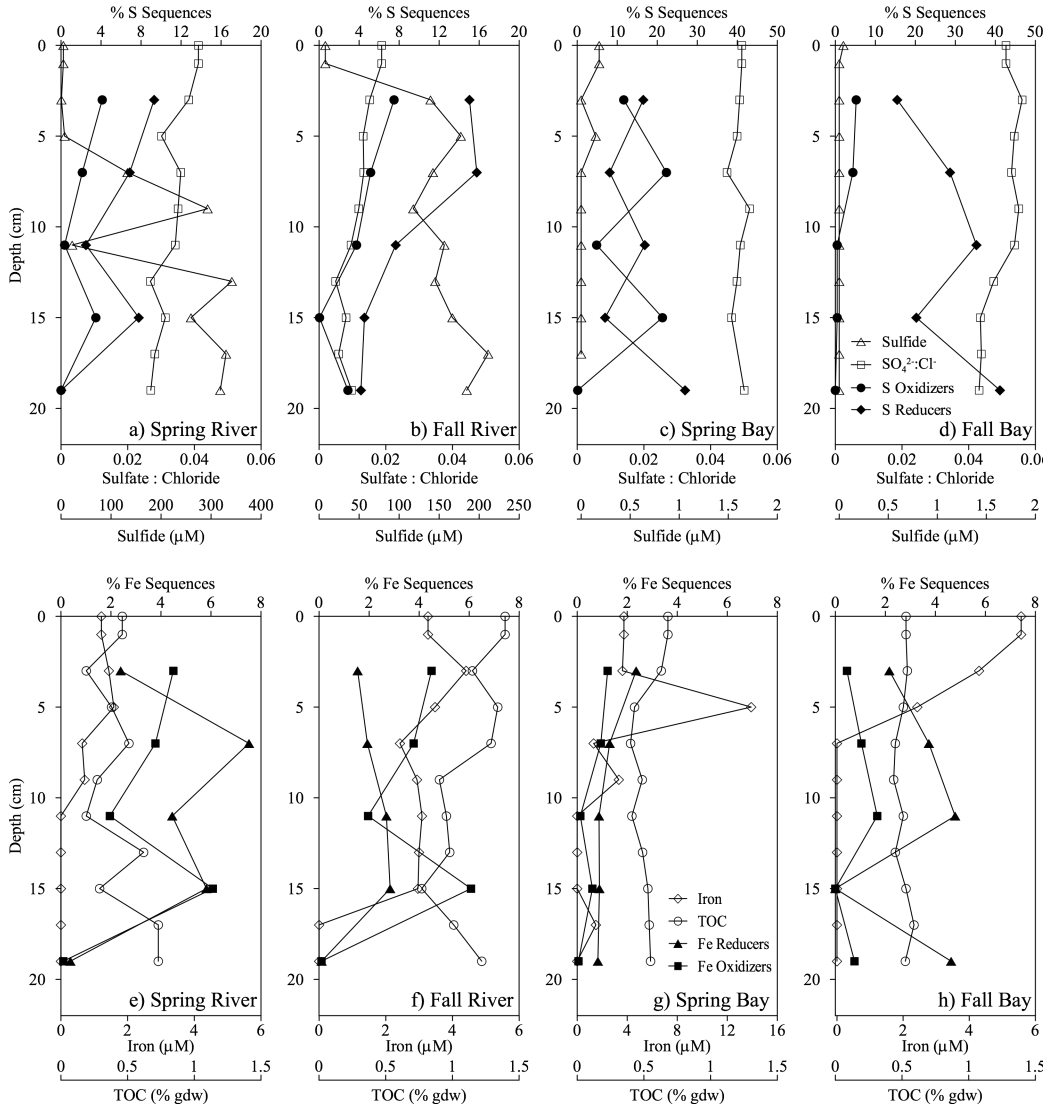

Figure 3.1. Depth profiles of geochemical species and microbial lineages related to sulfur cycling (panels a through d) and iron cycling (panels e through h) in the Nueces River, TX. Note that dissolved sulfide and iron are plotted on different concentration scales due to large observed variation. The functional groups shown represent all lineages detected with the potential for the specific metabolic process as described in the results. SRB = sulfate reducing bacteria: *Desulfobacteraceae*, *Desulfobulbaceae*, *Desulfuromonadaceae* and *Syntrophobacteraceae*; SOB = sulfide oxidizing bacteria: *Ectothiorhodospiraceae*, *Thiotricaceae* and *Chromatiaceae*; FeRB = iron reducing bacteria: *Geobacteraceae*, *Shewanellaceae*, *Campylobacteraceae*, *Pseudomonadaceae*, *Pelobacteraceae*, *Ferrimonadaceae*, and *Desulfuromondaceae*; FeOB = iron oxidizing bacteria: *Nitrospiraceae* and *Rhizobiales*.

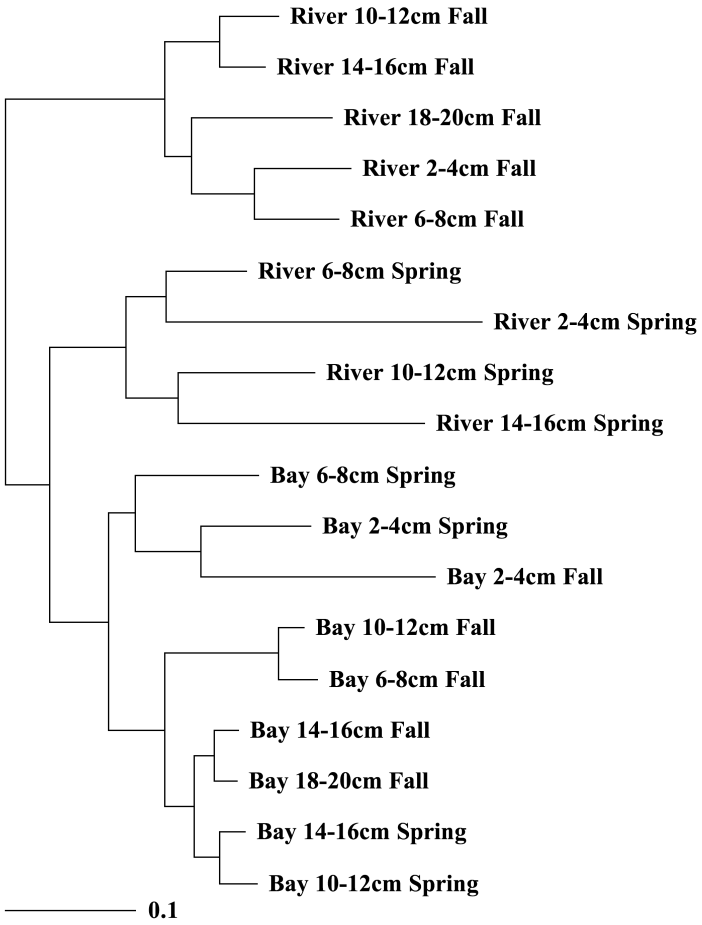

Figure 3.2. Hierarchal cluster analysis using geochemical characteristics of each sample. This included SO_4^{2-}:Cl^-, ΣH_2S, Fe, sulfate reduction rates, TOC, TC, grain size and porosity. A pairwise comparison using these geochemical parameters produced a similarity matrix. A dendrogram was constructed using a neighbor-joining algorithm. Scale bar indicates 10% difference.

The average SRR in the river was higher during the spring (62.0 mmol m^{-2} d^{-1}, 12-hr incubation) than during the fall (25.8 mmol m^{-2} d^{-1}, 12-hr incubation). In contrast, the average SRR in the bay location was higher during the fall (50.0 mmol m^{-2} d^{-1}, 12-hr incubation) than during the spring (26.6 mmol m^{-2} d^{-1}, 12-hr incubation). The highest

Table 3.1. Sulfate reduction rates (SRR) of the Nueces River and Nueces Bay during the spring and fall

		SRR (mmol m^{-2} d^{-1})			
Location	**Sample Depth**	**Spring**		**Fall**	
	(cm)	**6 hours**	**12 hours**	**6 hours**	**12 hours**
Nueces Bay	2-4	32.9	28.5	51.5	94.9
	6-8	84.6	50.1	47.6	59.3
	10-12	16.8	20.2	49.2	42.7
	14-16	18.8	7.5	21.4	23.9
	18-20			18.4	29.1
Nueces River	2-4	196.5	123.8	33.8	30.9
	6-8	112.4	38.4	19.1	23.0
	10-12	37.5	69.5	9.2	8.5
	14-16	5.7	16.3	12.5	20.2
	18-20			22.3	46.2

and lowest rates were observed in the river location during the spring at 2-4 cm depth (196.5 mmol m^{-2} d^{-1}, 6-hr incubation) and 14-16 cm depth (5.7 mmol m^{-2} d^{-1}, 12-hr incubation). The SRR showed a significant correlation ($p < 0.05$) to SO_4^{2-}:Cl^- in the river location but showed no correlation in the bay location.

Microbial characterization: A total of 198,467 sequences were produced after pyrosequencing of small subunit (SSU) rRNA transcripts extracted from the river and the bay locations during both sampling periods. Data presented herein were interpreted with the understanding and minimization of known biases associated with nucleic acid extractions, PCR amplification and sequence analysis. The average number of sequences per sediment depth was 9,923. Sequences were clustered into operational taxonomic units (OTU) based on a 95% sequence similarity, corresponding to a genus level classification. The average number of OTUs per sediment depth was 1,240, ranging from 128 OTUs in the fall bay 14-16 cm sample to 4,453 OTUs in fall bay 2-4 cm sample. Predicted total OTU, as calculated by the Chao1 estimator, suggested an upper range of 8,027 (7,658 – 8,439 at 95% CI) in the sample fall bay 2-4 cm. In general, sequences were evenly distributed within each OTU as indicated by an average evenness measured of $E > 0.83$. However, the evenness decreased with depth down each sediment core overall from 0.89 to 0.73. Rarefaction curves calculated from the OTUs suggested that additional sequences would be required to saturate the sample set, as no individual curve reached a slope of 0 (Figure 3.3). Despite under-saturation of the sample set as indicated by the rarefaction curve and Chao1, it is assumed that the most abundant members of the population, and thus the most geochemically relevant lineages, have been identified and characterized.

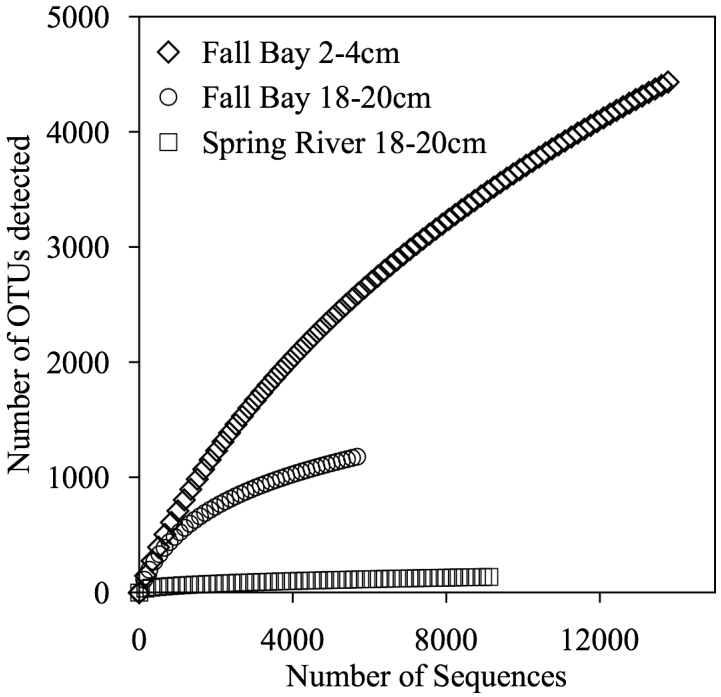

Figure 3.3. Rarefaction curves comparing the diversity of select sediment samples in Nueces Bay, TX. These three samples were chosen as they represent sequence data sets with the highest (Fall Bay 2-4 cm), lowest (Fall Bay 18-20 cm), and median (Spring River 18-20 cm) number of operational taxonomic units (OTU).

A Sorensen similarity index was used to characterize microbial communities based on season or location (Figure 3.4). The number of shared OTUs between any two samples defined similarity between communities. OTUs represented a classification at the genus level. The primary clade bifurcation separated samples by site. Secondary clades separated the river samples into spring and fall seasons, but the bay sample dates showed no further separation.

Proteobacteria phylogenetics: The metabolically active microbial community was divided among 16 phyla, with the most abundant phylum being *Proteobacteria*, comprising 46% of total classified sequences. Specifically, *Gammaproteobacteria* and *Deltaproteobacteria* were the most abundant classes within this phylum, each comprising an average of 19% of the total classified sequences. *Alphaproteobacteria* and *Betaproteobacteria* represented an average of 3-5% of the total sequences. The families *Rhizobiales*, *Rhizobiales* and *Rhodobacterales* within *Alphaproteobacteria* were detected most frequently; they were observed mainly in the river location. Interestingly, within *Betaproteobacteria*, the family *Burkholderiales* was identified in the bottom two depths of the river location during the spring at greater than 9% of the total sequences. These microorganisms are non-fermentative, aerobic, and have the potential to reduce nitrate to nitrite (Wen et al. 1999). *Epsilonproteobacteria* and *Zetaproteobacteria* were also represented at less than 2% of total sequences in any sample. *Gammaproteobacteria* decreased in abundance with depth at each location from an overall average of 33.3% at the top of the sediment core to 4.7% of total sequences at the deepest depth, whereas

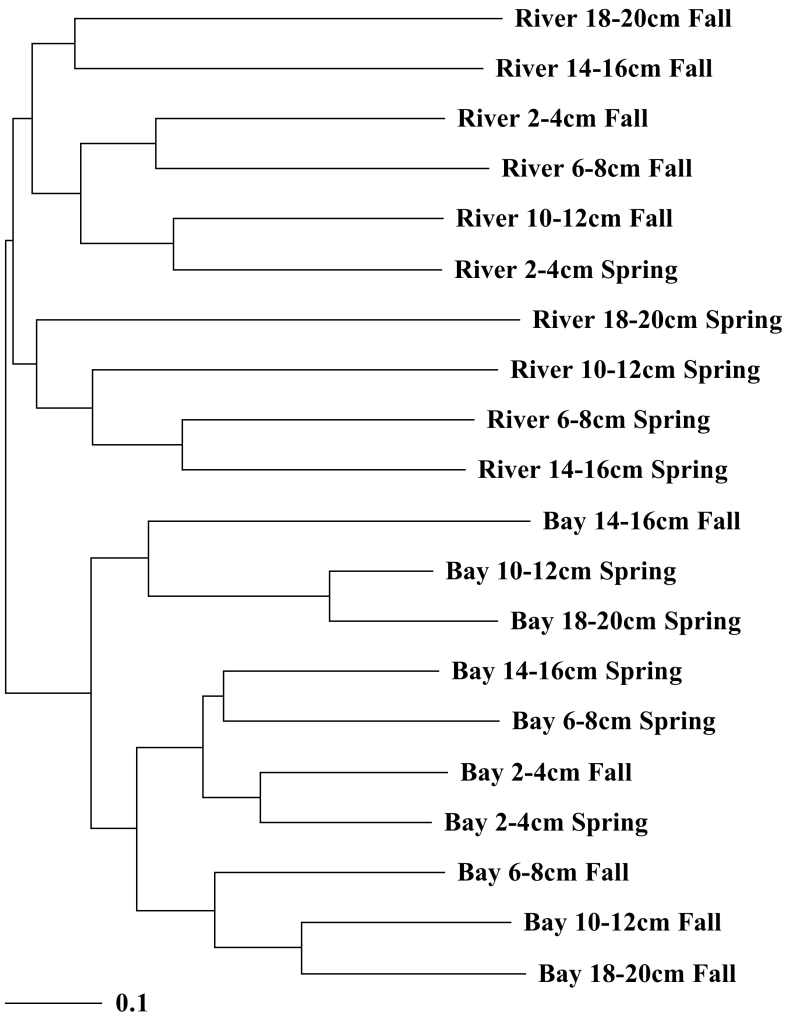

Figure 3.4. Phylogenetic similarity among sample locations and seasons in the Nueces Estuary. Dendrogram was created from Sorensen's diversity index. Scale bar indicates 10% community difference.

Deltaproteobacteria increased from 17.7% in the sediment surface to 23.0% at depth (Appendix A). The sequences related to *Gammaproteobacteria* were subdivided into 15 orders, including *Alteromonadales*, *Chromatiales*, *Methylococcales*, *Pseudomonadales*, and *Thiotrichales*. These five lineages were detected at all depths and at abundances of greater than 1% of the classified sequences. *Chromotiales*, more specifically the sulfur oxidizing families *Ectothiorhodospiracea* and *Chromatiaceae*, were observed more frequently in the upper sediment column at greater than 1% of total sequences. These families were also observed more often during the spring sampling period. *Pseudomonadaceae*, the most abundant family within *Pseudomonadales*, was observed in greater abundance (> 10% total classified sequences) during the fall sampling period and was highest at the surface in each sediment core. *Thiotricaceae* within the order *Thiotrichales* is also known to be capable of sulfur oxidation and was identified in all sediment cores with the most abundance during the spring in the bay location.

Members of the *Deltaproteobacteria* are commonly identified with the potential for sulfate reduction. This class was divided among 7 orders: *Bdellovibrionales*, *Desulfobacterales*, *Desulfovibrionales*, *Desulfurellales*, *Desulfuromonadales*, *Myxococcales*, and *Syntrophobacterales*. The most abundant (greater than 1% of total sequences) of these orders were *Desulfobacterales*, *Desulfuromonadales*, *Myxococcales*, and *Syntrophobacterales*. *Desulfobacterales*-related sequences represented an overall average of 14.4% of the classified sequences. The greatest frequency was observed during the fall sampling period (18.1%) and in the bay location (21.2%). *Desulfuromonadales* constituted as much as 7.6% of the classified sequences with an

average 2.8% of total sequences. This order was identified more frequently in the upper 10 cm of sediment at each site than in the deeper sediment. *Myxococcales* was observed in greater abundance in the upper sediment column of the bay location (1-2.3%). *Syntrophobacterales* was identified more frequently in the river location than the bay and in similar abundance in both seasons.

Non-*Proteobacteria* phylogenetics: *Acidobacteria*, *Bacteroidetes*, *Chloroflexi*, *Cyanobacteria*, *Firmicutes*, and *Planctomycetes* were the most abundant phyla after the *Proteobacteria*. The phylum *Acidobacteria*, more specifically the family *Acidobacteriaceae*, was observed in the top half of the sediment column at > 1% of the total sequences in each location and during both seasons. Sequences with high similarity to *Bacteroidetes* and the sub-family *Cytophagaceae* comprised as much as 5.1% of classified sequences in the fall river sediment with an overall average of 1.7% among all samples collected. As expected, trends were observed with the photosynthetic phylum *Cyanobacteria*-related sequences as they were detected most frequently (> 1% of the classified sequences) in the surface sediment in each of the cores. *Actinobacteria,* specifically the iron oxidizing family *Acidimicrobiaceae*, represented an average of 1.4% of the classified sequences and was detected in the river during the spring below 10 cm depth. Phylum *Firmicutes* was detected in all depths sampled ranging from 0.5% in the river sediment during the fall to 55.6% in the deepest sample within the bay location during the spring. The genus *Eubacterium*, within the phylum *Firmicutes*, was

identified as the most prevalent and abundant. This genus has the potential to contribute to fermentative processes.

Family lineages with potential functions related to sulfur or iron cycling have been combined in this study in order to identify trends (Figure 3.1). SOB families included *Ectothiorhodospiraceae*, *Thiotricaceae* and *Chromatiaceae*. Lineages that have been attributed to sulfate reducing bacteria (SRB) in marine systems included *Desulfobacteraceae*, *Desulfobulbaceae*, *Desulfuromonadaceae* and *Syntrophobacteraceae* (Nealson 1997; Pereira et al. 2007). Iron oxidizing bacteria (FeOB) included *Nitrospiraceae* and *Rhizobiales*. Lineages determined as iron reducing bacteria (FeRB) included *Geobacteraceae*, *Shewanellaceae*, *Campylobacteraceae*, *Pseudomonadaceae*, *Pelobacteraceae*, and *Ferrimonadaceae*.

Quantification of *dsrA* transcript: The abundance of the *dsrA* transcript was determined from the same sediment depths selected for ^{35}S quantification. Transcripts were calculated per gram of sediment to normalize variations in extraction volume. River sediment samples had on average an order of magnitude more *dsrA* transcripts per gram sediment compared to the bay samples with the spring river sediments having the highest overall abundance (Figure 3.5). In general, transcript abundance reduced with depth, with the fall river sample being an exception. Of note, all samples had a quantifiable number of transcripts present.

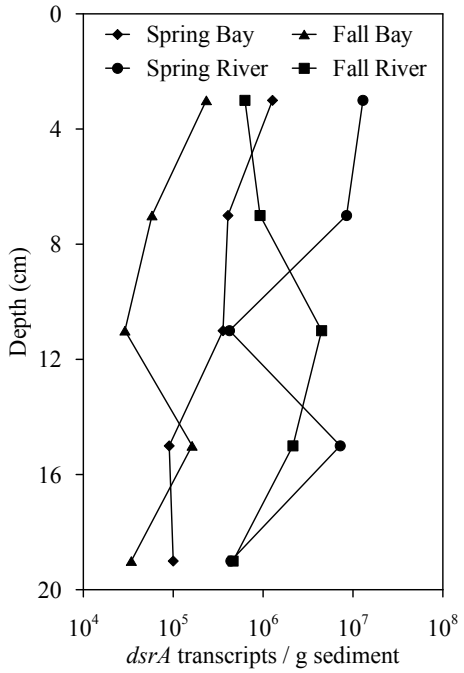

Figure 3.5. Quantitative PCR analysis of the *dsrA* transcript. Reverse transcribed cDNA amplicons of the *dsrA* gene transcript were quantified using real time PCR. Amplicons were compared to standards amplified simultaneously.

Discussion

Nueces River and Bay sediments represent two distinct geochemical and geotechnical areas within the Nueces estuary. The concentration of TOC (and TC) in the river was approximately 200% greater than in the bay. Sediment type (e.g., grain size and porosity) has been previously correlated to TOC in estuarine environments where sands with low pore volume contained < 0.6% dw TOC and muddy sand contained 1.5-1.6% dw TOC (Koster and Meyer-Reil 2001). Consistent with this, the porosity and grain size variation at each location correlated significantly ($p < 0.05$) to the amount of

TOC measured. The bay location sediments lacked the high levels of TOC common to biologically productive muds (Koster and Meyer-Reil 2001) whereas the river sediments would be classified as having the essential elements for biological productivity. However, other factors including composition of the microbial community and the availability of terminal electron acceptors also have a significant impact on the sediment environment.

Sulfate reduction rates: The Nueces River and Bay had high sulfate reduction rates (SRR) relative to those of coastal sandy sediments (Canfield 1991) and to other estuarine environments (Skyring 1987). Rates of similar magnitude to the current study have been observed in salt marshes that are high in organic matter (Howarth and Merkel 1984), microbial mats (Visscher et al. 1992), and comparable to those measured in the muddy subtidal sediments of Tomales Bay, California (30 mmol m^{-2} d^{-1}) (Chambers et al. 1994). The highest rates in this study were measured in near-surface sediments, which have been observed in previous studies as well (Chambers et al. 1994). Jorgensen (1978) noted that the top few centimeters of sediment was where the largest gradients in bacterial activity are located. Additionally, the fine-grained muddy sediments of the river location had rates exceeding those in the sandy bay location, which is consistent with findings in other locations (Canfield 1991; Chambers et al. 1994; Howarth and Merkel 1984). Overall, rate measurements in this study were consistent with other geochemical studies, providing a base for the molecular comparisons discussed below.

The rates found in this study during the spring were highest over the 6-hour incubation period, and the fall SRR was highest over the 12-hour incubation at both locations. This indicates that the microbial community utilized the labeled sulfate that was injected during the spring sampling period more quickly than during the fall. The optimal incubation time can depend on the SRR and can vary from one hour to one day. Many studies fail to report this discrepancy or adjust the incubation times to account for the variation. Additionally, the significant correlation ($p < 0.05$) of SRR to SO_4^{2-}:Cl^- observed in the predominantly freshwater river location indicates that the SRB community was likely lacking in its terminal electron acceptor (i.e., sulfate). The addition of sulfate caused an increase in their activity and the SRR was higher than predicted based on sulfate concentrations alone. The overall maximum SRR in this study was measured in the freshwater river environment indicating that the resident sulfate-reducing bacteria are able to survive with low sulfate concentrations until sulfate became available. This has been observed in previous studies of eutrophic lakes (Ingvorsen et al. 1981) and sediments in the freshwater part of an estuary (Trimmer et al. 1997).

It was interesting to note that SRR measured in this study showed no correlation with the abundance of SRB, overall. Pallud and Van Cappellan (2006) found that the size of the sulfate-reducing microbial community in the Scheldt estuary also did not correlate with potential sulfate reduction rates. In this current study, rate measurements were supported by in situ *dsrA* transcript abundance as determined by quantitative reverse transcription PCR analysis. This indicates that the abundance alone may not be

the driving factor of SRR, rather the activity of the key gene in dissimilatory reduction (*dsrA*/*B*) is likely the greater influence.

The SRR in the bay was negatively correlated ($p < 0.05$) to TOC, indicating that SRR increased as carbon was utilized. The bay sediments had lower concentrations of organic carbon than the river location, but the concentration of dissolved sulfate was greater in the bay. The Nueces River had higher rates, on average, compared to the Nueces Bay location and consistent with these findings, the TOC and TC was greater in the river than in the bay. In coastal and open ocean sediments, sulfate reduction rates are primarily controlled by the availability of degradable organic matter and secondarily by the sedimentation rate as it impacts the total carbon flux (Canfield 1991; Holmkvist et al. 2011). Electron acceptors are typically not limiting in this environment because of the high concentration of sulfate in marine waters. The availability of organic carbon has been shown in previous studies to be the primary limiting factor for sulfate reduction and SRB (Pallud and Van Cappellen 2006; Rudd et al. 1986). These results indicated successful site selection, providing a range of carbon concentrations and SRRs to characterize the microbial community using molecular techniques.

Fall river sediment: A classic sulfate reduction profile was observed in the river sediment during the fall sampling period in both the geochemical and molecular analyses. The geochemical profile in this location displayed sulfate loss with depth and a related sulfide accumulation over the 20 cm sediment column. In addition, lineages associated with sulfate reduction decreased as their primary terminal electron acceptor

(i.e., sulfate) decreased and were in greater abundance than the SOB. The lineages known to oxidize sulfide decreased with depth corresponding to a decrease in SRB as well. This microbial community and associated biogeochemical profiles have been observed in estuaries (Morse and Rowe 1999; Weston et al. 2006), salt marshes (Howarth and Merkel 1984; Roychoudhury 2007), and freshwater environments (Cook and Kelly 1992; Ingvorsen et al. 1981) and would not be disputed as a description of a sulfate-reducing environment from either the geochemical or microbiological viewpoint.

Spring bay sediment: In contrast to the fall river location, the depth profile for the spring sampling period in the bay location showed no significant loss of sulfate and very little sulfide accumulation across the 20 cm sediment column. However, SRR data indicated that sulfate reduction was occurring at every depth interval. The population abundance of SRB in the spring bay core was largely equal to the fall river core, but the SOB abundance in the spring bay samples was greater (approximately 25%) than in the fall river samples. The SRB and SOB abundance were equal to each other on average in the spring bay samples, but the abundances were out of phase throughout the length of the core. The lack of sulfide accumulation and decline in sulfate concentration is likely due to the cycling of geochemical products between the SRB and SOB within the sediment. During this process, a microbial population may utilize the metabolic products from another population in the reverse redox reaction, masking the initial microbial process and establishing a geochemically “cryptic” microbial cycle. The geochemical signature

of sulfate reduction in the spring bay sediment is thus camouflaged because SOB reoxidized the sulfide.

Co-localization of sulfur transformation processes has been previously described in a study of waters off the Chilean coast. Canfield et al. (2010) describe sulfide oxidizing and sulfate reducing taxa based only on bacterial DNA and bulk sulfate reduction rates coupled with nitrate reduction. The SOB community masked the chemical expression of the putative SRB. Although the findings described an important phenomenon, a drawback of the described research was the reliance on community DNA characterization, which has been shown to represent members of the population that are potentially non-relevant to the geochemical signatures observed.

It is important to note that although the terminal electron acceptors are exchanged in this process, the electron donors are variable for each of the microbes that comprise the SOB and SRB communities and therefore is not a perpetual exchange loop. Key to this predicted coupling of SRB and SOB is the ability of SOB to oxidize sulfide under anoxic conditions. *Beggiatoa* and *Thiothrix* are the dominant members (55% on average) of the SOB community within the sediments of the fall river core. These organisms, members of the order *Thiotrichales* (*Gammaproteobacteria*), are known for their ability to couple sulfide oxidation to nitrate reduction in an anoxic environment (Schulz et al. 1999; Teske and Nelson). Microorganisms that oxidize sulfide or elemental sulfur to sulfate (including *Acidithiobacillaceae* and *Ectothiorhodospiraceae*, found in this study) commonly thrive in a microaerophilic environment near the sediment-water interface in order to utilize molecular oxygen as the electron acceptor

while not losing sulfide to chemical oxidation reactions (Hallberg et al. 2011; Orcutt et al. 2011). Therefore, SOB activity should be considered when analyzing SRR and SRB activity in environmental systems.

Fall bay sediment: Within the sediment depth profile of the fall bay location, little to no sulfide accumulation and a slight loss of sulfate was observed. An initial assessment of the geochemical profile indicated that no sulfate reduction was occurring, however, each sample analyzed had quantifiable sulfate reduction. A comparatively high population abundance of SRB was noted in this sediment that increased from 15% to 41% of total classified sequences, and a correspondingly low abundance of SOB was observed that decreased from 5% to 0% of total sequences. The SRR in this sediment did not correlate significantly with the sulfate concentrations or sulfate reducing population abundance.

Interestingly, the SRB population paralleled the same trend and correlated significantly ($p < 0.05$) with FeRB. The TOC showed a high correlation ($p < 0.05$) to both the SRB and FeRB. TOC concentration in this core was likely limiting, as it was relatively low 0.5% gdw compared with that of typical marine mud environments (Pallud and Van Cappellen 2006). This suggests that both of these communities were competing for a common electron donor (i.e., TOC) or, more likely, codependent.

The soluble sulfide products that are produced as a result of SRB metabolism rapidly react with the Fe(II) products from FeRB respiration to form metal sulfides including iron monosulfide (FeS) and pyrite (FeS_2) by the following reactions:

$$9H_2S + 4Fe_2O_3 \rightarrow SO_4^{2-} + 8FeS + 8H_2O + 2H^+ \qquad \text{(Eq. 3.2)}$$

$$FeS + H_2S \rightarrow FeS_2 + H_2 \quad \text{(Eq. 3.3)}$$

The distribution of dissolved sulfide in Nueces Bay during the fall season was a balance between the rate of sulfate reduction and its removal by reaction with iron oxides to form total reducible sulfides (TRS; i.e., pyrite). Previous studies within the Nueces Bay have measured relatively high TRS concentrations (42 – 78 μmol gdw^{-1}) and a high degree of sulfidization (extent to which reactive iron has been transformed to sulfide) of 93% on average (Morse et al. 2007). This indicates that almost all sulfide produced is contributing to the formation of pyrite, which is consistent with the current study that found that dissolved sulfide was not present despite an active SRB population and measureable SRR. The binding of sulfide as different iron sulfides sets up a geochemical cryptic cycle, not unlike that observed in the spring bay sediment with the SRB and SOB in consortium. The products were again masked in the fall bay sediment, but through solid phase sequestration, which has also been described in several other coastal and estuarine systems (Canfield 1991; Holmkvist et al. 2011; Morse et al. 2007).

Despite initial appearances that sulfate reduction was not occurring in the last two scenarios, this study showed the importance of simultaneously analyzing the active microbial community and multiple geochemical reservoirs to determine the extent of sulfate reduction within sediments.

CHAPTER IV

LINKING MOLECULAR MICROBIAL ECOLOGY TO GEOCHEMISTRY IN A COASTAL HYPOXIC ZONE

Overview

Multiple environmental mechanisms have been proposed to control bottom water hypoxia (< 2 mg L^{-1} or 63 μmol L^{-1} O_2) in the northern Gulf of Mexico Louisiana shelf. Near-bottom hypoxia has been attributed to a direct consumption of oxygen through benthic microbial respiration and a secondary chemical reaction between oxygen and reduced metabolites (i.e. ferrous iron and total sulfide) from these populations. No studies to date have examined the metabolically active microbial community structure in conjunction with the geochemical profile in these sediments. Temporal and spatial differences in dissolved and solid phase geochemistry were investigated in the upper 20 cm of the sediment column. Pyrosequencing of reverse transcribed small subunit (SSU) ribosomal ribonucleic acid (rRNA) was used to determine population distribution. Results indicated that populations shallower than 10 cm below surface were temporally variable yet uniform between sites, while below this depth, populations were more site specific. This suggests a shallow interaction potential between the water column and the benthic microbial population. The presence of dissolved reduced iron in the upper sediment column was indicative of low oxygen concentration, yet sulfide was at or below detection limits. Sulfate and iron reducing and oxidizing populations were metabolically active at similar depths suggesting potential recycling of products. General

metabolic activity may be limited by low carbon concentrations, reducing the potential for microbial respiration.

Introduction

A balance between oxygen supplied from physical processes and biologic production, and oxygen depletion by chemical and biological consumption governs the concentration of dissolved oxygen within bodies of water. In the northern Gulf of Mexico, this balance is disrupted seasonally resulting in hypoxic water formation (oxygen concentration < 2 mg L^{-1} or 63 μmol L^{-1} O_2) between the inner and mid-continental shelf, beginning at the Mississippi River delta and extending westward to the upper Texas coast. The overall area varies in size, but can average over 15,600 km^2; making this the second-largest hypoxic zone in the world (Rabalais et al. 2007). The physical characteristics contributing to hypoxia including shallow water depths, weak summer winds, and thermal and density stratification from both the Mississippi and Atchafalaya rivers have been well characterized and modeled (Dagg and Breed 2003; Green et al. 2006; Rowe and Chapman 2002). The majority of the hypoxic water in this region is below the pycnocline as a result of limited mixing between surface oxygen rich top water and oxygen poor bottom water. The chemical and biological mechanisms for reducing oxygen concentrations below the pycnocline have not been well described. Understanding these mechanisms will provide a better assessment of the ecological impact of hypoxia (Leming and Stuntz 1984) and enhance the capacity of predictive models used for mitigation-based policy development.

Biogeochemical factors attributed to bottom water hypoxia focus on high nutrient loading promoting increased algal biomass production that ultimately contributes to increased pelagic and benthic respiration and carbon remineralization rates. To understand this potential benthic mechanism contributing to hypoxia, the sediment geochemistry and microbial ecology must be characterized. In coastal sediments, sulfate is the second most abundant anion in seawater and therefore the microbial reduction of sulfate to sulfide accounts for the majority of anaerobic carbon mineralization (Jorgensen 1977; 1982). Seasonal hypoxia typically produces sulfide in the sediments, which threatens aquatic organisms (Diaz and Rosenberg 1995). The sulfide produced also enhances the cycle of PO_4^{3-} release into the water column through the reduction of iron hydroxides, producing more organic mater to fuel hypoxia (Ma et al. 2006; Sutula et al. 2004). In order to determine the mechanisms controlling hypoxia, it is important to understand the production and fate of sulfide within the environment through biological and chemical reactions.

In hypoxic areas the biological production of sulfide has been linked to the chemical consumption of oxygen and assumed to be a proxy for overall metabolic activity in sediments (Luther et al. 2011; Reese et al. 2008). Previous studies in the Gulf of Mexico hypoxic zone have detected sulfide in sediments near the mouth of the Mississippi River at a sediment depth of 60 cm (Morse and Rowe 1999). While these results may be important for understanding hypoxia formation near the Mississippi River, sediments west of the Morse and Rowe (1999) sample locations had vastly different geochemical profiles (Lin and Morse 1991), yet were located well within the

hypoxic zone. The benthic mechanisms controlling hypoxia in the western region were uncharacterized prior to the current study. A review of the different hypoxic regions in the northern GoM can be found in (Dagg and Breed 2003; Green et al. 2006; Rowe and Chapman 2002).

Porewater and solid-phase geochemical analyses alone provides a snapshot of the benthic environment with no information on active biological processes, including the accumulation or depletion of specific compounds. Active biological or chemical consumption of sulfide may mask geochemical evidence for sulfate reduction. To enhance and possibly further explain the observed geochemistry, the metabolically active fraction of the microbial community must be characterized. Molecular characterization of the active community requires ribonucleic acid (RNA)-based analysis. Deoxyribonucleic acid (DNA) targets are detectable in dead and quiescent cells (Mills et al. 2004; Nogales et al. 1999) whereas ribosomal RNA (rRNA) has a short residence time within a cell when the cell is either inactive or dead. In addition, rRNA increases in concentration when metabolic activity increases. Changes in metabolic activity and rRNA concentration are the result of shifts in geochemical conditions. Therefore, determining the microbial populations that are metabolically active by characterizing rRNA can enhance the understanding of seasonal and spatial geochemistry.

The objective of this study was to determine the role of sediment microbial ecology as a mechanism contributing to bottom water hypoxia in the western GoM hypoxia region. Molecular techniques were used to enhance classic geochemical analysis

to provide a description of the benthic environment. We hypothesize that an active microbial community within the sediment contributed to water column hypoxia in the western region through respiration and the production of oxygen-depleting compounds (e.g., sulfide). Two sites were examined prior to and during hypoxic conditions to provide spatial and temporal analyses of the benthic environment. Fine scale sampling of individual sediment cores and high throughput nucleic acid extraction techniques combined with 454 FLX sequencing provided a robust understanding of the benthic microbial community. The resulting data conclude that benthic microbial populations have a limited contribution to water column hypoxia. Conclusions made herein will contribute to the development of future models describing mechanisms controlling hypoxia in this region.

Materials and methods

Sample collection: Sediment samples were collected from two locations (BC1: 28.8806^{o}N, 91.7373^{o}W and 8C: 28.9976^{o}N, 92.0051^{o}W) in the northern Gulf of Mexico (Figure 4.1) in April and July 2008 during Mechanisms Controlling Hypoxia (MCH) cruises 11 and 12, respectively. Both sites were located along the 20 m isobath. Sample dates corresponded to pre-hypoxic (April) and hypoxic (July) conditions in this region. Water column parameters including dissolved oxygen, PAR, and fluorescence were collected every hour for 24 hours via CTD (Sea-Bird Electronics, Bellevue, Washington). Sediment was collected via box core. Subcores were collected by hand using 7 cm diameter polystyrene core liners to a depth exceeding 20 cm. Lithology and

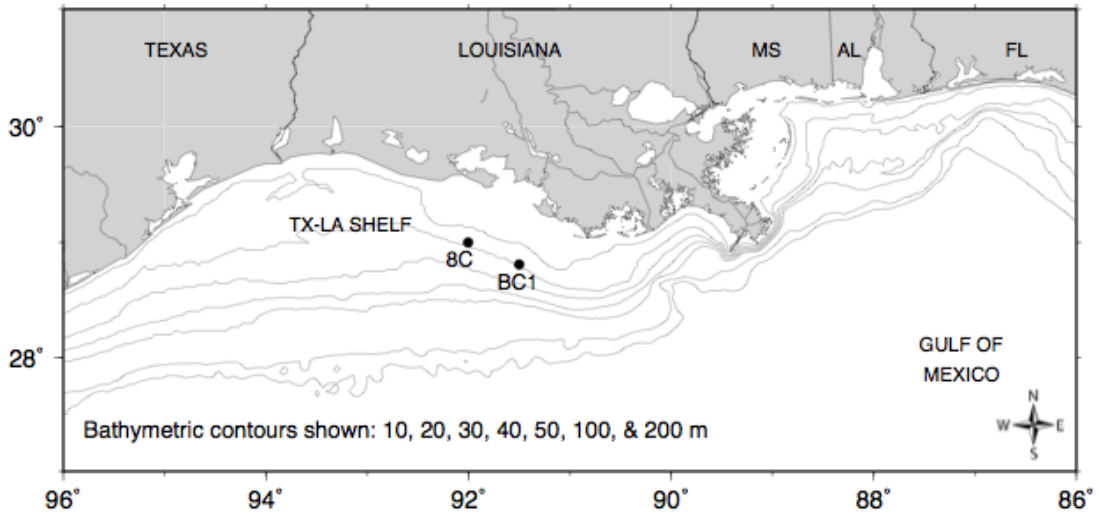

Figure 4.1. Location of the two sites (BC1: 28.8806°N, 91.7373°W and 8C: 28.9976°N, 92.0051°W) on the Texas-Louisiana shelf sampled during this study.

clay thickness prohibited some cores from reaching this target depth. Cores were sectioned in 2 cm intervals for both geochemistry and molecular analysis from the sediment surface (0 cm) to a max depth of 20 cm. For molecular analysis, three sediment cores were simultaneously sectioned with corresponding depth sections and homogenized. Three 2 g subsamples from each depth were frozen in liquid nitrogen and transferred to -80°C upon returning to Texas A&M University. Cores were collected in duplicate for geochemical analysis and immediately frozen intact at -20°C and transported to Texas A&M University on dry ice. Cores were sectioned (2 cm resolution) within an anaerobic chamber. Porewater was extracted via squeezing (Reeburgh 1967) and collected in gastight syringes. Squeezed sediments were stored at

-20^{o}C for acid volatile sulfide (AVS), total reducible sulfide (TRS) analysis, total carbon (TC) and total organic carbon (TOC).

Sediment and porewater geochemistry: An aliquot of porewater was immediately processed for dissolved iron and total sulfide using colorimetric methods (Reese et al. 2011a; Viollier et al. 2000). Dissolved Fe(II) was determined using the ferrozine method in the presence of an ammonium acetate buffer on a Shimadzu UV-1201 spectrophotometer (Shimadzu Scientific Instruments, Columbia, Maryland) at 562 nm wavelength (Viollier et al. 2000). Total dissolved sulfide ($\Sigma H_2S_{aq} = H_2S_{aq} + HS^- + S^{2-}$) was determined using a modified Cline (1969) method described in Reese et al. (2011a) on a Shimadzu UV-1201 and 667 nm wavelength. Additional porewater was filtered using 0.2 μm syringe filter and immediately frozen at -20^{o}C for later sulfate and chloride analysis. Dissolved sulfate and chloride was determined using precipitate gravimetric analysis with the use of $BaCl_2$ and $AgNO_3^-$, respectively (APHA 1998). Acid volatile sulfides (AVS) were analyzed by the cold 6N HCl + $SnCl_2$ method of Cornwell and Morse (1987) and total reducible sulfides (TRS) were analyzed by the hot $CrCl_2$ method of Canfield et al. (1986). AVS and TRS were determined using 5-6 g per 2 cm section of porewater-extracted sediment. TRS was extracted by distillation with reduced chromium and 12N HCl. The volatilized sulfide was trapped in 10 ml of sulfide antioxidant buffer (SAOB) (APHA 1998) and ultra-high purity N_2 carrier gas. The antioxidant buffer protected the sulfide from oxidation and the high pH converts all of the H_2S_{aq} and HS^-

into non-volatile S^{2-}. AVS was extracted using cold 6N HCl and 2% $SnCl_2$ and trapping the volatilized sulfide as described above for the TRS method.

The silt and clay fraction (wt% <63 mm) was measured by wet sieving. Porosity was determined by drying the sediment in an ~80°C oven and calculating the ratio of percent solid to percent water. TOC and total carbon TC was determined on unacidified and acidified oven-dried sediment, respectively, through coulometry using a UIC Model CM-5012 CO_2 coulometer attached to a modified version of the CM-5120 combustion furnace (UIC Inc, Joliet, IL) (Lyle et al. 2000).

Nucleic acid extraction and amplification: Total nucleic acids were extracted from all 36 sediment samples from MCH 11 and 12 using a method modified by Mills et al. (2008). Total nucleic acids were extracted from 0.5-0.6 g (wet weight) from each 2 cm sediment section. DNase was added to the nucleic acid extracts to remove deoxyribonucleic acid (DNA) prior to reverse amplification of ribonucleic acid (RNA) targets. Negative controls during polymerase chain reaction (PCR) confirmed no contaminating nucleic acids were present during the extraction process and no residual DNA remained in RNA extracts (data not shown). Small subunit (SSU) ribosomal RNA (rRNA) was reverse transcribed to complementary DNA (cDNA) using moloney murine leukemia virus (MMLV) reverse transcriptase (Promega, Madison, WI) during a 30 min incubation at 37^{o}C with reverse primer 518R (5'-CGT ATT ACC GCG GCT GCT GG-3') (Nogales et al. 1999). Aliquots of reverse transcribed SSU rRNA cDNA were screened through PCR-amplification using NEB Taq DNA Polymerase (New England Biolabs, Ipswich,

MA) and the *Bacteria* domain-specific SSU rRNA gene primers 27F (5'-AGR GTT TGA TCM TGG CTC AG-3') (Giovannoni et al. 1991) and 518R. Thermocycling was performed on an Applied Biosystems Veriti 96 well (ABI Inc., Foster City, CA) using the following protocol: initial incubation at 95^{o}C for 5 min, followed by 35 cycles of 95^{o}C for 1 min, 50^{o}C for 1 min and 72^{o}C for 1 min, with a final extension step at 72^{o}C for 10 min. Amplicons were visualized and size verified with gel electrophoresis using a 0.7% agarose gel (data not shown).

Pyrosequencing: Primers 28F (5'-GAG TTT GAT CNT GGC TCA G-3') and 519R (5'-GTN TTA CNG CGG CKG CTG-3') produced amplicons from cDNA that spanned three hyper-variable regions (V1 through V3) (Handl et al. 2011). PCR amplicons from each of the 36 sediment samples were sequenced at the Research and Testing Laboratory in (Lubbock, TX). Amplicons from each sample were first labeled with a 10 base unique multiplex identifier (MID) sequence to allow all samples to be sequenced on a single run of a Roche 454 FLX (454 Life Sciences, Branford, CT). Downstream sequence analysis parsed the individual sequences into sample specific libraries. Resulting libraries were screened for reads less than 200 bases, reads lacking a Roche-designed four base key sequence, and non-bacterial reads lacking specific 28F primer recognition site. All sequences passing quality control were deposited to the National Center for Biotechnology Information (NCBI) database using Sequence Read Archive (SRA).

Phylogenetic and statistical analysis: All sequences were taxonomically classified using the Ribosomal Database Project (RDP) classifier database (RDP MultiClassifier, Lansing, MI) (Wang et al. 2007). Classifications were checked randomly against the Basic Local Alignment Search Tool (BLAST) pipeline through National Center for Biotechnology Information (NCBI) database (accessed September 2010). A 70% confidence interval (CI) was used as a threshold to discern highest taxonomic level designation. Only sequences meeting this threshold at a desired taxonomic level were incorporated into statistical analyses. The average percentage of sequences classifiable above the 70% CI at the phyla level per sample was 77.8%, with the maximum percentage 91.2% in sample July 8C 6-8 cm (data not shown). Sequences were clustered into operational taxonomic units (OTU) using RDP and a 95% sequence similarity cutoff corresponding to a genus level classification. All statistical analyses were performed in Microsoft Excel using Pop Tools which included Singular Value Decomposition (SVD), Principal Component Analysis (PCA), and T-test where noted.

Results

Site description: Locations used in this study experience seasonal hypoxia from approximately mid April until mid September (Bianchi et al. 2010; Rabalais and Turner 2001). During this study, the water column dissolved oxygen (DO) concentrations at both sites indicated no hypoxia during the April sampling period. The DO was higher in the surface water (4.74 ml L^{-1} at 8C and 5.27 ml L^{-1} at BC1) than the bottom water (3.23 ml L^{-1} at 8C and 3.58 ml L^{-1} at BC1) at both locations. Both locations showed very slight

inverse thermal stratification in April with a difference in temperature (ΔT) between the surface and the bottom water of -2.07^{o}C at site 8C and -2.06^{o}C at site BC1. Both locations also displayed a slight pycnocline with a surface salinity of 28.45 practical salinity units (PSU) at 8C and 25.50 PSU at BC1 and bottom water salinities of 35.80 PSU and 36.10 PSU, respectively. Benthic light levels (as photosynthetically available radiation, or PAR) were never less than 1% of the surface PAR indicating the presence of limited light near the sediment.

Although a small part of the CTD data from site BC1 was compromised during the July sampling, the water column parameters at this location appeared to be largely similar to site 8C. Subsequent annual cruises in 2009 and 2010 support this observation (data not shown). Water column thermal stratification was slightly stronger in the July sampling period with a daytime ΔT of 5.09^{o}C from the surface to the bottom at site 8C. The same trend in salinity was seen in July as was observed in April with fresher water (24.36 PSU) on the surface and more saline water (35.91 PSU) in the bottom waters. The daytime DO, however, showed the highest concentration in the surface water of 4.48 ml L^{-1}, decreased to a minimum of 0.19 ml L^{-1} in the mid-column at 9 m, increased again at 11 m to 2.02 ml L^{-1}, then gradually decreased to 0.81 ml L^{-1} in the bottom waters. The bottom water DO was always less than 1 ml L^{-1} starting at 14 m during both the day and night at site 8C. This general trend of hypoxia at mid-depth was observed in both locations during both day and night and has been noted in this area on other cruises and dates as well (DiMarco et al. 2010).

Sediment and porewater geochemistry: Initial analysis of the geochemical data from April and July indicated little, if any, seasonal or spatial variation among the sites. Variations with sediment depth were observed using SVD and PCA analyses, which are noted where appropriate. The porosity decreased significantly ($p<0.05$) with depth from 0.86 at the surface to 0.75 at 18-20 cm in April BC1 and from 0.78 at the surface to 0.73 at 12-14 cm in April 8C. The July cores showed similar decreases in porosity with depth. Additionally, Student's t-tests showed that the overall porosity at the eastern location (BC1) was significantly ($p<0.05$) greater than the porosity at the western location (8C). Based on the grain size the sites can be classified as mostly sandy (%<63 μm <25), intermediate (25 < %<63 μm <75), or mostly fine-grained (%<63 μm >75). Overall, the sediments were mostly fine-grained; however, the sediments at site BC1 contained more sandy material than site 8C. The sediment cores from site BC1 contained a mostly sandy layer at the surface (24% <63 μm) and a mostly sandy lens at 12-14 cm (21% <63 μm). No seasonality was observed with porosity or grain size.

Figure 4.2. Depth profiles of geochemical species and microbial lineages related to sulfur cycling (panels a through d) and iron cycling (panels e through h). Data were collected at 2 cm intervals. The functional groups presented represent all lineages detected with the potential for that specific metabolic process as described in the results. SRB = sulfate reducing bacteria: *Desulfobacteraceae*, *Desulfobulbaceae*, *Desulfuromonadaceae* and *Syntrophobacteraceae*; SOB = sulfide oxidizing bacteria: *Ectothiorhodospiraceae*, *Thiotricaceae* and *Chromatiaceae*; FeRB = iron reducing bacteria: *Geobacteraceae*, *Shewanellaceae*, *Campylobacteraceae*, *Pseudomonadaceae*, *Pelobacteraceae*, *Ferrimonadaceae*, and *Desulfuromondaceae*; FeOB = iron oxidizing bacteria: *Nitrospiraceae* and *Rhizobiales*.

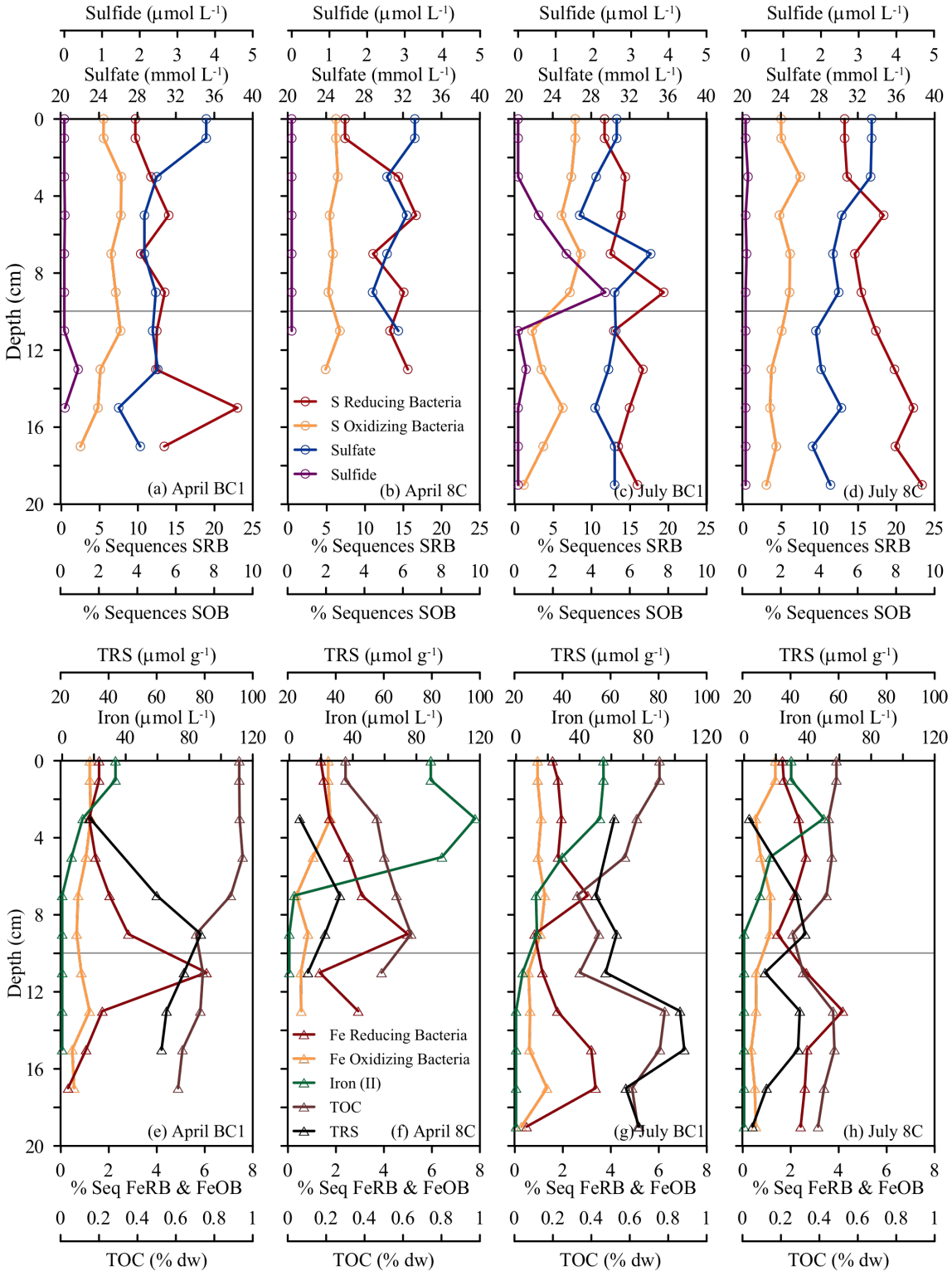
Sulfide (µmol L-1)
Sulfate (mmol L-1)
Depth (cm)
% Sequences SRB
% Sequences SOB
S Reducing Bacteria
S Oxidizing Bacteria
Sulfate
Sulfide
(a) April BC1
(b) April 8C
(c) July BC1
(d) July 8C
TRS (µmol g-1)
Iron (µmol L-1)
% Seq FeRB & FeOB
TOC (% dw)
Fe Reducing Bacteria
Fe Oxidizing Bacteria
Iron (II)
TOC
TRS
(e) April BC1
(f) April 8C
(g) July BC1
(h) July 8C

The overall depth profiles for each site and sample date were similar. Each profile showed few seasonal differences overall and were highly variable with depth (Figure 4.2). Chloride and sulfate concentrations were slightly greater in the surface sediments showed slight but insignificant decrease with depth in each of the sediment cores. Converting chloride and sulfate concentrations to a sulfate to chloride ratio (SO_4^{2-}:Cl^-) normalized the sulfate concentration, which showed an overall decrease with depth as seen through the singular value decomposition ($p<0.05$). The down-core average sulfate and chloride concentrations were consistent with typical marine sediment (30 mmol L^{-1} and 657 mmol L^{-1}, respectively).

The dissolved total sulfide concentration showed accumulation above the method detection limits (1 μmol L^{-1}) during the summer sampling period in samples July BC1 6-8 cm (1.28 μmol L^{-1}) and 8-10 cm (2.31 μmol L^{-1}). Sulfide was not observed in detectable concentrations any of the shallow sediment samples on any sampling date (Figure 4.2a-d).

Dissolved Fe(III) and Fe(II) concentrations showed similar trends of a decrease with depth in each core with concentrations terminating to undetectable at approximately 8-10 cm depth (Figure 4.2e-h). Overall, the Fe(II) concentrations exceeded the Fe(III) concentrations in each sample by as much as 32% to 100% (data not shown). The maximum Fe(II) concentration was seen in April 8C 2-4 cm (116.9 μmol L^{-1}). The site located further east, BC1, contained higher iron concentrations ($p<0.05$) overall during both seasons (Figures 4.2e and 4.2g).

Total carbon (TC) and total organic carbon (TOC) was low on average (< 1.5% dry weight (dw) and < 1% dw, respectively) in all of the sediment cores (Figure 4.2e-h). The distribution of either TC or TOC with depth showed no significant trend with depth. The percent TC (data not shown) was significantly (p<0.05) greater in the spring (1.29% at BC1 and 1.12% at 8C) than in the summer (1.08% at BC1 and 0.95% at 8C). The percent TOC at the eastern site, BC1, (0.79% in April and 0.59% in July) was significantly (p<0.05) greater than the western site, 8C, (0.5% in April and 0.42% in July).

Acid volatile sulfides (AVS) and total reduced sulfur (TRS) are operationally defined measurements to describe the percentage of ΣH_2S_{aq} along with iron monosulfides (FeS) and pyrite (FeS_2), respectively. AVS was low or below the method detection limits in all of the samples (data not shown). Based on SVD analysis, a significant (p<0.05) increase in TRS was observed as Fe(II) began to terminate to below method detection limits (Figure 4.2e-h). The TRS concentrations in April were on average 12.8% and 7.9% lower at sites BC1 and 8C, respectively, than they were in July.

Microbial phylogenetic characterization: Pyrosequencing of small subunit (SSU) rRNA transcripts from 36 individual sediment depths collected during MCH 11 and MCH 12 yielded 168,760 total sequences after quality control analysis. Data presented herein are interpreted with the understanding and minimization of known biases associated with nucleic acid extractions, PCR-based gene amplification and sequence-based analysis. The average number of sequences per sediment depth was 4,688, ranging from 2,891

sequences in April BC1 12-14 cm to 7,131 sequences in July 8C 10-12 cm. Sequences were clustered into 19,745 operational taxonomic units (OTU) based upon a 95% sequence similarity, corresponding to a genus level classification. The average number of OTUs per sediment depth was 1,473, ranging from 800 OTUs in the April 8C 0-2 cm sample to 2,254 OTUs in July 8C 10-12 cm sample (Appendix B). Predicted total OTU, as calculated by Chao1 estimator, suggested an upper range of 28,008 (27,523 – 28,525 at 95% CI) with individual samples having as many as 3,868 OTUs (sample July 8C 10-12 cm). The observed OTUs were evenly distributed ($E>0.81$) in each sample as well as throughout each sediment core ($E>0.84$). Rarefaction curves calculated from the OTUs suggested additional sequences would be required to saturate the sample set as no individual curve reached a slope of 0 (Figure 4.3). Despite under-saturation of the sample set as indicated by the rarefaction curve and Chao1, it is assumed that the most abundant members of the population thus the more geochemically relevant lineages have been identified and characterized.

Taxonomic classification of the 168,760 sequences using the RDP database yielded a total of 131,343 sequences that surpassed the 70% confidence interval for classification at the phylum level (Appendix B). A total of 20 phyla were identified across all samples (Figure 4.4), with the fewest number of phyla detected in an individual sample being 17. The top 10 cm of the sediment column contained significantly ($p<0.05$) more classified lineages than the bottom 10 cm.

A Sorensen's index analysis was used to determine similarity between sample-specific microbial communities. Community similarity was defined by the number of

shared OTUs and represented a commonality at the genus-level of classification. A comparison of the calculated percent similarities revealed that the communities grouped into three main clusters (Figure 4.5). Cluster I represented communities from the upper 10 cm of sediment (Figure 4.5). Subgroups within Cluster I further divided based on seasonality as shown in Group IA (April) and Group IB (July). These communities were similar despite a physical separation of approximately 29 km, supporting a seasonal shift in specific community composition. Clusters II and III represent the lower 10 cm of the sediment column sampled (i.e., 10-20 cm below surface). No seasonality effects were observed, however the samples did cluster based on location. All the BC1 samples (Cluster II) grouping separately from the 8C samples (Cluster III) despite the date of sampling. Only a couple of exceptions were noted in which samples (April BC1 12-14 cm and July BC1 16-18 cm) grouped into the upper 10 cm of sediment. This is perhaps due to fringe effects or a localized change in geochemistry, however this does not impact the overall trend observed.

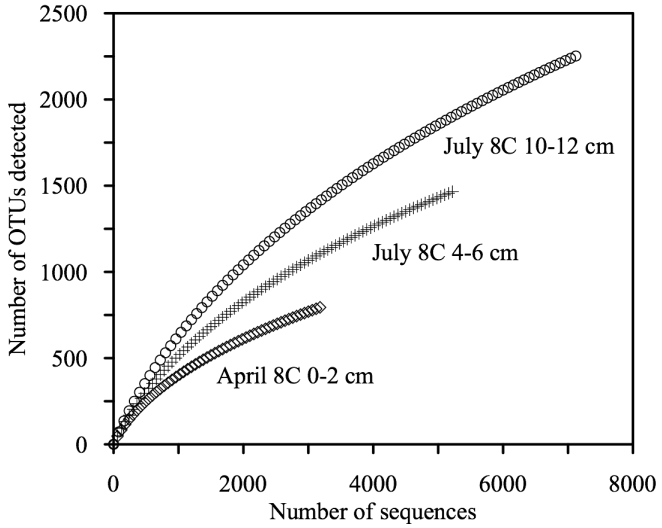

Figure 4.3. Rarefaction curves comparing the diversity of samples April 8C 0-2 cm, July 8C 4-6 cm, and July 8-C 10-12 cm. These three samples were chosen as they represent sequence data sets with the highest (July 8C 10-12 cm), lowest (April 8C 0-2 cm), and median (July 8C 4-6 cm) number of operational taxonomic units (OTU).

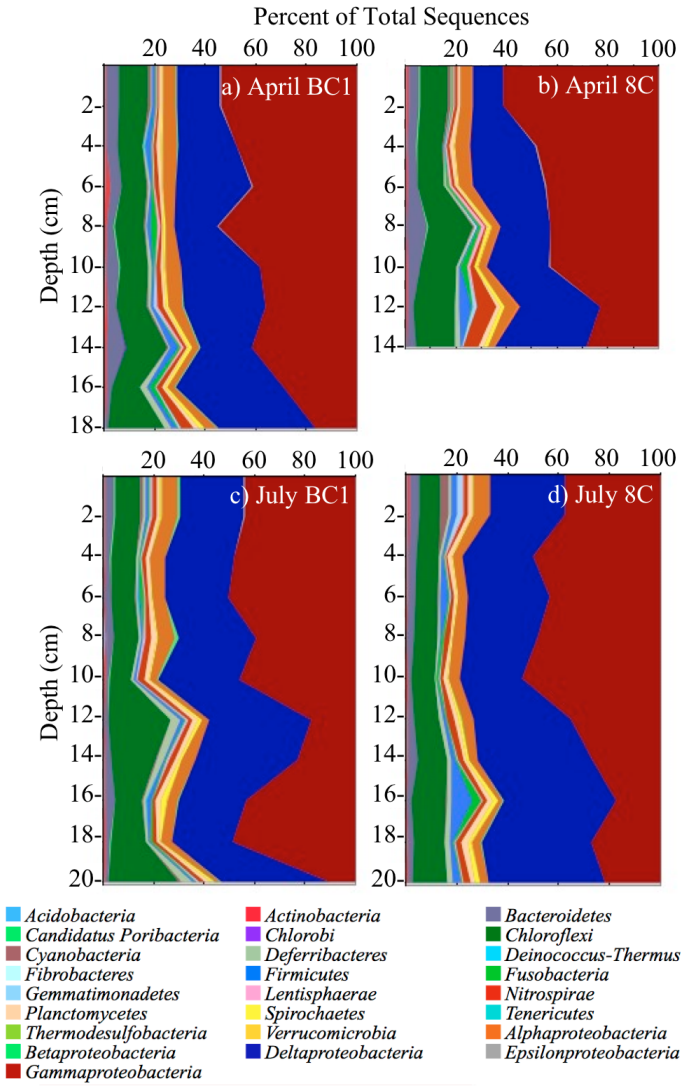

Figure 4.4. Taxonomic distribution of sequences at the phyla and class level. A total of 168,760 sequences were classified at a 70% confidence interval. Percentages were based on total sequences obtained at a given sample depth. A majority of sequences at all depths were related to *Gamma-* and *Deltaproteobacteria*, with the *Gammaproteobacteria* decreasing in frequency detected with depth while the *Deltaproteobacteria* increases.

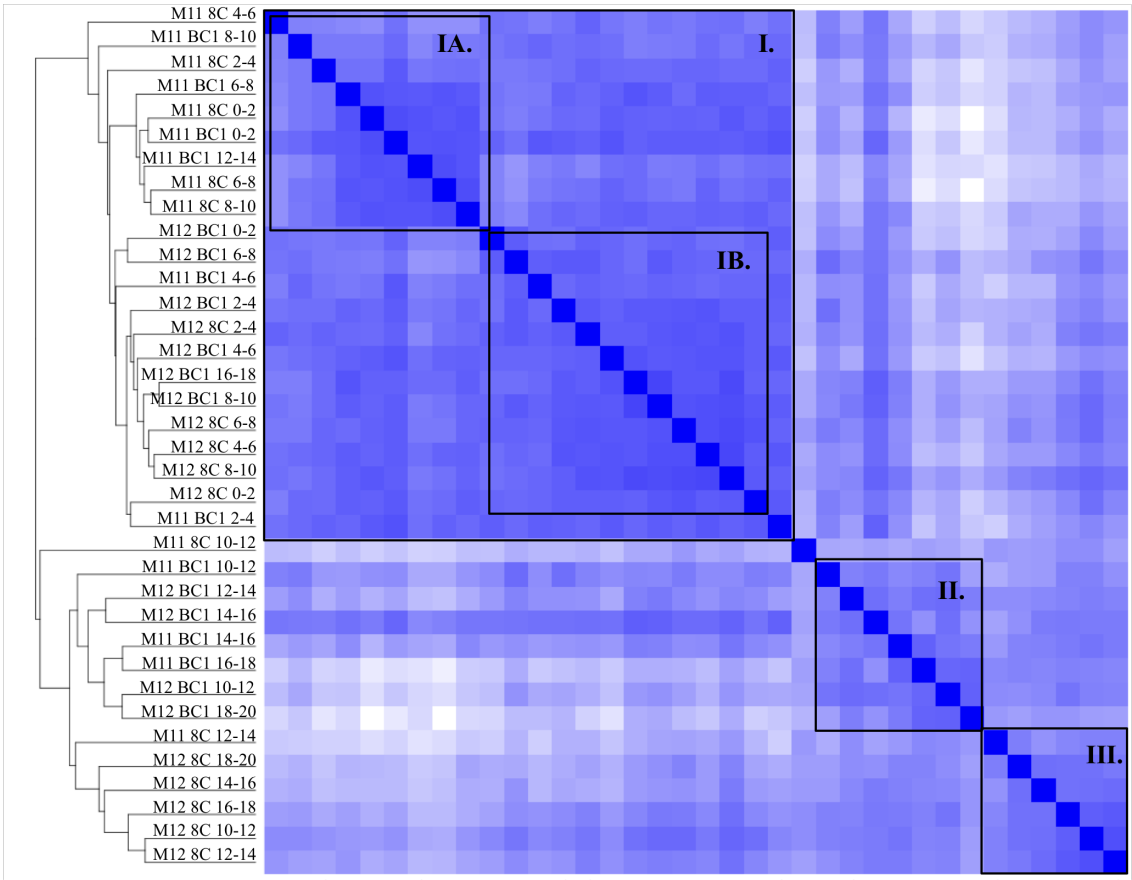

Figure 4.5. Heatmap and associated dendrogram of Sorensen's diversity index comparing all 36 samples. Communities from the upper 10 cm clustered together (Group I) based on sample date (April: Group IA and July: Group IB). Communities from the lower 10 cm cluster based on individual site (BC1: Group II and 8C: Group III).

Lineage specific microbial characterization of *Proteobacteria* phyla: The most frequently detected phyla were *Proteobacteria*, which comprised 71.2% - 89.4% of the classified sequences (Figure 4.4a-d). Specifically, *Gammaproteobacteria* (13.12% in sample July BC1 18-20 cm – 65.94% in sample April 8C 0-2 cm; general decrease with depth) and *Deltaproteobacteria* (12.7% in sample April 8C 0-2 cm - 53.7% in sample July BC1 18-20 cm; general increase with depth) were the most abundant classes within all of the classified *Proteobacteria*. The remaining three classes of *Proteobacteria* were also detected in lower abundances. *Alphaproteobacteria* represented 1.37% - 5.12% of the classified sequences and decreased in frequency with depth in each of the cores. *Epsilonproteobacteria*, notably the microaerophilic sulfur oxidizing family *Campylobacterales*, was also observed, but only at depths shallower than 10 cm and represented less than 1% of the classified sequences.

The most frequently detected *Gammaproteobacteria* lineages relevant to this study included *Chromotiales* and *Altermonadales*. These lineages were detected in all depths and were often greater than 1% of the classified sequences. *Chromotiales*, including the sulfur oxidizing family *Ectothiorhodospiracea*, were observed more frequently in April samples, while decreasing in frequency with depth in each of the sediment cores.

Within *Deltaproteobacteria*, the most abundant orders detected included *Desulfobacterales*, *Desulfuromonadales*, and *Syntrophobacterales*. All of these lineages have the potential to reduce oxidized sulfur species. Additionally, *Desulfuromonadales* have been linked to iron reduction processes. The family *Desulfuromonadaceae*, has

been shown to tolerate salt, use acetate as an electron donor, and of most importance for this study, use sulfur compounds as alternative electron acceptors (Coates et al. 1995; Roden and Lovley 1993). *Desulfobacterales*-related sequences represented greater than 10% of the classified sequences in all of the samples except April 8C 0-2 cm (7.05%). *Desulfuromonadales* comprised between 0.68% and 8.03% of the classified sequences. *Myxococcales* was observed in greater abundance in July than in April while *Syntrophobacterales*-related sequences were observed to increase with depth in each of the sediment core libraries.

Lineage specific microbial characterization of Non-*Proteobacteria* phyla: The next most abundant phyla after the *Proteobacteria* are the *Chloroflexi*, *Bacteroidetes*, *Cyanobacteria* and *Actinobacteria*. Both are common marine lineages and were detected in relatively high abundances throughout all samples and all depths. *Chloroflexi*, including the strictly anaerobic, fermentative class *Anaerolineae*, ranged from 2.78% in April BC1 2-4 cm to 9.65% in July BC1 18-20 cm. Sequences with high similarity to *Bacteroidetes*, specifically classes *Flavobacteria* and *Sphingobacteria*, ranged from 1.20% to 8.17% of classified sequences with an overall average of 3.21%. No distinct trend was noted spatially or temporally with these two classes. Trends were observed, as expected, with the phylum *Cyanobacteria*-related sequences as they were observed most frequently (>1% of the classified sequences) in the 0-2 cm sediment depth in each of the cores. In contrast, *Actinobacteria,* specifically the iron oxidizing family *Acidimicrobiaceae*, represented 0.31% - 2.03% of the classified sequences and was detected more frequently below 10 cm depth.

Additional phyla that have physiologies not within the scope of this study included: *Acidobacteria* (0.30% - 5.64%), *Firmicutes* (0.07% - 8.24%), *Fusobacteria* (0.14% - 4.05%), *Lentispheraea* (not detected - 2.79%) and *Planctomycetes* (0.38% - 2.76%). Other phyla detected in all the sediment depths at less than 1% of the classified sequences included: *Chlorobi*, *Deinococcus-Thermus*, *Gemmatimonadetes*, *Nitrospiria*, *Spirochaetes*, *Tenericutes* and candidate divisions OD1 and OP10.

Family lineages identified in this study with common functions related to sulfur or iron cycling were combined in order to identify trends (Figure 4.2). Family lineages of sulfide oxidizing bacteria (SOB) included *Ectothiorhodospiraceae*, *Thiotricaceae* and *Chromatiaceae*. Lineages commonly attributed to sulfate reduction in marine systems included *Desulfobacteraceae*, *Desulfobulbaceae*, *Desulfuromonadaceae* and *Syntrophobacteraceae* (Nealson 1997; Pereira et al. 2007) and will be collectively referred to as sulfate reducing bacteria (SRB) throughout this study. Lineages detected as iron reducing bacteria (FeRB) included *Geobacteraceae*, *Shewanellaceae*, *Campylobacteraceae*, *Pseudomonadaceae*, *Pelobacteraceae*, *Ferrimonadaceae*, and *Desulfuromondaceae*. Iron oxidizing bacteria (FeOB) included *Nitrospiraceae* and *Rhizobiales*.

Discussion

This study represents a substantial advance in the understanding of geochemical and microbiological characteristics of the shallow sediments of the northern Gulf of Mexico hypoxic zone. Data presented herein represents the first simultaneous analysis of porewater chemistry and RNA-based pyrosequencing analysis of the microbial

community structure in the Gulf of Mexico. Characterizing the microbial community using an RNA target is required to correlate molecular sequence data of the active community to the geochemical profiles. DNA is more stable in the environment due to its double-stranded structure, has an extracellular residence time of weeks or months and is also detectable in dead and quiescent cells (Mills et al. 2004; Nogales et al. 1999). Ribosomal RNA (rRNA) has a residence time of minutes to hours and increases in concentration when metabolic activity increases. Characterizing the rRNA enhances the understanding of the microbial populations that are actively influencing the geochemical environment, providing a better description of seasonal and spatial biogeochemical relationships in the environment. This study also highlights the feasibility of a high throughput, multidisciplinary strategy to describe fine scale variations in sediment microbial ecology and geochemistry.

Multiple mechanisms have been proposed to controlling hypoxia in this region of the northern Gulf of Mexico (Bianchi et al. 2010; Rabalais and Turner 2001; Rabalais et al. 2007). Numerous models proposed that the production of benthic sulfide contributed to water column hypoxia in the western region of the hypoxic zone (Dagg and Breed 2003; Green et al. 2006; Rowe and Chapman 2002). However, these models were based on the detection of sulfide at relatively deep depths (e.g., 60 cm) in the eastern hypoxic zone (Morse and Rowe 1999) and extrapolating that finding to more western and shallow regions. These models lack direct analysis of the microbial community activity with a corresponding geochemical profile description.

During the current study of the western hypoxic zone, low oxygen (< 2 mg L^{-1} or 63 μmol L^{-1} O_2) was observed within the water column during the July sampling period. Therefore, data collected provided a unique environmental assessment before and during hypoxia. To properly determine the potential benthic microbial community and associated geochemistry impact on hypoxia formation in the western zone, three key factors were addressed: depth of water column influence on the benthic environment, profile of redox processes within the sediments, and carbon limitation on biologic activity.

Depth of water column influence: Previous models describing mechanisms controlling hypoxia have proposed benthic microbial processes contribute to bottom water hypoxia directly (i.e., respiration) and indirectly (i.e., production of metabolites) (Green et al. 2006; Hetland and DiMarco 2008; Rowe and Chapman 2002). Seasonal shifts in the hypoxic zone water column chemistry would be a result of changes in the benthic microbial community metabolic activity (Bianchi et al. 2010) and may then be observed as shifts in microbial community structure and sediment geochemistry. The first step to analyze the benthic potential to impact water column oxygen concentration is to determine the depth at which the sediment microbial community responds to changes in the overlying water chemistry.

The geochemically pertinent members of a population are those that are metabolically active (Mills et al. 2004; Nogales et al. 1999). In this region, lineages that respond to changes in the geochemistry over time scales relevant to the onset and

dissipation of hypoxia are the most relevant to this study. Community characterization based on RNA sequences provided identification of the metabolically active fraction of the population. Resulting data indicated that the microbial populations in only the top 10 cm of the sediment column changed between sampling dates. The shallow populations were highly similar at both locations during their respective sampling dates. This similarity between sites can be the result of physical transport of sediment and/or common water column chemistry being advected into the sediment. Physical transport from BC1 to 8C is unlikely as previous studies have shown that a majority of sediment transport in this area is a result of wintertime resuspension and deposition events and the mobile mud layer is only limited to the top 3-5 cm (Corbett et al. 2004). Geochemical data (discussed below) further refute this conjecture. Thus, population similarities are more likely the result of common water chemistry flux into the sediment. The effective depth of water column influence is restricted to 10 cm as populations below this depth are site specific and did not display temporal variations.

Previous radioisotope studies measuring both ^{7}Be and ^{210}Pb support shallow mixing of water into the sediment to a depth of 8 cm at the 20-25 m isobath off the Atchafalaya River (Allison et al. 2000), near the current study area. Jaramillo and others (2009) determined that the maximum depth of water penetration in the NGoM, during a non-tropical storm event, is greatest during the passage of cold fronts in the winter. An average wave height of 1-2 m resuspended the upper few centimeters of sediment when water depths were greater than 10 m (Jaramillo et al. 2009). Bioturbation of nematodes was only observed on a very limited basis in a couple of cores during the current study

and it was limited to the top several centimeters. This is consistent with other studies conducted in the eastern hypoxic zone, closer to the Mississippi River (Rabalais et al. 2001). Triplicate cores were collected (Materials and methods) and as such the effect of bioturbation in the few samples would not be as evident as a whole. These studies support the data presented herein that the geochemical changes in the water column only impact the benthic microbial community to a limited depth. Therefore, only the geochemical compounds within the top 10 cm of sediment would affect the overlying water column.

Redox profiles: Microbial activity in the sediments has been proposed as a mechanism controlling hypoxia in the overlying water due to the biological production of reduced chemical compounds (i.e., sulfide) (Bianchi et al. 2010; Eldridge and Morse 2008; Hetland and DiMarco 2008). Sulfate reducing bacteria (SRB) lineages collectively represented a large percentage (15% on average) of total sequences obtained. However, only one core in this study had sulfide concentrations exceeding 1 μmol L^{-1} (i.e., detection limit) measured to a depth of 20 cm below sediment surface. Lack of measurable sulfide in a marine environment where active sulfate reducing lineages are present may suggest that any sulfide produced is 1) bound in a reduced form to metals (i.e., iron), 2) chemically oxidized to sulfate, or 3) biologically recycled during respiration.

Sulfur sequestration in sediments: The formation of total reducible sulfides (TRS) results in the sequestering of reduced sulfur within the sediment in a solid phase

and is a significant way to remove sulfide from the system (Jorgensen 1977). The reaction is operationally defined as the sum of dissolved sulfide, iron monosulfude (FeS) and pyrite (FeS_2) and is the product of reduced sulfur compounds bound to reactive iron (dissolved or particulate). TRS concentration in this study increased with depth, after dissolved Fe(II) disappeared, supporting phylogenetic data suggesting biological formation of sulfide and Fe(II) within the sediment column. However, the biological production of sulfide appears limited by available TOC because TRS concentrations correlate significantly with TOC ($p<0.05$) as sediment depth increases. The increased Fe(II) concentrations and reduced TRS concentrations in the upper sediment column suggest lower sulfide production in the uppermost sediment column. The available Fe(II) may serve as a possible sequestering mechanism to prevent sulfide from interacting with the water column if higher biological production of sulfide were to occur. Due to the presence of dissolved Fe(II) and TRS, which would otherwise be oxidized under aerobic conditions, it is unlikely that the fate of dissolved sulfide was chemical oxidation.

Chemical oxidation of sulfide: The relatively high and consistent concentrations of sulfate with depth in the sediment and reduced bottom water oxygen concentrations observed in this study could be explained through the chemical oxidation of sulfide to sulfate. However, sulfide oxidation by molecular O_2 is unfavorable and is kinetically slow due to the transfer of single electrons (Luther et al. 2011; Ma et al. 2006; Vazquez et al. 1989). When the oxidation reaction of H_2S is catalyzed by the oxygenated forms of iron and manganese (i.e., $Fe(OH)_3$ and MnO_2, respectively), the kinetics are much faster and the half-life decreases from a couple of days to minutes. The absence of sulfide does

not necessarily indicate an oxygenated sediment environment; rather it suggests that iron and manganese hydroxide minerals may be coupled to sulfide oxidation. The presence of dissolved Fe(II) and iron sulfides in the near surface sediments in this study further refute the possibility of an aerobic sediment environment. Additionally, the presence of oxygen would inhibit oxygen-sensitive sulfate reducing populations determined as being metabolically active.

Previous studies have further shown that biological sulfide oxidation rates far exceed abiotic sulfide oxidation rates by more than three orders of magnitude under both aerobic and anaerobic conditions (Luther et al. 2011). The experiments conducted in this study were conducted in strict trace metal clean conditions suggesting that prior oxidation rates have been over-estimated due to the potential catalysts of oxygenated Fe and Mn species within the reactions (described above). This study and others indicated that a majority of the reoxidation of sulfide in the environment is largely due to sulfide oxidizing bacteria (SOB) rather than chemical oxidation alone (Luther et al. 2011; Zhang and Millero 1994). Therefore, the population size and activity of microbial communities in aerobic-anaerobic transitions zones will determine any flux of sulfide.

Biological recycling: Microbial metabolic processes can be determined geochemically by the production or consumption of conjugate oxidation-reduction (redox) pairs. Redox processes are commonly presented as being stratified, establishing recognizable diagenetic zones within an environment. As noted by Boudreau (2000), sediment zonation is not solely unidimensional as it is typically presented, but rather a mosaic of microenvironments with different redox conditions and with different

bacterial populations. Microbial populations that coexist may utilize the redox products from another population in the reverse reaction. This could mask the initial microbial process and set-up a “cryptic” microbial cycle. For example, the disappearance of sulfate combined with the appearance of sulfide would be a reliable indicator of microbial sulfate reduction. However, sulfate reduction can be camouflaged when SOB utilize the sulfide that is produced (reoxidized).

Based on the geochemical data from the sediments, the oxidized state of sulfur is dominant within the upper 20 cm, which is evident by the lack of a defined zone of sulfate reduction and sulfide accumulation. SSU rRNA transcript analysis indicated the presence of metabolically active sulfate reducing lineages was paralleled by sulfide oxidizing lineages at all sediment depths tested (Figure 4.2a-d). As shown in the SVD and PCA analyses, the SOB lineages displayed a significant overall decline in abundance with depth ($p<0.05$) while the SRB lineages increased in abundance ($p<0.05$). Such an overlap of lineages in an area of low concentrations of reduced compounds and minimal loss of sulfate is expected during an active cryptic sulfur cycle and would explain why no obvious *in situ* geochemical signature for sulfate reduction was observed. The presence of molecular oxygen may not be required for the reoxidation of sulfur as Canfield et al. (2010) linked cryptic, nitrate-driven sulfur cycling to characteristic sulfur-oxidizing microbial communities observed in a water column oxygen minimal zone off the coast of northern Chile. The data presented herein advances their conclusions of active cryptic cycles by using RNA-based targets and direct geochemical analysis.

Active iron reducers and iron oxidizers were also observed in close proximity and each displayed similar trends throughout the sediment column setting up a potential cryptic cycling of iron similar to that of the sulfur cycle. Of the identified iron reducing lineages, *Desulfuromonadaceae* has been detected the most frequently when molecular techniques have been used to assess microbial community composition in Fe(III) reducing marine environments (Holmes et al. 2004; Ravenschlag et al. 1999). The FeRB population sequences within the data set were, on average, higher in abundance than the FeOB sequences. According to SVD and PCA analyses, FeRB displayed a significant increase with depth while FeOB decreased with depth in each core ($p<0.05$), similar to the trend observed in the sulfur cycle. The overall peak in abundance for FeRB lineages was observed at mid-depth (i.e., 8-12 cm), located above the peak in abundance of SRB lineages. The depth at which the peak was observed correlated with the predicted depth of water column influence (discussed above). Active FeRB lineages and their relative abundance to FeOB lineages provides a mechanism for the Fe(II) concentrations detected near the surface and additional reduced iron species at depth. The general trend of iron reducer sequence abundance is positively correlated with changes in the TRS and TOC concentrations mentioned above ($p<0.05$) suggesting a potential carbon limitation for the iron and/or sulfate reducing lineages. These lineages may be dependent on the limited availability of carbon to actively reduce iron and that this iron is being locally bound to reduced sulfide, forming predominantly pyrite.

Carbon limitation: Both sites had relatively low TOC concentrations as compared to typical marine mud environments (Berner 1982; Koster and Meyer-Reil 2001; Pallud and Van Cappellen 2006) and as defined by the Environmental Protection Agency (≤1% dw) (EPA) 2002). TOC is the fraction of the total carbon (TC) that is typically derived from the decomposition of plants and animals but excludes the inorganic fraction (i.e., carbonates). The site located further west (8C) had a lesser percentage of organic carbon compared to the site further east (BC1), which is expected given the proximity of BC1 to the mouth of the Mississippi River. The TOC was on average 43-61% of the TC and remained relatively unchanged with depth. Redox profiles suggest that the fraction of the population capable of iron reduction would utilize the limited carbon available before the sulfate reducing lineages (Froelich et al. 1979). This has been supported by previous studies that have shown FeRB outcompeting SRB for carbon substrates and predominate over the oxidation of organic matter (Kostka et al. 2002).

Sediment type (e.g., grain size and porosity) has been previously correlated to TOC in estuarine environments where sands with low pore volume contained <0.6% dw TOC and muddy sand contained 1.5-1.6% dw TOC (Koster and Meyer-Reil 2001). It is interesting to note that the Gulf of Mexico sediments analyzed in this study had a grain size and porosity indicative of a sandy mud to muddy sand, yet the average TOC (0.45% dw at 8C and 0.70 % dw at BC1) was more typical of a sandy sediment. The advantages associated with high advective flow through sands (i.e., increased influx of carbon and flushing of metabolites) (Buhring et al. 2006; Jahnke et al. 2005) would not be observed

in these sediments. Additionally, these sediments lack the high levels of TOC common to biologically productive muds (Koster and Meyer-Reil 2001).

The low concentrations of organic matter detected and the lack of terminal electron acceptor depletion with depth suggests that despite the detection of multiple active SRB and FeRB populations, their benthic contribution to water column hypoxia appears limited. We conclude that the primary factor inhibiting activity within these sediments is carbon availability.

Summary

Geochemical profiles determined in the present study (Figure 4.2) suggested that prior incorporation of elevated near surface sulfide concentrations into models describing hypoxia formation might be overestimated (Hetland and DiMarco 2008). This study emphasizes the importance and feasibility of coupling geochemical and molecular analysis when describing sedimentary processes. Geochemical data revealed within the upper sediment a lack of sulfide accumulation, presence of Fe(II) and relatively low organic carbon. Examining the geochemical profiles alone would support the assumption that the sediments have a low sulfate reducing activity and would be a minor contributor to the mechanisms controlling hypoxia in the western region. Conversely, sequence analysis of the metabolically active portion of the microbial community showed a high frequency of sequences related to sulfate reducing lineages. These contradictory findings, explained through analysis of the total data set, suggest that either the products from sulfate reduction are recycled by sulfur oxidizing lineages or the sulfate reducing

populations that are active are limited by low concentrations of electron donors (i.e., organic carbon). Both the geochemistry and molecular biology suggest the lack of organic carbon within the sediments inhibits microbial activity. Conclusions presented here are novel for the NGoM hypoxic zone and can be tested in future studies to determine additional implications for model development.

CHAPTER V

CHARACTERIZATION OF IRON AND SULFUR CYCLING BIOGEOGRAPHY USING SOLID AND AQUEOUS GEOCHEMICAL ANALYSES

Overview

Most biogeochemical studies describe microbial ecology using only aqueous geochemistry. However these studies neglect to characterize the bioavailable, solid-phase portions as it relates to the local environment. Solid phase species of key elements, including sulfur and iron, are typically underestimated sources for microbial activity. The objective of this study was to determine spatial and temporal variability of the benthic ecosystem through biogeochemical and molecular analysis while focusing on the sulfur and iron cycles. The central hypothesis is that the microbial ecology will be distinctly independent at each location and reflect the aqueous and solid phase geochemical constituents. During this study, sediment samples were collected from three locations and to a sediment depth of 20 cm in the northern Gulf of Mexico hypoxic zone. Sulfate and iron reducing bacteria community structure was determined every 2 cm using 454 FLX pyrosequencing of SSU rRNA transcripts. Aqueous and solid phase iron and sulfur compounds were also analyzed in combination with molecular characterization, and the degree of pyritization was determined. Variations in iron and sulfur bioavailability altered the microbial ecology, both in terms of structure and function. In turn, community activity can contribute to small spatial scale changes in the geochemistry providing a potential for geographic and geochemical isolation. Therefore,

localized feedback loops between available geochemistry and the microbial community can result in population divergence, exhibiting biogeography with sediments.

Introduction

Iron and sulfur are two critical elements within marine sediments, contributing to a significant portion of carbon remineralization. The most dynamic regions to examine the biogeochemical interactions between iron and sulfur occur where iron-rich river water flows onto shallow, oxygen-starved continental shelf regions. In these coastal environments, the concentrations of iron, sulfur and carbon are highly variable and are dependent upon localized physical, chemical and biological factors. To characterize the transformations, sinks and sources, and how these elements interact with the cycling of other molecules, an integrated biogeochemical approach is required. Previous strategies have relied heavily on geochemical techniques because they have been well developed, suitable for field research, and widely available (Berner 1982). The biological component has historically been treated as an assumption that everything was everywhere (Baas-Becking 1934), or that the biological processes were insignificant. In part, this has spearheaded the relatively new field of environmental molecular biogeochemistry.

Significant advancements in microbial ecology through the use of molecular tools have helped further the study of prokaryotic biogeography and speciation (Xu 2006). Identifying bacterial communities that thrive in a given environment and, likewise, the evolutionary forces that shape it can aid in the development and

understanding of biogeochemical models. An increasing number of studies have focused on describing microbial diversity at the genotype level in marine ecosystems (Horner-Devine et al. 2003; Papke et al. 2003); however, these studies often overlook the importance of the geochemical environment. Bacterial populations tend to reflect the geochemical conditions while they evolve. In addition, these populations can influence the surrounding geochemistry creating an independent feedback loop vastly different from the parent population. Observations in biogeographical variations have been made on large basin-wide scales and on smaller scales within niches (Ramette and Tiedje 2007). The smaller scale variability is particularly important within coastal sediments that are highly dynamic and experience temporal shifts.

It is not an uncommon understanding that a microbial community within the environment is shown to have an effect on the surrounding geochemistry. Additionally, most studies describe this interaction as a side effect of bacterial metabolism and mineralogical changes are merely a coincidental outcome of respiration (Rogers and Bennett 2004). The fundamental problem is not how the system is perturbed by microbial activity, but rather why each community develops in the manner that is does and what advantage is gained by the population dynamics. It has been best summarized by the idea that evolution impacts geochemistry as equally and as directly as it does biochemistry (Bennett and Omelon 2011).

Precipitation and dissolution of minerals are not coincidental outcomes of microbial respiration; there is a selective advantage to this process, especially in areas with limiting nutrients. Most of the focus on biogeochemical reactions is given to the

dissolved geochemical phases as this has been considered the most bioavailable. Studies have shown, however, that different mineral surfaces offer different selective habitats and microbes purposely attach based on beneficial needs (Rogers and Bennett 2004).

The use of oxidized iron and sulfur by microbes as a terminal electron acceptor (coupled to simple organic carbon) to derive energy has been well characterized in numerous environments. Many microorganisms have developed strategies of dissolving solid-phase Fe to increase its bioavailability (Lovley et al. 1996; Roden and Zachara 1996). Combining the reduced iron (Fe^{2+}) generated from bacterial biomineralization and sulfide generated from dissimilatory sulfate reduction, iron monosulfides (FeS) and eventually pyrite (FeS_2) precipitate locally.

Most biogeochemical studies describe the aqueous geochemistry as it relates to the microbial ecology; yet neglect to characterize the bioavailable, solid-phase portion of the iron and sulfur cycle. With the advancement in molecular techniques, the structure of the total bacterial community has been well studied in other environments. However, the interaction of the active (RNA-based) microbial population with the full geochemical suite, and resulting spatial variability has not been fully elucidated.

The objective of this study was to determine spatial and temporal variability of the benthic ecosystem through biogeochemical and molecular analysis. This paper focuses on two important elements in the coastal marine system that contributes a large portion of the benthic respiration, iron and sulfur (Jorgensen 1982). The central hypothesis is that the microbial ecology will be distinctly independent at each location and reflect the aqueous and solid phase geochemical constituents. Furthermore, we

expect to observe a diurnal variation in the top few centimeters of the sediment column. Understanding the implications of a heterogeneous environment will provide the basis for more informed models coupling the reactions within the benthic and pelagic environments. This study combines state-of-the-art molecular techniques aimed at characterizing the metabolically active community with robust dissolved and solid phase geochemical analysis.

Materials and methods

Location and sampling: The Northern Gulf of Mexico hypoxic zone is an area along the Texas-Louisiana shelf that is characterized by low oxygen concentrations (< 63 μmol L^{-1}) during the summer. This system is dominated by large seasonal inputs of freshwater along with inorganic and organic nutrients from the Mississippi and Atchafalaya Rivers (Bianchi et al. 2010).

Samples for this study were collected in July 2009 (during hypoxic conditions) from three stations (AB5: 29.0801°N, 89.9493°W; 10B: 28.6290°N, 90.55133°W; 8C: 29.0004°W, 92.0039°N) along the 20 m isobath (Figure 5.1). Water column parameters, including dissolved oxygen, PAR, and fluorescence, were collected every two hours for 24 hours via CTD (Sea-Bird Electronics, Bellevue, WA). Box-cores were collected at each location at midday and at midnight. Triplicate cores were collected for molecular analysis and duplicate cores were collected for geochemical analysis in 7 cm diameter polystyrene core liners. Cores were sectioned in 2 cm intervals for both geochemistry and molecular analysis from the sediment surface (0 cm) to a maximum depth of 20 cm.

The three triplicate molecular cores were simultaneously sectioned shipboard with corresponding depth sections, homogenized and frozen at -80^{o}C. The duplicate cores for geochemical analysis were immediately frozen upright at -20^{o}C. All samples were transported to Texas A&M University for processing.

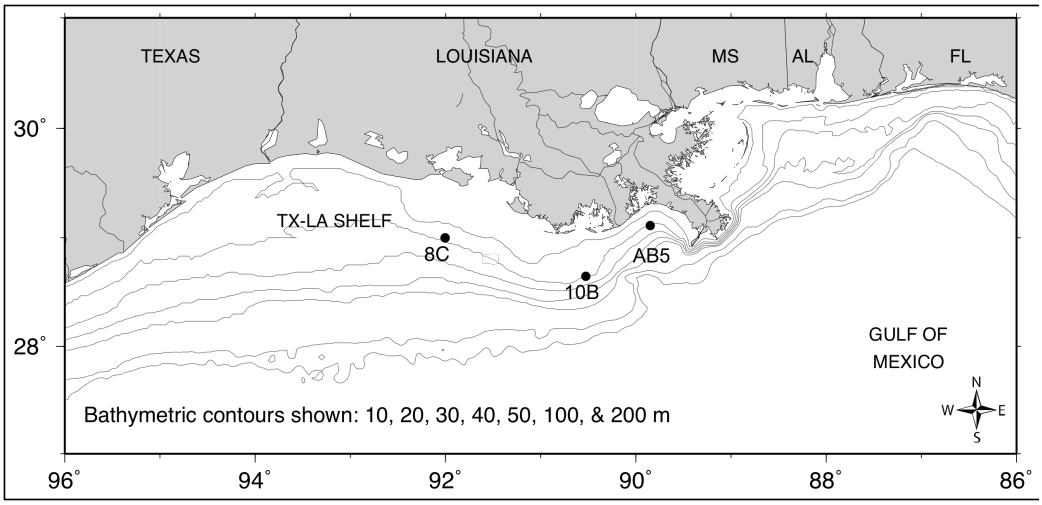

Figure 5.1. Map of the three sample locations in the northern Gulf of Mexico (AB5: 29.0801^{o}N, 89.9493^{o}W; 10B: 28.6290^{o}N, 90.55133^{o}W; 8C: 29.0004^{o}W, 92.0039^{o}N) along the 20 m isobath.

Geochemical analysis: Cores collected for geochemistry were sectioned (2 cm resolution) within an anaerobic chamber. Porewater was extracted via squeezing (Reeburgh 1967) and collected in gastight syringes. Squeezed sediments were stored at -20^{o}C for acid volatile sulfide (AVS), total reducible sulfide (TRS) analysis, total carbon (TC) and total organic carbon (TOC).

Porosity was determined on oven-dried (~80^{o}C) sediment and by calculating the ratio of percent solid to percent water. Total organic carbon was determined in acidified (to remove $CaCO_3$) dry sediment samples in a UIC CM-5120 combustion furnace (UIC Inc, Jolliet, IL) that was coupled to a UIC CM-5012 carbon coulometer (Lyle et al. 2000).

Total dissolved sulfide ($\Sigma H_2S_{aq} = H_2S_{aq} + HS^- + S^{2-}$) was determined using the method described in Reese et al. (2011a). Porewater iron speciation was determined using the ferrozine method (Viollier et al.). Dissolved sulfate and chloride was determined using ion chromatography with an IonPac ASII high capacity anion-exchange column (Dionex, Sunnyvale, CA).

Acid volatile sulfide (AVS), defined as ΣH_2S_{aq} + iron monosulfides (FeS), within the sediment was analyzed by the cold 6N HCl + $SnCl_2$ method (Cornwell and Morse 1987). Total reduced sulfur (TRS), defined as AVS + pyrite (FeS_2), was analyzed by the hot $CrCl_2$ method (Canfield et al. 1986). Solid phase reactive-Fe was extracted using the cold 1 mol L^{-1} HCl (2 h incubation; room temperature) and citrate-dithionate (4 h incubation; 60^{o}C) methods (Kostka and Luther 1994; Raiswell et al. 1994). The resulting extract supernatant was analyzed for dissolved iron speciation using HEPES-buffered

ferrozine (Kostka and Luther 1994) on a Shimadzu UV-1201 spectrophotometer (Shimadzu Scientific Instruments, Columbia, MD).

Highly reactive iron was calculated as the sum of the dithionite extractable iron (FeCD) and the iron that is present in the form of pyrite (defined as TRS). Poorly reactive iron was determined as the difference between the HCl extractable iron (FeH) and the FeCD. The unreactive iron was defined as the total iron pool minus FeH and TRS (Raiswell and Canfield 1998). The degree of pyritization (DOP), representing the extent to which reactive Fe was transformed to pyrite, was calculated by the following equation (Berner 1970; Morse et al. 2007):

$$DOP = \frac{\text{Pyrite-Fe}}{\text{Pyrite-Fe} + \text{Reactive-Fe}}, \text{where Pyrite-Fe} = \frac{1}{2}(\text{TRS} - \text{AVS}) \qquad \text{(eq. 5.1)}$$

Nucleic acid extraction: Total community DNA and RNA were extracted from ~0.5 g wet sediment from every 2-cm slice using a phenol-chloroform procedure adapted from (Mills et al. 2008) Mills et al. (2008) and (Kerkhof and Ward 1993) Kerkhof and Ward (1993). Modifications include the omission of glycogen and all solutions were buffered for RNA preservation. Residual DNA was removed from the extracts with RNase-free DNase (Promega, Madison, WI) according to the manufacture's instructions. Negative controls were carried throughout to verify no contaminating nucleic acids during the extraction procedure and no DNA remained in the RNA extracts.

Reverse transcription and PCR amplification: Aliquots of small subunit ribosomal RNA (rRNA) were reverse transcribed to complimentary DNA (cDNA) using moloney murine

leukemia virus (MMLV) reverse transcriptase (Promega, Madison, WI) and *Bacteria*-specific SSU rRNA primer 518R (Nogales et al. 1999). The cDNA (10 to 50 ng) was PCR amplified using NEB Taq DNA Polymerase (New England Biolabs, Ipswich, MA) and bacterial primers 27F (Giovannoni et al. 1991) and 518R. PCR amplification included initial denaturing at 95^{o}C for 5 min; followed by 35 cycles of denaturation at 95^{o}C for 1 min, annealing at 50^{o}C for 1 min, and elongation at 72^{o}C for 1 min; with a final extension step at 72^{o}C for 10 min. RNA extracts were monitored by PCR amplification of the rRNA aliquot prior to reverse transcription to confirm no contaminating DNA. Amplicons were visualized and size verified by gel electrophoresis stained with ethidium bromide and UV illuminated.

Pyrosequencing: Aliquots of amplified cDNA that passed quality control assurances were prepared for 454 sequencing at the Research and Testing Laboratory (RTL; Lubbock, TX). Initial generation of the sequence library used a one-step PCR with HotStarTaq Plus Master Mix Kit (Qiagen, Valencia, CA), with a universal primer (5'-GAG TTT GAT CNT GGC TCA G-3') and *Bacteria*-specific 519R primer (5'-GTN TTA CNG CGG CKG CTG-3') (Handl et al. 2011). A secondary PCR was performed for FLX (Roche, Nutley, NJ) amplicon sequencing under the same condition by using designed special fusion primers with a 10-base unique multiplex identifier (MID) sequence. The use of a secondary PCR prevented amplification of any potential bias that might have been caused by inclusion of tag and linkers during initial template amplification reactions. Tag-encoded amplicon pyrosequencing analyses utilized a

Roche 454 FLX instrument with Titanium reagents, titanium procedures performed at the RTL based upon their protocols (www.researchandtesting.com).

Quality trimmed sequence reads were derived directly from FLX sequencing run output files. Sequences were extracted from the multi-FASTA file into individual sample specific libraries based upon the tag sequence. Tags that did not have 100% homology to the sample designation were not considered. Sequences which were less than 200 base-pair (bp) after quality trimming were not considered. All sequences passing quality control were deposited in the National Center for Biotechnology Information (NCBI) database using Sequence Read Archive (SRA).

Phylogenetic analysis: Initial sequence analysis was performed according to standard protocols at the Research and Technology Laboratories, Lubbock, TX. In brief, sequences were denoised, assembled into clusters and queried using a distributed BLASTn .NET algorithm (Dowd et al. 2005) against a database of high quality SSU bacterial sequences derived and curated monthly from NCBI (accessed January 2011). Database sequences were characterized as high quality based upon criteria utilized by Ribosomal Database Project (RDP; University of Michigan, Lansing, MI). Using a .NET and C# analysis pipeline the resulting BLASTn outputs were compiled, validated using taxonomic distance methods, and data reduction analysis performed as described previously (Handl et al. 2011).

The BLASTn derived sequence identity, defined as the percent of total length query sequence that aligns with a given database sequence, was used for classification at

the appropriate taxonomic levels based upon the following criteria: Sequences with identity scores, to known or well characterized SSU rRNA sequences, greater than 97% identity (<3% divergence) were resolved at the species level, between 95% and 97% at the genus level, between 90% and 95% at the family and between 85% and 90% at the order level , 80 and 85% at the class and 77% to 80% at phyla. The percentage of sequences classified to each lineage was determined for individual samples providing relative abundance information within and among all samples. Data presented at each taxonomic level, including percentage compilations, represent all sequences resolved to their primary identification or their closest relative.

Statistical analysis: Sequences were clustered into operational taxonomic units (OTU) using RDP and a 95% sequence similarity cutoff (corresponding to a genus level classification). Pairwise comparisons examined the null hypotheses of no differences (α=0.05) in the biological composition or geochemistry between sites or seasons. Differences between sites, depths and seasons by OTU, functional groups, and geochemical composition were evaluated through one-way ANOVA in varied combinations. A post-hoc least significant difference (LSD) test was performed when significant differences were identified. Correlation analysis was conducted to identify strength of relatedness in geochemical and physical variables. Statistical analyses were performed using Microsoft Excel 2008 and SPSS v. 16.0. Evenness, Shannon diversity index, species richness and rarefaction analysis were computed in RDP. Cluster analysis using Ward's linkages was performed to examine relationship of site and depth through

geochemistry and functional groups using JMP v. 9.0 (SAS Analytics, Cary, NC). Dendrograms were constructed using Phylip (http://www.phylip.com), NJ Plot (Perriere and Gouy 1996) and TreeView (http://taxonomy.zoology.gla.ac.uk/rod/treeview.html).

Results

Site description: Water column hypoxia (< 2 mg L^{-1} or 63 μmol L^{-1} O_2) was observed at locations AB5 and 10B during the study period; location 8C had low oxygen concentrations, but was not hypoxic. The dissolved oxygen concentration (DO) at AB5 during the midday period decreased from 4.4 mg L^{-1} in the surface water to 0.2 mg L^{-1} at 19 m depth. Likewise, site 10B showed a decrease in DO from 4.4 mg L^{-1} to 1.5 mg L^{-1}. However, site 8C was inversely stratified slightly with the lowest DO concentrations of 3.4 mg L^{-1} at the surface and 4.2 mg L^{-1} at 19 m depth. All three locations showed slight variation between the day and night DO concentrations, with the maximum surface water DO during the night (approximately 23:00 – 01:00 hour).

The maximum daytime difference in temperature (ΔT) between the surface and bottom water was 2.76°C at 8C, 5.25°C at 10B, and 4.33°C at AB5. The variation in salinity from the surface water to the bottom was -1.72 PSU at 8C (indicating more saline water on the bottom), -6.84 PSU at 10B, and -5.83 PSU at AB5. Overall, the strongest thermal and density stratification was observed in the water column at 10B and AB5, whereas site 8C was very weakly stratified. Nighttime thermal stratification was slightly weaker at all locations; however, density stratification remained relatively unchanged. Daytime benthic light levels (defined as photosynthetically available

radiation, or PAR) were never less than 1% of the surface PAR indicating the presence of limited light near the sediment.

Sediment and porewater analysis: The geochemical data suite (i.e., sulfate, sulfide, dissolved iron, sulfate reduction rates, porosity, TOC, and TC) from all three locations was compiled to calculate a similarity index using SPSS v. 16.0. The pairwise comparison between samples resulted in the formation of a similarity matrix and the construction of a dendrogram using a neighbor-joining algorithm (Figure 5.2). Clade formation within the dendrogram indicated the three sample locations had distinctly different geochemical characteristics (Figure 5.2). All geochemical measurements reported herein are the average of duplicate sampling.

The porosity at each location did not show any differences between the day and night sampling periods. The average overall porosity at AB5 was greatest (0.84) and the lowest porosity was observed at 10B (0.78). A significant ($p<0.05$) decrease in porosity with depth was noted in the cores from site AB5 and 8C, but the cores from 10B showed no change in porosity with depth. Overall, the porosity showed a strong positive correlation to sulfide, Fe(II), TOC and TC (n=57; $p<0.05$).

Figure 5.2. Depth profiles of geochemical species and microbial lineages related to sulfur cycling (panels a through f) and iron cycling (panels g through l). Note that dissolved iron and TOC are plotted on different concentration scales due to large observed variations. The functional groups shown represent the sum of all lineages detected with the potential for the specific metabolic process as described in the results. SRB = sulfate reducing bacteria: *Desulfobacteraceae, Desulfobulbaceae, Desulfuromonadaceae and Syntrophobacteraceae*; SOB = sulfide oxidizing bacteria: *Hydrogenophilaceae*, *Ectothiorhodospiraceae*, *Thiotricaceae* and *Chromatiaceae*; FeRB = iron reducing bacteria: *Geobacteraceae*, *Shewanellaceae*, *Campylobacteraceae*, *Pseudomonadaceae*, *Pelobacteraceae*, *Ferrimonadaceae*; FeOB = iron oxidizing bacteria: *Nitrospiraceae* and *Burkholderiales*.

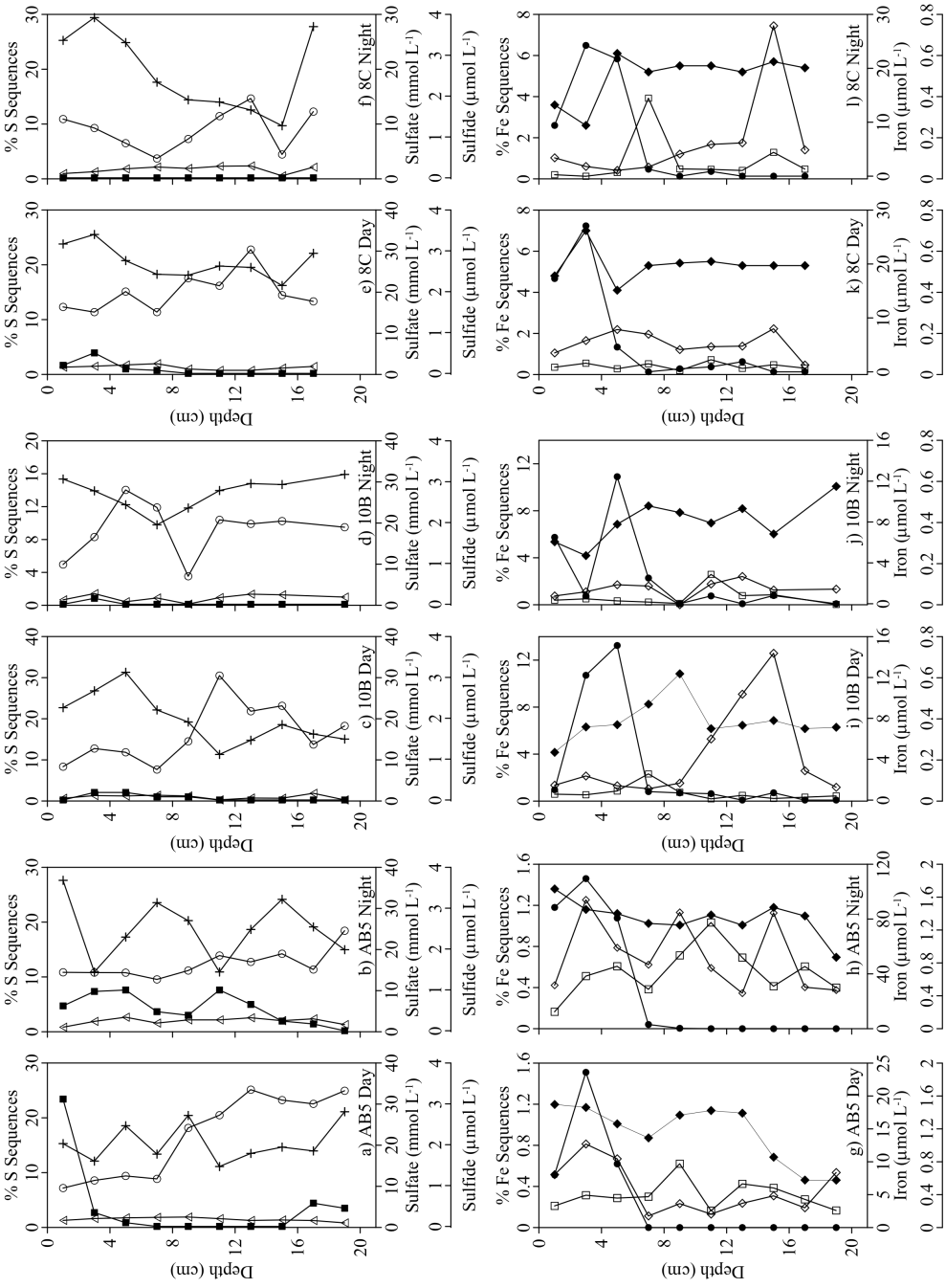
a) AB5 Day
b) AB5 Night
c) 10B Day
d) 10B Night
e) 8C Day
f) 8C Night
g) AB5 Day
h) AB5 Night
i) 10B Day
j) 10B Night
k) 8C Day
l) 8C Night
% S Sequences
% Fe Sequences
Depth (cm)
Sulfate (mmol L-1)
Sulfide (µmol L-1)
Iron (µmol L-1)
TOC (% gdw)
TOC (% gdw-1)
FeRB
FeOB
Iron
TOC
SRB
SOB
Sulfate
Sulfide

Total dissolved sulfide within the sediment porewater was measured above the method detection limit (1 mmol L^{-1}) only at site AB5 with the highest daytime concentration at 0-2 cm (3.1 mmol L^{-1}) and the highest nighttime concentration at 4-6 cm (1.2 mmol L^{-1}). Overall, the sulfate concentration was relatively uniform throughout all depths and no significant loss was observed; however, the SO_4^{2-}:Cl^- showed a small but significant ($p<0.05$) loss with depth. No significant differences in sulfate concentration were observed among the sample locations. A significant ($p<0.05$) difference was measured in sulfate concentrations from the day and the night sampling at sites 10B and 8C, but not at site AB5. The average bulk sulfate concentrations at AB5, 10B, and 8C were 22.8 mmol L^{-1}, 23.7 mmol L^{-1}, and 23.4 mmol L^{-1}, respectively.

Dissolved Fe(II) was only observed in the upper 10 cm of sediment at each location with concentrations decreasing to below the detection limit at approximately 10-12 cm depth (Figure 5.2g-l). On average, site AB5 had the highest bulk concentration (16.2 mmol L^{-1}). The highest concentration overall was measured at site AB5, 2-4 cm depth (109.5 mmol L^{-1}). No significant difference was noted in the iron concentrations measured during the day and during the night.

Acid volatile sulfides (AVS) and total reduced sulfur (TRS) are operationally defined measurements to describe the percentage of ΣH_2S_{aq} along with iron monosulfides and pyrite, respectively. AVS was measured below the detection limit at each sample location. TRS was highest on average at site AB5 with 84.1 mmol gdw^{-1} (gram dry weight) and lowest at 8C with 40.3 mmol gdw^{-1} (Table 5.1). Site 10B had an

average TRS concentration of 75.0 mmol gdw^{-1}. No significant difference in the TRS was noted between the daytime and nighttime sampling at all locations.

Table 5.1. Data for total reduced sulfur (TRS), extractable iron analysis and porosity given as average and range for each sample location

	TRS			Extractable Iron-CD			Extractable Iron-HCl			
Location	Average (μmol gdw^{-1})	Range (μmol gdw^{-1})	Depth of max (cm)	Average (μmol gdw^{-1})	Range (μmol gdw^{-1})	Depth of max (cm)	Average (μmol gdw^{-1})	Range (μmol gdw^{-1})	Depth of max (cm)	Porosity (Φ)
AB5	84.1	47.8 - 118.7	18 - 20	292.9	205.4 - 328.5	10 - 12	272.0	226.3 - 316.2	18-20	0.84
10B	75.0	27.1 - 105.5	10 - 12	93.3	79.4 - 104.2	10 - 12	198.6	137.0 - 262.5	14-16	0.78
8C	40.3	26.2 - 55.9	12 - 14	147.6	122.6 - 196.9	18 - 20	21.4	15.4 - 30.0	2 - 4	0.81

The concentration of solid-phase reactive iron by the HCl method was greater than by the citrate-dithionite (CD) method at site 10B by an average of 51%. At site AB5, the percent difference was minimal and the CD method showed greater concentrations than the HCl method by 8.9%. The greatest difference in the two methods was observed at site 8C; the concentration of extractable iron was 598% greater on average by the CD method than the HCl method. Similar to the TRS concentrations, the greatest concentration of reactive iron was measured at AB5 (292.2 mmol gdw^{-1}) and the lowest was measured at 8C (21.4 mmol gdw^{-1}).

Total organic carbon (TOC) and total carbon (TC) showed a strong correlation to each other across all samples ($p<0.05$). The TOC and TC concentrations were low on average (<1.2% dry weight (dw) and <0.7% dw, respectively) in all samples from sites 8C and 10B (Figure 5.2i-l). Site AB5 had the significantly greater ($p<0.05$) TOC concentrations than the other locations with 1.7% dw at the surface to 0.6% dw at 18-20 cm depth (Figure 5.2g-h). Both TC and TOC also decreased significantly ($p<0.05$) with depth in each sediment core. No significant difference was noted between the day and night sampling for TOC and TC concentrations at any location.

A geochemical similarity index was calculated to determine the percent similarity between individual parameters. Geochemical parameters tested included sulfate, sulfide, dissolved iron, sulfate reduction rates, porosity, TRS, TOC, and TC. A pairwise comparison between samples resulted in the formation of a similarity matrix and the construction of a dendrogram using a neighbor-joining algorithm (Figure 5.3). The dendrogram showed distinct groups with different geochemical characteristics that divided samples based on location (Figure 5.3).

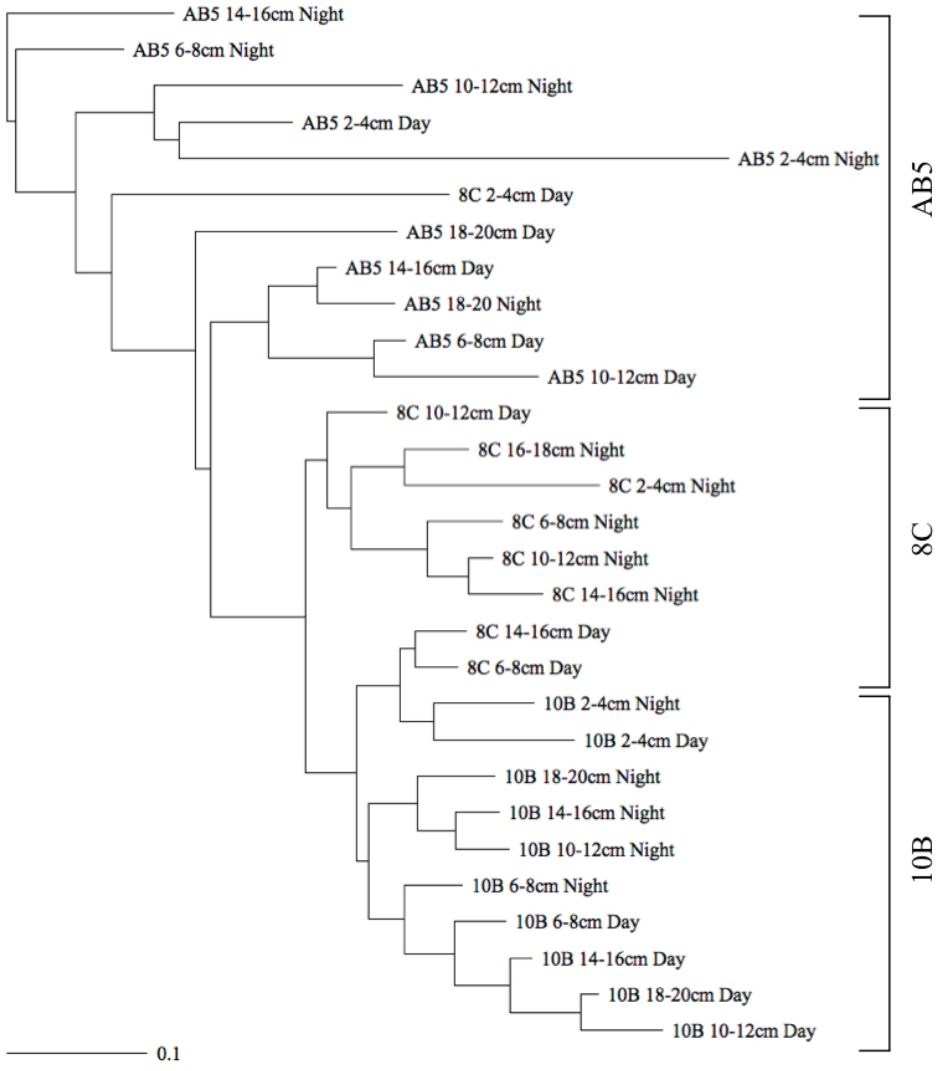

Figure 5.3. Hierarchal cluster analysis using geochemical characteristics of each sample including SO_4^{2-}, ΣH_2S, Fe, TOC, TC, TRS, and porosity. A pairwise comparison using these geochemical parameters produced a similarity matrix. A dendrogram was constructed using a neighbor-joining algorithm. Scale bar indicates 10% difference.

Molecular analysis: Pyrosequencing yielded 264,365 total sequences from 58 individual samples. The average number of sequences per depth was 4,558, which clustered into an average 2,073 OTUs per depth based upon a 95% sequence similarity (corresponding to a genus level classification). The greatest number of OTUs were noted in the surface sediments and the least number of OTUs were noted at depth. No significant difference in the OUT abundance was noted in the daytime and nighttime sampling. Site 8C had significantly ($p<0.05$) greater abundance of OTUs than sites 10B and AB5. Estimates of OTUs increased with number of sequences. A plot of OTUs versus the number of sequences yielded a rarefaction curve that approached a maximum, which corresponds to the Chao1 nonparametric estimate of species diversity (Figure 5.4). The Chao1 predicted that the total OTUs were under-sampled by an average of 139%. The upper estimate of OTU richness was calculated to be 11,957 in the sample 10B 2-4 cm (Figure 5.4). In general, sequences were evenly distributed within each OTU as indicated by an average evenness measured of $E>0.91$. Evenness and Chao1 estimates decreased with depth in each sediment core, similar to the trend in OTU abundance.

A Sorensen diversity index was used to characterize microbial communities based on time of sampling, location, or depth within the sediment column (Figure 5.5). The resulting matrix and the subsequent dendrogram illustrated the deepest branching lineages between the three sites. Additional secondary divisions within the tree formed distinct clades between the bottom of the core (>10 cm below surface) and the top of the core (<10 cm below surface).

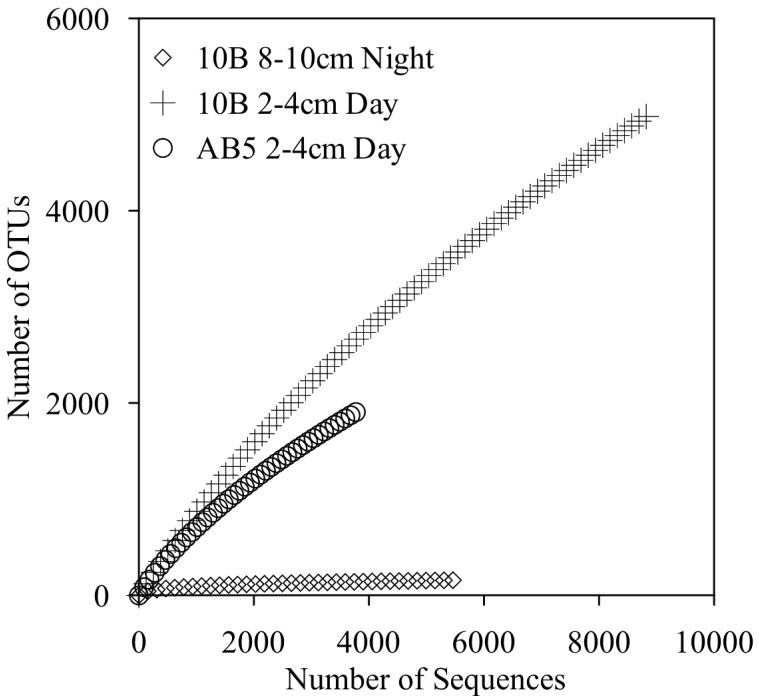

Figure 5.4. Rarefaction curves comparing the diversity of select samples. These three samples were chosen as they represent sequence data sets with the highest (10B Day 2-4 cm), lowest (10B Night 8-10 cm), and median (AB5 Day 2-4 cm) number of operational taxonomic units (OTU).

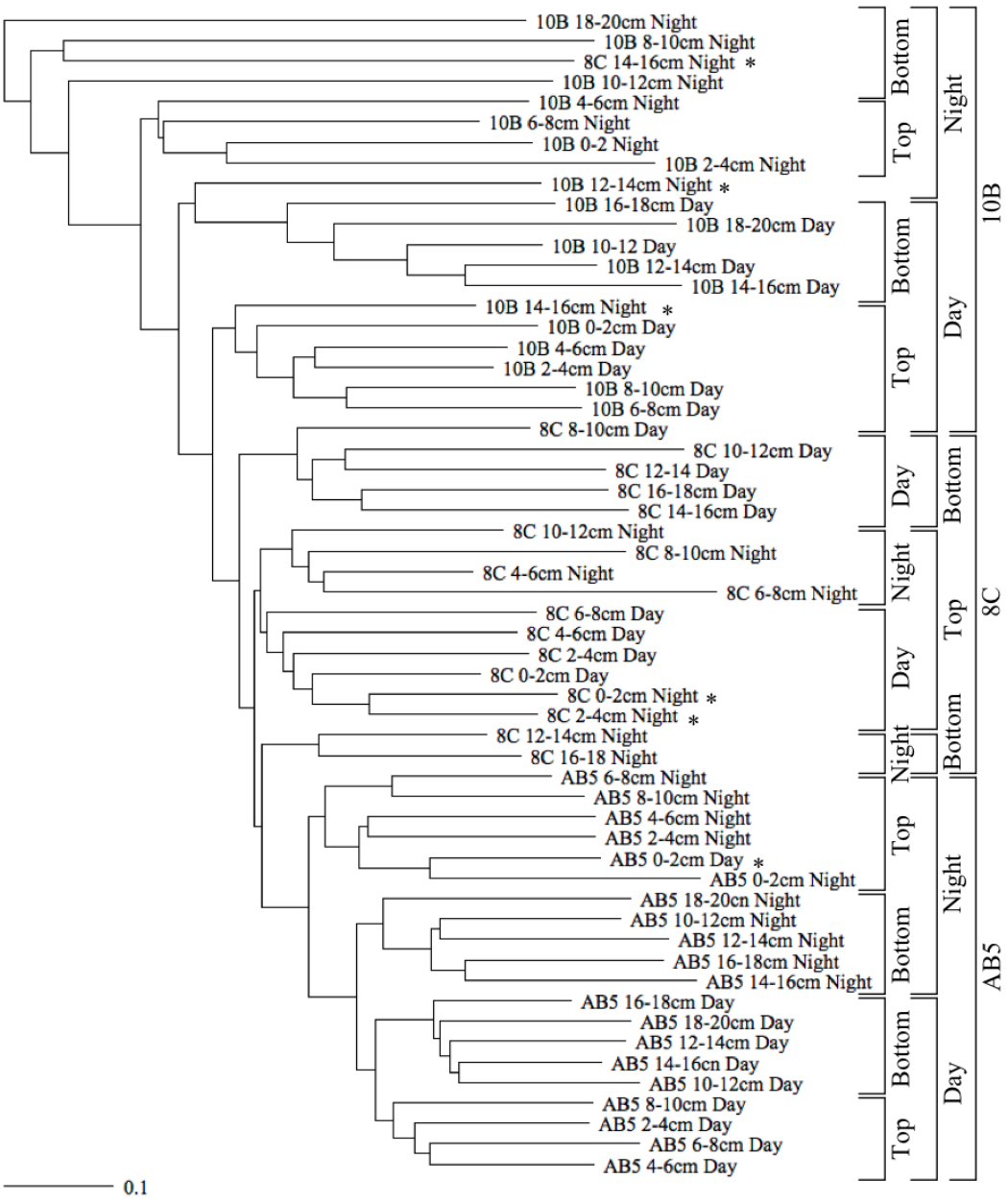

Figure 5.5. Phylogenetic similarity among locations and time of sample collection. Dendrogram was created from Sorensen's diversity index. Scale bar indicates 10% community difference.

Proteobacteria phylogenetics: An average of 76.9% of the total sequences were classifiable at the 70% confidence interval (CI) using the RDP database. The classified sequences were divided among 27 phyla. The single largest metabolically active phylum was *Proteobacteria*, with an overall average of 60.3% of total classified sequences. Among the *Proteobacteria*-related phylotypes, 89.4% could be classified above the CI and were divided among five classes, *Alphaproteobacteria* (average 2.3% of the total sequences), *Betaproteobacteria* (0.3%), *Deltaproteobacteria* (21.8%), *Epsilonproteobacteria* (0.1%) and *Gammaproteobacteria* (32.2%). *Alphaproteobacteria* was observed most frequently in the surface sediments and in greater abundance in the night cores. *Rhizobiales* and *Rhodobacterales* were the most frequently detected orders within *Alphaproteobacteria*. Within *Betaproteobacteria*, the order *Burkholderiales* was observed most frequently. *Epsilonproteobacteria*, specifically *Campylobacterales*, was only greater than 1% in one sample, 10B 6-8 cm Night.

Gammaproteobacteria–related sequences were detected in every sample and ranged from 6.7% of total sequences in 10B 16-18 cm Day depth to 70.9% in 8C 4-6 cm Night. A general decrease with depth was noted in each core. The abundance of *Gammaproteobacteria* within site 10B was significantly ($p<0.05$) less than sites AB5 and 8C; however, sites AB5 and 8C were not significantly different than each other. Furthermore, the difference between the abundance in the day and night cores was significant ($p<0.05$) at site AB5 and 8C, but not at site 10B. Within *Gammaproteobacteria*, sequences related to the orders *Alteromonadales*, *Chromatiales*, *Oceanospirillales*, and *Pseudomonadales* were detected most frequently. *Chromatiales*,

specifically *Chromatiaceae* and *Ectothiorhodospiraceae* families, was detected at each sample depth (0.08% in 10B 16-18 cm Night to 4.5% in 8C 10-12 cm Night). *Oceanospirillales* was less than 1% of the total classified sequences in all samples, except for 10B 14-16 cm Night and 8C 0-2 cm Night. The family *Pseudomonadaceae* within *Pseudomonadales* was observed in the highest abundance in 8C and lowest in AB5.

Deltaproteobacteria was observed to increase in abundance with depth and was highest at site AB5 and lowest at 8C. A significant difference ($p<0.05$) was noted in the sequence abundance between the daytime and nighttime sampling at 10B and 8C, but not at AB5. Overall, no significant difference in the abundance of *Deltaproteobacteria* was observed among the three sites. Within *Deltaproteobacteria*, the most abundant orders detected included *Desulfobacterales* and *Desulfuromonadales*. All of these lineages have been shown to reduce sulfate to sulfide. Sequences related to *Desulfobacterales* comprised more than 10% of the total classified sequences, on average, and was measured to be greatest in the bottom of the sediment column. Interestingly, lineages related to the family *Desulfobulbaceae* (within *Desulfobacterales*) showed the greatest frequency just below the sediment water interface at approximately 4-8 cm depth. *Desulfuromonadales*, including *Desulfuromonadaceae*, averaged 2.0% of all classified sequences and was highest in cores from 10B (1.1% - 14.1%) and lowest at AB5 (0.2% - 1.7%). Other notable lineage orders that were detected, but in lesser abundance, within *Deltaproteobacteria* included, *Desulfarculales*, *Desulfovibrionales*, *Desulfurellales*, *Myxococcales*, and *Syntrophobacterales*.

Non-*Proteobacteria* phylogenetics: The most abundant non-*Proteobacteria* phyla (> 1% of total sequences on average) outside of *Proteobacteria* included *Acidobacteria*, *Bacteroidetes*, *Chloroflexi*, *Cyanobacteria*, *Firmicutes*, *Fusobacteria* and *Planctomycetes*. Within *Acidobacteria*, *Holophagae* was the predominant class and was observed most frequently in the surface samples at site 10B and at mid-depth (6-12 cm below surface) at sites AB5 and 8C. *Bacteroidetes* and the sub-class *Bacteroidia* comprised as much as 24.0% of the total sequences in sample 10B 14-16 cm Night and 3.8% of the overall sequence abundance.

Anaerolineae, the prevalent class within *Chloroflexi*, was observed in every sample except 10B 8-10 cm Night with the greatest abundance in the top 10 cm of sediment. Sequences related to the *Cyanobacteria* phylum were also noted predominantly in the top few centimeters of sediment at each site, with the exception of 10B 16-18 cm Night in which this group was 24.9% of the total sequences.

The most abundant classes within *Firmicutes* were *Bacilli* and *Clostridia*. The *Firmicutes* ranged from 0.1% in AB5 10-12 cm Day to 60.4% in 10B 8-10 cm Night with the overall average 3.7% of total classified sequences. Despite the anomalously high abundance in the 10B Night core, no significant difference between the day and night sampling was noted in the *Firmicutes* phylum at all locations. Furthermore, no significant difference was noted between sites.

Fusobacteria phylum and the sub-class *Fusobacteria* averaged 1.0% of the total classified sequences and were most abundant in the deepest sediment at AB5 and at the mid-depth layers in 10B and 8C. *Planctomycetacia* class (*Planctomycetes*) was detected

more frequently in 10B and 8C than site AB5. The average abundance was 1.2% of total sequences and the maximum abundance was 3.9% in sample 10B 16-18 cm Day depth.

The abundances of active lineages detected within this study with known potential functions related to sulfur or iron cycling have been combined in order to identify trends (Figure 5.2). Sulfide oxidizing bacteria (SOB) families included *Hydrogenophilaceae*, *Ectothiorhodospiraceae*, *Thiotricaceae* and *Chromatiaceae* (Orcutt et al. 2011). Combined, these groups showed a significant ($p<0.05$) decrease with depth in each sediment core. Lineages that have been attributed to sulfate reducing bacteria (SRB) in marine systems included *Desulfobacteraceae*, *Desulfobulbaceae*, *Desulfuromonadaceae* and *Syntrophobacteraceae* (Nealson 1997; Pereira et al. 2007). A small, but significant ($p<0.05$) decrease with depth was observed with the SRB lineages. Iron oxidizing bacteria (FeOB) included *Nitrospiraceae* and *Burkholderiales* (Coates et al. 1999; Emerson et al. 2010). No significant change with depth was noted in the FeOB lineages. Sequences phylogenetically related to the *Geobacteraceae*, *Shewanellaceae*, *Campylobacteraceae*, *Pseudomonadaceae*, *Pelobacteraceae*, *Ferrimonadaceae* (Fredrickson and Gorby 1996; Orcutt et al. 2011) genera were lineages determined as capable of iron reduction (FeRB) and combined were observed to significantly ($p<0.05$) increase with depth.

Discussion

The interpretation of the structure and function of the microbial ecology during this study was based on the active bacterial cells using rRNA gene transcripts and not

DNA. Due to the stability of DNA in quiescent, dead, and active cells, studies based on DNA genetics describe the taxa and metabolic pathways from the total microbial community present in the sediment. Therefore, the taxa and metabolic pathways identified within the microbial community may not be relevant to observed changes in the geochemistry. However, the metabolically active taxa within the total population can be identified by isolation and characterization of small subunit (SSU) rRNA. The concentration of ribosomes, and thus copies of SSU rRNA within a cell, is linearly correlated to cellular metabolic activity (Delong et al. 1989; Kerkhof and Ward 1993), with quiescent and dead cells having few to no ribosomes present (Fegatella et al. 1998). All phylogenetic classifications in this study were interpreted with the understanding and minimization of known analytical biases and therefore were checked for quality assurance. Only one of the 58 total samples was discarded during the phylogenetic and statistical analysis. Sample 10B 16-18 cm Night was excluded because a high frequency of *Cyanobacteria* (24.9% of total sequences) was observed, indicative of water column intrusion. This conclusion is supported by phylogenetic research of the microbial community within the water column in this area indicating the dominance of *Cyanobacteria* (unpublished data).

The communities were compared pairwise using the Sorensen's index. This index only calculates absence or presence of common lineage and does not account for frequency shifts. Such a comparison becomes less statistically significant as the number of OTU (i.e., points of comparison) near one or the populations are not evenly distributed. The most deep branching communities on the dendrogram (i.e., 10B 8-10 cm

Night, 10B 10-12 cm Night, 10B 18-20 cm Night, and 8C 14-16 cm Night) may be a result of the latter. The OTUs calculated for these communities ranged from 160 to 552, while the evenness for these groups were calculated to be less than 0.8.

Sequence analysis sample 10B 8-10 cm Night indicated a very high frequency of the orders *Bacillales* and *Lactobacillales* (>60% of the total classified sequences) compared to other samples in this study. Other phyla (e.g., *Proteobacteria*) were abnormally low in this sample as well. Additional samples that were biased toward *Firmicutes* included 10B 10-12 cm Night, 10B 18-20 cm Night, and 8C 14-16 cm Night. Likely, these samples are a reflection of an infaunal polychaete burrow or cast that skewed the analysis toward fermenting bacteria. *Bacillus* (*Firmicutes*) clones have been shown in previous studies to increase in abundance within the biofilm that lined worm casts as compared to the surrounding soil phylogeny (Furlong et al. 2002). Several unidentified polychaetes were observed during the sediment sectioning at similar depths to these samples. Although the phylogenetic analysis reflects this abnormality, geochemical evidence was not seen because of the sampling procedures. The burrow was likely limited to one of the cores designated for molecular analysis, and the geochemical measurements were an average of duplicate sampling. The effects of bioturbation at depth appear to be minimal within these sediments.

Linking geochemical observations to microbial community: The description of microbial function through the use of phylogenetic analyses relies on the assumptions that functional properties are conserved among populations that are phylogenetically related,

and that the biochemical processes of culturable microorganisms are also carried out by phylogenetically related non-culturable species (Lambais et al. 2008).

Typical biogeochemical zonation (Boudreau and Jorgensen 2000) with depth was not observed in the sediment profile at any of the three locations. Similar results were observed in a previous study that focused on site 8C in the western hypoxic zone (Reese et al. 2011b). Sulfide, a geochemical signature of sulfate reduction within the sediment, was only measured at AB5. However, an active sulfate reducing bacteria (SRB) population was ubiquitous throughout all samples analyzed, which indicated the presence of sulfate reduction at all locations. In conjunction with an active SRB community, active SOB were observed at all depths which indicates that a portion of sulfide produced was likely reoxidized to sulfate. A previous study measuring sulfate reduction rates using ^{35}S analysis detected sulfate reduction within sediments with active sulfur oxidizing bacteria (Reese et al. 2011c). Similar low sulfide concentrations were detected. Iron reducing bacteria (FeRB) and iron oxidizing bacteria (FeOB) were observed in juxtaposition with one another indicating a similar scenario for the iron cycle. Additionally, reactive iron has been shown to be an effective sequestration mechanism for sulfide in the environment, inhibiting the detection of sulfide within the pore water. Redox zonation was not well-defined in each of the sites in this study. This agrees with previous research in coastal sediments that found crystalline Fe-oxyhydroxides and sulfate reduction was not limited to one depth (Postma and Jakobsen 1996). Previous studies have shown that sulfate reduction occurs once amorphous Fe is depleted (Postma and Jakobsen 1996).

Reactive iron and degree of pyritization: The pool of total sediment iron can be partitioned into three operationally defined iron fractions with respect to their reactivity towards dissolved microbially-produced sulfide (Raiswell and Canfield 1998). The assumption is that extractable iron represents a labile fraction of sedimentary iron that is available for pyrite formation. The degree of reactivity towards sulfide among the various forms of iron present in marine sediments differs from hours to geologic timescales (Holmkvist et al. 2011; Raiswell and Canfield 1998). Poorly reactive iron (e.g., iron extracted by HCl method minus iron extracted by citrate dithionate (CD) method) primarily consists of iron silicates that are not highly reactive towards sulfide on early diagenetic time scales (half life time > 105 yr) (Canfield et al. 1992). The HCl method leaches iron from silicate minerals as well as amorphous Fe(III) oxides, whereas the CD method extracts all amorphous Fe(III) oxides and crystalline iron oxides (e.g., ferrihydrite, lepidocrite, hematite) (Kostka and Luther 1994; Lyons and Severmann 2006). The amount of iron extractable by the HCl method exceeded the amount extractable by the CD method at site 10B and the deep sediments (> 10 cm) of AB5, indicating these areas are dominated by iron that is poorly reactive toward sulfide. Site 8C and the shallow sediment of AB5 (< 10 cm) was dominated by iron that it is extractable by the CD method, indicating these areas was abundant in crystalline Fe(III) oxides and very low in non-reactive silicates. These sediments would react rapidly with sulfide produced during biological sulfate reduction and inhibit detection within the porewater.

Raiswell and Canfield (1998) have defined highly reactive iron (e.g., iron extracted by CD method plus TRS) as the fraction of iron that may react with sulfide to form iron sulfide minerals. Site AB5 had a whole-core average of 51.2% more highly reactive iron than sites 8C and 10B, in which the later two were relatively equal in abundance. This indicates that AB5 site had the highest potential for pyrite formation and perhaps younger sediments. Although the potential exists for iron sulfide minerals to be produced, reactive organic matter and thus microbial sulfide production has been shown to limit actual pyritization in marine sediments (Burdige 2006), as shown by the degree of pyritization (DOP).

The DOP is a measure of the extent to which reactive Fe has been converted to pyrite and was first used to distinguish environments where FeS_2 is either Fe or carbon limited (Raiswell and Berner 1985). The DOP using HCl at AB5 (0.23) and 10B (0.28) were the lowest on average, and highest at 8C (0.70). The high DOP values at 8C indicated an iron-limited environment and low values at AB5 and 10C indicated an iron-rich environment. The DOP calculated at 8C in the northern Gulf of Mexico was similar to brackish and marine estuaries (Morse et al. 2007) and gas hydrate cores (Morse et al. 2002). Furthermore, Raiswell et al. (1988) reported typical values of DOP based on HCl extraction method were less than 0.42 for sediments deposited during oxygenated conditions, 0.42 to 0.8 for intermediate oxygen environments and 0.55 to 0.93 for euxinic depositional conditions. This indicates that the top 20 cm of sediment analyzed during this study at site 8C were deposited in a low oxygen or euxinic environment,

according to the DOP. Sites AB5 and 10B were possibly deposited during oxygenated conditions.

DOP calculations based on the CD method have been used as a measure of reactive iron because it extracts only a small fraction of the poorly reactive iron silicates (Raiswell et al. 1994). While iron extracted using the HCl method (FeH) is important on geologic timescales, iron extracted using the CD method (FeCD) is a better indicator of short-term processes occurring in estuary sediments. The DOP based on the CD extraction method showed that AB5 (0.22) and 8C (0.26) were lowest and 10B was highest (0.44), indicating that less than half of the reactive iron was converted to pyrite and therefore an additional factor, such as carbon, may be limiting. The apparent discrepancy in this study between the DOP based on the HCl method and the CD method reflects the different types of sedimentary iron released by the two techniques.
The resulting pyrite (i.e., TRS) concentrations at AB5 were higher than sites 10B and 8C. This indicates a higher potential for iron sulfide mineral formation at AB5 because 1) the availability of reactive iron or 2) the availability of organic carbon for sulfide production. Results suggest both of these cases were true for site AB5. However, sites 10B and 8C had equal potential for pyritization, yet the TRS concentrations at 10B were nearly twice that of 8C. The availability of highly reactive iron was also greater at 8C than 10B. This leads to the supposition that the availability of organic matter and thus microbially produced sulfide was limiting at 8C.

At all locations, lineages related to FeRB were most abundant in zones with the highest FeCD. This small but significant increase in FeRB abundance indicates that the

microbial activity increased where their primary electron donor concentrations were greatest. A relatively high concentration of TRS was also noted in the same zone, suggesting the occurrence of sulfate reduction. This is in agreement with the high frequency of SRB observed at this depth as well. No dissolved sulfide was measured above the method detection limit, and was likely sequestered as pyrite.

Spatial and temporal variability of microbial community: High resolution community analysis indicated biogeochemical spatial heterogeneity between the three sites within the northern Gulf of Mexico hypoxic zone. The deepest branching clades (i.e., greatest community difference) in the dendrogram were observed when comparing each of the three locations (Figure 5.5). The low percentage of shared lineages between the clades suggests the potential for geographic and geochemical isolation within the region. Similar conclusions have been noted in other studies describing biogeographic isolation in which spatial separation of two or more populations lead to genetic diversity (Cho and Tiedje 2000; Papke et al. 2003; Papke and Ward 2004), including a study in the western hypoxic zone (Reese et al. 2011b). However, this study also supports geochemistry as an additional driver for population divergence.

Populations tend to evolve based on local geochemical conditions. In turn, these populations can influence the surrounding geochemistry creating an independent feedback loop vastly different from the parent population. This feedback was evident in the geochemical dendrogram as it supported the basic branching patterns of the phylogenetic tree. The concentrations of TOC, TC, sulfide, iron, and reactive iron were

significantly different at AB5 than at 8C or 10B. In addition, the higher abundance of the dissolved and reactive compounds lead to the development of a more pronounced solid-phase geochemical signature at AB5. The combination of benthic population and geochemical variability within the sediments should be considered in general models describing mechanisms controlling hypoxia in this region.

The large geographic clades within the phylogenetic dendrogram further divided into differences based on depth. The top and bottom 10 cm of sediment from each core clustered independent of each other indicating a shift in population at that depth. A noticeable influence on the microbial community variation was the increase of TOC as sediment depth increased. The significant variation between the top and bottom sediment communities has been observed in other studies (Mills et al. 2008; Reese et al. 2011b; Tsertova et al. 2011). This was also reflected in the geochemical dendrogram in which the geographic clades were also subdivided into clusters based on depth. At 8C, the top 10 cm from both Day and Night sampling points clustered on one clade with the 0-2 cm and 2-4 cm samples having the most community similarity. The same general trend was observed at sites AB5 and 10B, but only AB5 had the 0-2 cm Night and Day samples grouping together. The depth of similarity between cores suggests a surface water influence homogenizing the chemistry and microbial communities. It is interesting to hypothesize that the advective flow into the sediment is greatest at 8C and least at 10B. In addition, higher microbial activity in the sediments can rapidly alter the surface water geochemically as it enters the sediment. If 10B has high metabolic activity at the surface, the deeper depths would be geochemically isolated, promoting localized divergence of

populations. These observations further support the importance and connectivity of the microbial ecology and the geochemical environment.

The collection of cores during the day (noon) and night (midnight) provided the opportunity to explore a hypothesized diurnal shift in the microbial ecology. Although, the phylogenetic dendrogram showed slight clustering based on temporal variability, the geochemical dendrogram showed no diurnal connection. The highest variability was predicted to be at the surface, however two of the three sites had the surface samples as most closely pair. The clusters are therefore concluded to be a reflection of inter-core variability. Future targeted studies are needed to address the level of heterogeneity within sites.

CHAPTER VI

SUMMARY

The study of biogeochemical cycles has emerged as a dominant field of marine research over the past 50 years. As this field has evolved and new technologies have been developed, the ability and need to intertwine various disciplines has become critical. Shallow coastal sediments found in the northern Gulf of Mexico and along the Texas coast have proven to be an ideal, dynamic location to test many hypotheses regarding the interaction of the active microbial ecology with the geochemical environment. In coastal and estuarine environments, a large portion of benthic respiration has been attributed to sulfate reduction (Canfield 1989; Chambers et al. 1994; Jorgensen 1982) and implicated as an important mechanism in hypoxia formation (Ma et al. 2006). This research focuses on sulfur and iron cycling. Data collected showed their interdependence with each other and was able to provide further understanding of the connectivity to the microbial population. Additionally, the use of high-resolution sampling of individual sediment cores and high throughput nucleic acid extraction techniques combined with 454 FLX sequencing provided a robust understanding of the benthic microbial community.

A colorimetric method was developed to accurately determine dissolved hydrogen sulfide concentrations based on the methylene blue method of Cline (1969). The modifications allowed the researcher to easily adapt the method sampling, preservation, and analytical techniques to a variety of environments. The procedure

outlined also allowed the researcher to determine the concentration range and refine the method by making a mixed diamine reagent to suit the situation.

Linking sulfate reduction rate measurements to the phylogenetics derived from SSU rRNA gene transcripts, three distinct communities were observed in the Nueces estuary: 1) a classic sulfate reduction profile in which sulfate was depleted and sulfide was accumulated along with a corresponding increase in abundance of sulfate reducing bacteria with sediment depth; 2) a profile with no sulfate loss or sulfide accumulation, but an equal abundance of sulfate reducers and sulfide oxidizers indicative of a cryptic sulfur cycle; and 3) a profile with equal abundance of sulfate reducers and iron reducers producing compounds which react to form solid phase iron sulfides, therefore sulfate reduction geochemical signatures are masked within the sediment column. Despite initial appearances that sulfate reduction was not occurring in the last two scenarios, this study showed the importance of simultaneously analyzing the active microbial community and multiple geochemical reservoirs to determine the extent of sulfate reduction within sediments.

Elucidating the effects of the active microbial ecology and the mechanisms of sequestration on sulfide produced within the sediment provided an opportunity to understand the mechanisms controlling hypoxia in the western portion of the Gulf of Mexico hypoxic zone. Historical models of the area indicated that sulfide release from the sediments is a contributing factor to water column hypoxia along the coastal shelf. However, the current research herein showed that aqueous sulfide did not accumulate within the sediment pore water due to microbial recycling and sequestration as iron

sulfides. Additionally, a discontinuity was observed in the microbial community between the upper and lower portions of the sediment column, indicating that only the top 10 cm interacts with the water column and varies with seasons while the bottom 10 cm was specific to the location. Both the geochemistry and molecular biology also suggested the lack of organic carbon within the sediments inhibited microbial activity.

The results from the western portion of the Gulf of Mexico hypoxic zone were used to further hypothesize diurnal variability as well as greater spatial diversity among the geochemistry and microbial community in other locations closer to the Mississippi River. Multiple geochemical assays were used to determine the degree of pyritization, a ratio that determined iron limitation and the potential for sulfide dissolution in the pore water. Site specific differences were observed, however each site had a low potential for sulfide accumulation. Although marginal differences were noted in the day and night cores both geochemically and biologically, a prominent difference was observed between the sample locations and with depth into the sediment column. This indicates the importance of studies and models to consider the biogeography of the microbial community along with understanding small-scale variations that impact the overall biogeochemical cycling of redox elements.

REFERENCES

Akob DM, Mills HJ, Gihring TM, Kerkhof L, Stucki JW, Anastacio AS, Chin KJ, Kusel K, Palumbo AV, Watson DB et al. 2008. Functional diversity and electron donor dependence of microbial populations capable of U(VI) reduction in radionuclide-contaminated subsurface sediments. Applied and Environmental Microbiology 74:3159-3170.

Akob DM, Mills HJ, Kostka JE. 2007. Metabolically active microbial communities in uranium-contaminated subsurface sediments. Fems Microbiology Ecology 59(1):95-107.

Allison MA, Kineke GC, Gordon ES, Goni MA. 2000. Development and reworking of a seasonal flood deposit on the inner continental shelf off the Atchafalaya River. Continental Shelf Research 20(16):2267-2294.

APHA (American Public Health Association). 1998. Standard methods for the examination of water and wastewater. 9 ed. Washington, DC: American Public Health Association, American Water Works Association, and Water Pollution Control Federation. p. 4127-4127

Baumgartner LK, Reid RP, Dupraz C, Decho AW, Buckley DH, Spear JR, Przekop KM, Visscher PT. 2006. Sulfate reducing bacteria in microbial mats: Changing paradigms, new discoveries. Sedimentary Geology 185(3-4):131-145.

Belasco JG. 1993. mRNA degradation in prokaryotic cells: An overview. In: Belasco JG, Brawerman G, editors. Control of messenger RNA stability. San Diego, CA: Academic Press. p. 3–12.

Bennett P, Omelon C. 2011. Microbial geochemistry: An intersection of disciplines. In: Harmon R, Parker A, editors. Frontiers in Geochemistry: Contribution of geochemistry to the study of Earth. Oxford, UK: John Wiley and Sons. p. 175-194.

Berner R. 1970. Sedimentary pyrite formation. American Journal of Science 268(1):1-23.

Berner R. 1982. Burial of organic cabon and pyrite sulfur in the modern ocean: its geochemical and environmental significance. American Journal of Science 282:451-473.

Bianchi TS, DiMarco SF, Cowan JH, Hetland RD, Chapman P, Day JW, Allison MA. 2010. The science of hypoxia in the Northern Gulf of Mexico: A review. Science of the Total Environment 408(7):1471-1484.

Boudreau BP, Jorgensen BB. 2000. The Benthic Boundary Layer: Transport Processes and Biogeochemistry. New York, NY: Oxford University Press.

Budd MS, Bewick HA. 1952. Photometric determination of sulfide and redicible sulfur in alkalies. Analytical Chemistry 24:1536-1540.

Buhring SI, Ehrenhauss S, Kamp A, Moodley L, Witte U. 2006. Enhanced benthic activity in sandy sublittoral sediments: Evidence from 13C tracer experiments. Marine Biology Research 2:120-129.

Burdige DJ. 2006. Geochemistry of marine sediments. Princeton, NJ: Princeton University Press.

Canfield DE. 1989. Reactive iron in sediments. Geochimica Cosmochim Acta 53:619-632.

Canfield DE. 1991. Sulfate reduction in deep-sea sediments. American Journal of Science 291(2):177-188.

Canfield DE, Berner RA. 1987. Dissolution and pyritization of magnetite in anoxic marine sediments. Geochimica et Cosmochimica Acta 51(3):645-659.

Canfield DE, Raiswell R, Bottrell S. 1992. The reactivity of sedimentary iron minerals toward sulfide. American Journal of Science 292(9):659-683.

Canfield DE, Raiswell R, Westrich JT, Reaves CM, Berner RA. 1986. The use of chromium reduction in the analysis of reduced inorganic sulfur in sediments and shales. Chemical Geology 54(1-2):149-155.

Canfield DE, Stewart FJ, Thamdrup B, De Brabandere L, Dalsgaard T, Delong EF, Revsbech NP, Ulloa O. 2010. A cryptic sulfur cycle in oxygen-minimum-zone waters off the Chilean coast. Science 330(6009):1375-1378.

Canfield DE, Thamdrup B, Kristensen E. 2005. Aquatic Geomicrobiology. San Diego, CA: Elsevier Academic Press.

Capone DG, Kiene RP. 1988. Comparison of microbial dynamics in marine and fresh-water sediments - Contrasts in anaerobic carbon catabolism. Limnology and Oceanography 33(4):725-749.

Chambers RM, Hollibaugh JT, Vink SM. 1994. Sulfate reduction and sediment metabolism in Tomales Bay, California Biogeochemistry 25(1):1-18.

Chin K-J, Esteve-Nunez A, Leang C, Lovley DR. 2004. Direct correlation between rates of anaerobic respiration and levels of mRNA for key respiatory genes in *Geobacter sulfurreducens*. Applied and Environmental Microbiology 70:5183-5189.

Chin K-J, Sharma ML, Russell LA, O'Neill KR, Lovley DR. 2008. Quantifying expression of a dissimilatory (bi) sulfite reductase gene in petroleum-contaminated marine harbor sediments. Microbial Ecology 55(3):489-499.

Cho JC, Tiedje JM. 2000. Biogeography and degree of endemicity of fluorescent *Pseudomonas* strains in soil. Applied and Environmental Microbiology 66(12):5448-5456.

Cline JD. 1969. Spectrophotometric determination of hydrogen sulfide in natural waters. Limnology and Oceanography 14:454-458.

Coates JD, Lonergan DJ, Phillips EJP, Jenter H, Lovley DR. 1995. *Desulfuromonas palmitatis* sp. nov., a marine dissimilatory Fe(III) reducer that can oxidize long-chain fatty acids. Archael Microbiology 164:406-413.

Coates JD, Michaelidou U, Bruce RA, O'Connor SM, Crespi JN, Achenbach LA. 1999. Ubiquity and Diversity of Dissimilatory (Per)chlorate-Reducing Bacteria. Applied and Environmental Microbiology 65(12):5234-3445.

Cook RC, Kelly CA. 1992. Sulphur cycling and fluxes in temperate dimictic lakes. In: Howarth RW, Stewart JWB, Ivanov MU, editors. Sulphur cycling on the continents: wetlands, terrestrial ecosystems and associated water bodies. Oxford, UK: John Wiley and Sons.

Corbett DR, McKee B, Duncan D. 2004. An evaluation of mobile mud dynamics in the Mississippi River deltaic region. Marine Geology 209(1-4):91-112.

Cornwell JC, Morse JW. 1987. The characterization of iron sulfide minerals in anoxic marine sediments. Marine Chemistry 22(2-4):193-206.

Cypionka H, Widdel F, Pfenning N. 1985. Survival of sulfate-reducing bacteria after oxygen stress, and growth in sulfate-free oxygen-sulfide gradients. Fems Microbiology Ecology 31(1):39-45.

Dagg MJ, Breed GA. 2003. Biological effects of Mississippi River nitrogen on the northern gulf of Mexico - a review and synthesis. Journal of Marine Systems 43(3-4):133-152.

Delong EF, Wickham GS, Pace NR. 1989. Phylogenetic stains - Ribosomal RNA-based probes for the identification of single cells. Science 243(4896):1360-1363.

Diaz RJ, Rosenberg R. 1995. Marine benthic hypoxia: A review of its ecological effects and the behavioural responses of benthic macrofauna. Oceanography and Marine Biology - an Annual Review 33:245-303.

Diaz RJ, Rosenberg R. 2008. Spreading dead zones and consequences for marine ecosystems. Science 321(5891):926-929.

DiMarco SF, Chapman P, Walker N, Hetland RD. 2010. Does local topography control hypoxia on the eastern Texas-Louisiana shelf? Journal of Marine Systems 80(1-2):25-35.

Dowd SE, Zaragoza J, Rodriguez JR, Oliver MJ, Payton PR. 2005. Windows.NET network distributed basic local alignment search toolkit (W.ND-BLAST). BMC Bioinformatics 6:93. DOI: 10.1186/1471-2105-6-93.

Eldridge PM, Morse JW. 2008. Origins and temporal scales of hypoxia on the Louisiana shelf: Importance of benthic and sub-pycnocline water metabolism. Marine Chemistry 108(3-4):159-171.

Emerson D, Fleming EJ, McBeth JM. 2010. Iron-oxidizing bacteria: An environmental and genomic perspective. Annual Review of Microbiology 64: 561-583.

EPA (United States Environmental Protection Agency). 2002. Mid-Atlantic Integrated Assessment (MAIA) Estuaries 1997-98: Summary Report, EPA/620/R-02/003. No. EPA/620/R-02/003.

Fegatella F, Lim J, Kjelleberg S, Cavicchioli R. 1998. Implications of rRNA operon copy number and ribosome content in the marine oligotrophic ultramicrobacterium *Sphingomonas* sp. strain RB2256. Applied and Environmental Microbiology 64(11):4433-4438.

Felsenstein J. 1989. PHYLIP- Phylogeny inference package (version 3.2). Cladistics 5:164-166.

Fischer E. 1883. Bildung von Methyleblau als Reaction auf Schwefelsasserstoff. Chem. Ber. 26:2234-2236.

Fleming JT, Sanseverino J, Sayler GS. 1993. Quantitative relationship between napthalene catabolic gene-frequency and expression in predicting PAH degradation in soils at soils at town gas manufacturing sites. Environmental Science and Technology 27(6):1068-1074.

Fogo JK, Popowsky M. 1949. Spectrophotometric determination of hydrogen sulfide-methylene blue method. Analytical Chemistry 21:732-734.

Fossing H, Jorgensen BB. 1989. Measurement of bacterial sulfate reduction in sediments: Evaluation of single-step chromium reduction methods. Biogeochemistry 8:223-245.

Fredrickson JK, Gorby YA. 1996. Environmental processes mediated by iron-reducing bacteria. Current Opinion in Biotechnology 7(3):287-294.

Froelich PN, Klinkhammer GP, Bender ML, Luedtke NA, Heath GR, Cullen D, Dauphin P, Hammond D, Hartman B, Maynard V. 1979. Early oxidation of organic matter in pelagic sediments of the eastern equatorial Atlantic - suboxic diagenesis. Geochimica et Cosmochimica Acta 43(7):1075-1090.

Furlong MA, Singleton DR, Coleman DC, Whitman WB. 2002. Molecular and culture-based analyses of prokaryotic communities from an agricultural soil and the burrows and casts of the earthworm Lumbricus rubellus. Applied and Environmental Microbiology 68(3):1265-1279.

Gardner WS, McCarthy MJ, Carini SA, Souza AC, Lijun H, McNeal KS, Puckett MK, Pennington J. 2009. Collection of intact sediment cores with overlying water to study nitrogen- and oxygen-dynamics in regions with seasonal hypoxia. Continental Shelf Research 29(18):2207-2213.

Giovannoni JJ, Wing RA, Ganal MW, Tanksley SD. 1991. Isolation of molecular markers from specific chromosomal intervals using DNA pools from existing mapping populations. Nucleic Acids Research 19:6553-6558.

Gontcharova V, Youn E, Wolcott RD, Hollister EB, Gentry TJ, Dowd SE. 2010. Black box chimera check (B2C2): A windows-based software for batch depletion of chimeras from bacterial 16S rRNA gene datasets. Open Microbiology Journal 4:47-52.

Green RE, Bianchi TS, Dagg MJ, Walker ND, Breed GA. 2006. An organic carbon budget for the Mississippi River turbidity plume and plume contributions to air-sea CO2 fluxes and bottom water hypoxia. Estuaries and Coasts 29(4):579-597.

Hallberg KB, Hedrich S, Johnson DB. 2011. *Acidiferrobacter thiooxydans*, gen. nov. sp. nov.; an acidophilic, thermo-tolerant, facultatively anaerobic iron- and sulfur-oxidizer of the family *Ectothiorhodospiraceae*. Extremophiles 15(2):271-279.

Handl S, Dowd SE, Garcia-Mazcorro JF, Steiner JM, Suchodolski JS. 2011. Massive parallel 16S rRNA gene pyrosequencing reveals highly diverse fecal bacterial and fungal communities in healthy dogs and cats. FEMS Microbial Ecology:1-10.

Hartig E, Zumft WG. 1999. Kinetics of nirS expression (cytochrome cd(1) nitrite reductase) in *Pseudomonas stutzeri* during the transition from aerobic respiration to denitrification: Evidence for a denitrification-specific nitrate- and nitrite-responsive regulatory system. Journal of Bacteriology 181(1):161-166.

Hetland RD, DiMarco SF. 2008. How does the character of oxygen demand control the structure of hypoxia on the Texas-Louisiana continental shelf? Journal of Marine Systems 70(1-2):49-62.

Holmes DE, Bond DR, O'Neil RA, Reimers CE, Tender LR, Lovley DR. 2004. Microbial communities associated with electrodes harvesting electricity from a variety of aquatic sediments. Microbial Ecology 48:178-190.

Holmkvist L, Ferdelman TG, Jorgensen BB. 2011. A cryptic sulfur cycle driven by iron in the methane zone of marine sediment (Aarhus Bay, Denmark). Geochimica et Cosmochimica Acta 75(12):3581-3599.

Horner-Devine MC, Leibold MA, Smith VH, Bohannan BJM. 2003. Bacterial diversity patterns along a gradient of primary productivity. Ecology Letters 6(7):613-622.

Howarth RW, Merkel S. 1984. Pyrite formation and the measurement of sulfate reduction in salt-marsh sediments. Limnology and Oceanography 29(3):598-608.

Ingvorsen K, Zeikus JG, Brock TD. 1981. Dynamics of bacterial sulfate reduction in a eutrophic lake. Applied and Environmental Microbiology 42(6):1029-1036.

Jahnke R, Richards M, Nelson J, Robertson C, Rao A, Jahnke D. 2005. Organic matter remineralization and porewater exchange rates in permeable South Atlantic Bight continental shelf sediments. Continental Shelf Research 25(12-13):1433-1452.

Jaramillo S, Sheremet A, Allison MA, Reed AH, Holland KT. 2009. Wave-mud interactions over the muddy Atchafalaya subaqueous clinoform, Louisiana, United States: Wave-supported sediment transport. Journal of Geophysical Research-Oceans 114:C04002. DOI: 10.1029/2008JC004821.

Jeffrey WH, VonHaven R, Hoch MP, Coffin RB. 1996. Bacterioplankton RNA, DNA, protein content and relationships to rates of thymidine and leucine incorporation. Aquatic Microbial Ecology 10(1):87-95.

Jorgensen BB. 1977. Sulfur cycle of a coastal marine sediment (Limfjorden, Denmark). Limnology and Oceanography 22(5):814-832.

Jorgensen BB. 1978. Comparison of methods for the quantification of bacterial sulfate reduction in coastal marine sediments. 1. Measurement with radiotracer techniques. Geomicrobiology Journal 1(1):11-27.

Jorgensen BB. 1982. Mineralization of organic matter in the sea bed - The role of sulfate reduction. Nature 296(5858):643-645.

Jorgensen BB, Postgate JR. 1982. Ecology of the bacteria of the sulfur cycle with special reference to anoxic oxic interface environments. Philosophical Transactions of the Royal Society of London Series B-Biological Sciences 298(1093):543-561.

Kashefi K, Lovley DR. 2003. Extending the upper temperature limit for life. Science 301(5635):934-934.

Kerkhof LJ, Ward BB. 1993. Comparison of nucleic acid hybridization and fluorometry for measurement of RNA/DNA relationship with growth rate in a marine bacterium. Applied and Environmental Microbiology 59:1303-1307.

Kloster MB, King MP. 1977. The determination of sulfide with DPD. Journal American Water Works Association 69:544-546.

Koster M, Meyer-Reil LA. 2001. Characterization of carbon and microbial biomass pools in shallow water coastal sediments of the southern Baltic Sea (Nordrugensche Bodden). Marine Ecology-Progress Series 214:25-41.

Kostka JE, Gribsholt B, Petrie E, Dalton D, Skelton H, Kristensen E. 2002. The rates and pathways of carbon oxidation in bioturbated saltmarsh sediments. Limnology and Oceanography 47:230-240.

Kostka JE, Luther GW. 1994. Partitioning and speciation of solid-phase iron in salt marsh sediments. Geochimica et Cosmochimica Acta 58(7):1701-1710.

Kostka JE, Nealson KH. 1995. Dissolution and reduction of magnetite by bacteria. Environmental Science and Technology 29(10):2535-2540.

Laier T, Jorgensen NO, Buchardt B, Cederberg T, Kuijpers A. 1992. Accumulation and seepages of biogenic gas in northern Denmark. Continental Shelf Research 12(10).

Lambais MR, Otero XL, Cury JC. 2008. Bacterial communities and biogeochemical transformations of iron and sulfur in a high saltmarsh soil profile. Soil Biology and Biochemistry 40(11):2854-2864.

Lawrence NS, Davis J, Compton RG. 2000. Analytical strategies for the detection of sulfide: A review. Talanta 52(5):771-784.

Leming TD, Stuntz WE. 1984. Zones of coastal hypoxia revealed by satellite scanning have implications for strategic fishing. Nature 310(5973):136-138.

Lin S, Morse JW. 1991. Sulfate reduction and iron sulfide mineral formation in the Gulf of Mexico anoxic sediments. American Journal of Science 291(1):55-89.

Lindsay WG. 1901. On a colorimetric method for the estimation of sulphur in pig iron. The School of Mines Quarterly 23:24-27.

Lindsay SS, Baedecker MJ. 1988. Determination of aqueous sulfide in contaminated and natural water using the methylene blue method. In: Collins AG, Johnson AI, editors. Ground-Water Contamination: Field Methods, ASTM STP 963. Philadelphia: American Society for Testing and Materials. P 349-357.

Lonergan DJ, Jenter H, Coates JD, Phillips EJP, Schmidt TM, Lovley DR. 1996. Phylogenetic analysis of dissimilatory Fe(III)-reducing bacteria. J Bacteriol 178:2402-2408.

Lord CJ, Church TM. 1983. A quantitative model for pyritization in salt-marsh sediments. Estuaries 6(3):295-296.

Lovley DR, Woodward JC, Chapelle FH. 1996. Rapid anaerobic benzene oxidation with a variety of chelated Fe(III) forms. Applied and Environmental Microbiology 62(1):288-291.

Luther GW, Church TM. 1988. Seasonal cycling of sulfur and iron in porewaters of a Delaware salt marsh. Marine Chemistry 23(3-4):295-309.

Luther GW, Findlay AJ, MacDonald DJ, Owings SM, Hanson TE, Beinart RA, Girguis PR. 2011. Thermodynamics and kinetics of sulfide oxidation by oxygen: A look at inorganically controlled reactions and biologically mediated processes in the environment. Frontiers in Microbiology 2:62. DOI: 10.3389/fmicb.2011.00062.

Lyle M, Mix A, Ravelo AC, Andreasen D, Heusser L, Olivarez A. 2000. Millennial-scale CaCO3 and CORG events along the northern and central California margins: Stratigraphy and origins. College Station, TX: Proceedings of the Ocean Drilling Program.

Lyons TW, Severmann S. 2006. A critical look at iron paleoredox proxies: New insights from modern euxinic marine basins. Geochimica et Cosmochimica Acta 70(23):5698-5722.

Ma SF, Noble A, Butcher D, Trouwborst RE, Luther GW. 2006. Removal of H2S via an iron catalytic cycle and iron sulfide precipitation in the water column of dead end tributaries. Estuarine Coastal and Shelf Science 70(3):461-472.

Mannino A, Montagna PA. 1997. Small-scale spatial variation of macrobenthic community structure. Estuaries 20(1):159-173.

Marvin-DiPasquale MC, Capone DG. 1998. Benthic sulfate reduction along the Chesapeake Bay central channel. I. Spatial trends and controls. Marine Ecology Progress Series 168:213-228.

Mecklenburg W. and Rosenkranzer F. 1914. Uber eine methode zur kolorimetrischen bestimmung kleiner schwefelwasserstoffmengen. Zeitschrift für anorganische Chemie 86:143-153.

Middelburg JJ, Levin LA. 2009. Coastal hypoxia and sediment biogeochemistry. Biogeosciences 6(7):1273-1293.

Mills HJ, Hunter E, Humphrys M, Kerkhof L, McGuinness LM, Huettel M, Kostka JE. 2008. Characterization of nitrifying, denitrifying, and overall bacterial communities in permeable marine sediments of the northeastern Gulf of Mexico. Applied and Environmental Microbiology 74:4440-4453.

Mills HJ, Martinez RJ, Story S, Sobecky PA. 2004. Identification of members of the metabolically active microbial populations associated with Beggiatoa species mat communities from Gulf of Mexico cold-seep sediments. Applied and Environmental Microbiology 70:5447-5458.

Moeseneder MM, Arrieta JM, Herndl GJ. 2005. A comparison of DNA- and RNA-based clone libraries from the same marine bacterioplankton community. Fems Microbiology Ecology 51(3):341-352.

Morse JW, Eldridge PM. 2007. A non-steady state diagenetic model for changes in sediment biogeochemistry in response to seasonally hypoxic/anoxic conditions in the "dead zone" of the Louisiana shelf. Marine Chemistry 106(1-2):239-255.

Morse JW, Gledhill DK, Sell KS, Arvidson RS. 2002. Pyritization of iron in sediments from the continental slope of the Northern Gulf of Mexico. Aquatic Geochemistry 8(1):3-13.

Morse JW, Millero FJ, Cornwell JC, Rickard D. 1987. The chemistry of the hydrogen sulfide and iron sulfide systems in natural waters. Earth-Science Reviews 24(1):1-42.

Morse JW, Rowe GT. 1999. Benthic biogeochemistry beneath the Mississippi River plume. Estuaries 22(2A):206-214.

Morse JW, Thomson H, Finneran DW. 2007. Factors controlling sulfide geochemisty in sub-tropical estuarine and bay sediments. Aquatic Geochemistry 13:143-156.

Nazaret S, Jeffrey WH, Saouter E, Vonhaven R, Barkay T. 1994. *merA* gene-expression in aquatic environments measured by messenger RNA production and Hg(II) volatilization. Applied and Environmental Microbiology 60(11):4059-4065.

Nealson KH. 1997. Sediment bacteria: Who's there, what are they doing, and what's new? Annual Review of Earth and Planetary Sciences 25:403-434.

Nogales B, Moore ERB, Abraham W-R, Timmis KN. 1999. Identification of the metabolically active members of a bacterial community in a polychlorinated biphenyl-polluted moorland soil. Environmental Microbiology 1(3):199-212.

Nusbaum I. 1965. Determining sulfides in water and wastewater. Water and Sewage Works 112:113-114.

Orcutt BN, Sylvan JB, Knab NJ, Edwards KJ. 2011. Microbial ecology of the dark ocean above, at, and below the seafloor. Microbiology and Molecular Biology Reviews 75(2):361-422.

Pallud C, Van Cappellen P. 2006. Kinetics of microbial sulfate reduction in estuarine sediments. Geochimica et Cosmochimica Acta 70(5):1148-1162.

Papke RT, Ramsing NB, Bateson MM, Ward DM. 2003. Geographical isolation in hot spring cyanobacteria. Environmental Microbiology 5(8):650-659.

Papke RT, Ward DM. 2004. The importance of physical isolation to microbial diversification. Fems Microbiology Ecology 48(3):293-303.

Parsons TR, Maita Y, Lalli CM. 1984. A manual of chemical and biological methods for seawater analysis. New York, NY: Pergamon Press. 144 p.

Patterson GD. 1978. Sulphur. In: Boltz DF, editor. Colorimetric Determination of Nonmetals. New York, NY: John Wiley and Sons. P 261-308.

Pereira IAC, Haveman SA, Voordouw G. 2007. Biochemical, genetic and genomic characterization of anaerobic electron transport pathways in sulphate-reducing *Deltaproteobacteria*. In: Barton LH, Hamilton WA, editors. Sulphate-Reducing Bacteria. Cambridge, U.K.: Cambridge University Press. p. 214-241.

Perriere G, Gouy M. 1996. WWW-Query: An on-line retrieval system for biological sequence banks. Biochimie 78(5):364-369.

Plas C, Harant H, Danner H, Jelinek E, Wimmer K, Holubar P, Braun R. 1992. Ratio of biological and chemical oxidation during the aerobic elimination of sulfide by colorless sulfur bacteria. Applied Microbiology and Biotechnology 36(6):817-822.

Pomeroy R. 1936. The determination of sulphides in sewage. Sewage Works Journal 8:572-591.

Pomeroy R. 1941. Hydrogen sulfide in sewage. Sewage Works Journal 13:498-505.

Poretsky RS, Bano N, Buchan A, LeCleir G, Kleikemper J, Pickering M, Pate WM, Moran MA, Hollibaugh JT. 2005. Analysis of microbial gene transcripts in environmental samples. Applied and Environmental Microbiology 71(7):4121-4126.

Postma D, Jakobsen R. 1996. Redox zonation: Equilibrium constraints on the Fe(III)/SO4-reduction interface. Geochimica et Cosmochimica Acta 60(17):3169-3175.

Poulsen LK, Ballard G, Stahl DA. 1993. Use of ribosomal-RNA fluorescence insitu hybridization for measuring the activity of measuring the activity of single cells in young and established biofilms. Applied and Environmental Microbiology 59(5):1354-1360.

Rabalais NN, Smith LE, Harper DE, Justic D. 2001. Effects of seasonal hypoxia on continental shelf benthos. In: Rabalais NN, editor. Coastal and Estuarine Sciences, Vol 58: Coastal Hypoxia: Consequences for Living Resources and Ecosystems. Washington, DC: American Geophysical Union. P 211-240.

Rabalais NN, Turner RE. 2001a. Hypoxia in the northern Gulf of Mexico: Description, causes and change. In: Rabalais NN, editor. Coastal and Estuarine Sciences, Vol

58: Coastal Hypoxia: Consequences for Living Resources and Ecosystems. Washington, DC: American Geophysical Union. P 1-36.

Rabalais NN, Turner RE, Sen Gupta BK, Boesch DF, Chapman P, Murrell MC. 2007. Hypoxia in the northern Gulf of Mexico: Does the science support the plan to reduce, mitigate, and control hypoxia? Estuaries and Coasts 30(5):753-772.

Raiswell R, Berner RA. 1985. Pyrite formation in euxinic and semi-euxinic sediments. American Journal of Science 285(8):710-724.

Raiswell R, Buckley F, Berner RA, Anderson TF. 1988. Degree of pyritization of iron as a paleoenvironmental indicator of bottom water oxygenation. Journal of Sedimentary Petrology 58(5):812-819.

Raiswell R, Canfield DE. 1998. Sources of iron for pyrite formation in marine sediments. American Journal of Science 298(3):219-245.

Raiswell R, Canfield DE, Berner RA. 1994. A comparison of iron extraction methods for the determination of degree of pyritisation and the recognition of iron-limited pytite formation. Chemical Geology 111(1-4):101-110.

Ramette A, Tiedje JM. 2007. Biogeography: An emerging cornerstone for understanding prokaryotic diversity, ecology, and evolution. Microbial Ecology 53(2):197-207.

Ravenschlag K, Sahm K, Pernthaler J, Amann R. 1999. High bacterial diversity in permanently cold marine sediments. Applied and Environmental Microbiology 65(9):3982-3989.

Reeburgh WS. 1967. An improved interstitial water sampler. Limnology and Oceanography 12(1):163.

Reese BK, Anderson MA, Amrhein C. 2008. Hydrogen sulfide production and volatilization in a polymictic eutrophic saline lake, Salton Sea, California. Science of the Total Environment 406(1-2):205-218.

Reese BK, Finneran DW, Mills HJ, Xu MX, Morse JW. 2011a. Examination and refinement of the determination of aqueous hydrogen sulfide by the methylene blue method. Aquatic Geochemistry 17(4):567-582. DOI: 10.1007/s10498-011-9128-1.

Reese BK, Mills HJ, Dowd S, Morse JW. 2011b. Benthic biogeochemistry of microbial iron and sulfate reduction in the Gulf of Mexico hypoxic zone. Geomicrobiology In press.

Reese BK, Mills HJ, Witmer AW, Dowd S, Shepard AK, Morse JW. 2011c. Factors affecting molecular and geochemical characterization of sulfur cycling within an estuarine system. Submitted.

Rickard D, Morse JW. 2005. Acid volatile sulfide (AVS). Marine Chemistry 97(3-4):141-197.

Roden EE, Lovley DR. 1993. Dissimilatory Fe(III) reduction by the marine microorganism *Desulfuromonas acetoxidans*. Applied and Environmental Microbiology 59:734-742.

Roden EE, Tuttle JH. 1992. Sulfide release from estuarine sediments underlying anoxic bottom water. Limnology and Oceanography 37(4):725-738.

Roden EE, Zachara JM. 1996. Microbial reduction of crystalline iron(III) oxides: Influence of oxide surface area and potential for cell growth. Environmental Science and Technology 30(5):1618-1628.

Rogers JR, Bennett PC. 2004. Mineral stimulation of subsurface microorganisms: release of limiting nutrients from silicates. Chemical Geology 203(1-2):91-108.

Rowe GT, Chapman P. 2002. Continental shelf hypoxia: Some nagging questions. Gulf of Mexico Science 2:153-160.

Rowe GT, Cruz Kaegi ME, Morse JW, Boland GS, Escobar Briones EG. 2002. Sediment community metabolism associated with continental shelf hypoxia, Northern Gulf of Mexico. Estuaries 25:1097-1106.

Roychoudhury AN. 2007. Spatial and seasonal variations in depth profile of trace metals in saltmarsh sediments from Sapelo Island, Georgia, USA. Estuarine Coastal and Shelf Science 72(4):675-689.

Rudd JWM, Kelly CA, Furutani A. 1986. The role of sulfate reduction in long term accumulation of organic and inorganic sulfur in lake sediments. Limnology and Oceanography 31(6):1281-1291.

Sands AE, Grafius MA, Wainwright HW, Wilson MW. 1949. The determination of low concentrations of hydrogen sulfide in gas by the methylene blue method. U.S. Bureau of Mines, Report of Investigation 4547: 1-19.

Schulz HN, Brinkhoff T, Ferdelman TG, Marine MH, Teske A, Jorgensen BB. 1999. Dense populations of a giant sulfur bacterium in Namibian shelf sediments. Science 284(5413):493-495.

Skyring GW. 1987. Sulfate reduction in coastal ecosystems. Geomicrobiology Journal 5(3-4):295-374.

St. Lorant I. 1929. Uber eine neue colorimetrische: Mikromethode zur bestimmung des schwefels in sulfiden sulfaten usw. Z. Physiol. Chem. 185:245-266.

Stackebrandt E, Stahl DA, Devereux R. 1995. Taxonomic relationships. In: Barton LL, editor. Sulfate Reducing Bacteria. New York: Plenum. P 49-87.

Sutula M, Bianchi TS, McKee BA. 2004. Effect of seasonal sediment storage in the lower Mississippi River on the flux of reactive particulate phosphorus to the Gulf of Mexico. Limnology and Oceanography 49(6):2223-2235.

Teske A, Nelson DC. 2006. The Genera *Beggiatoa* and *Thioploca*. In: Dworkin M, Falkow S, Rosenberg E, Schleifer K-H, Stackebrandt E, editors. The Prokaryotes. New York, NY: Springer. P 784-810.

Trimmer M, Purdy KJ, Nedwell DB. 1997. Process measurement and phylogenetic analysis of the sulfate reducing bacterial communities of two contrasting benthic sites in the upper estuary of the Great Ouse, Norfolk, UK. Fems Microbiology Ecology 24(4):333-342.

Tsertova N, Kisand A, Tammert H, Kisand V. 2011. Low seasonal variability in community composition of sediment bacteria in large and shallow lake. Environmental Microbiology Reports 3(2):270-277.

Tuttle JH, Jonas RB, Malone TC. 1987. Origin, development and significance of Chesapeake Bay anoxia. In: Majumdar SK, Hall LW, Austin HM, editors. Contaminant Problems and Management of Living Chesapeake Bay Resources. Philadelphia, PA: The Pennsylvania Academy of Science. P 442–472.

Vazquez F, Zhang JZ, Millero FJ. 1989. Effect of metals on the rate of the oxidation of H2S in seawater. Geophysical Research Letters 16(12):1363-1366.

Viollier E, Inglett PW, Hunter K, Roychoudhury AN, Van Cappellen P. 2000. The ferrozine method revisited: Fe(II)/Fe(III) determination in natural waters. Applied Geochemistry 15(6):785-790.

Visscher PT, Prins RA, Vangemerden H. 1992. Rates of sulfate reduction and thiosulfate consumption in a marine microbial mat. Fems Microbiology Ecology 86(4):283-293.

Wang Q, Garrity GM, Tiedje JM, Cole JR. 2007. Naive Bayesian classifier for rapid assignment of rRNA sequences into the new bacterial taxonomy. Applied and Environmental Microbiology 73(16):5261-5267.

Wawer C, Jetten MSM, Muyzer G. 1997. Genetic diversity and expression of the NiFe hydrogenase large-subunit gene of *Desulfovibrio* spp. in environmental samples. Applied and Environmental Microbiology 63(11):4360-4369.

Wen AM, Fegan M, Hayward C, Chakraborty S, Sly LI. 1999. Phylogenetic relationships among members of the *Comamonadaceae*, and description of *Delftia acidovorans* (den Dooren de Jong 1926 and Tamaoka et al. 1987) gen. nov., comb. nov. International Journal of Systematic Bacteriology 49:567-576.

Weston NB, Porubsky WP, Samarkin VA, Erickson M, Macavoy SE, Joye SB. 2006. Porewater stoichiometry of terminal metabolic products, sulfate, and dissolved organic carbon and nitrogen in estuarine intertidal creek-bank sediments. Biogeochemistry 77(3):375-408.

Xu JP. 2006. Microbial ecology in the age of genomics and metagenomics: concepts, tools, and recent advances. Molecular Ecology 15(7):1713-1731.

Zhang J, Gilbert D, Gooday AJ, Levin L, Naqvi SWA, Middelburg JJ, Scranton M, Ekau W, Pena A, Dewitte B et al. . 2010. Natural and human-induced hypoxia and consequences for coastal areas: Synthesis and future development. Biogeosciences 7(5):1443-1467.

Zhang JZ, Millero FJ. 1994. Kinetics of oxidation of hydrogen sulfide in natural waters. In: Alpers CN, Blowes DW, editors. Environmental Geochemistry of Sulfide Oxidation. P 393-409.

APPENDIX A

CLASSIFICATION TABLE FOR LINEAGES IDENTIFIED IN CHAPTER III

Appendix A is contained in a separate Microsoft Excel file and includes all lineages identified during this study.

APPENDIX B

CLASSIFICATION TABLE FOR LINEAGES IDENTIFIED IN CHAPTER IV

Appendix B is contained in a separate Microsoft Excel file and includes all lineages identified during this study.

APPENDIX C

CLASSIFICATION TABLE FOR LINEAGES IDENTIFIED IN CHAPTER V

Appendix C is contained in a separate Microsoft Excel file and includes all lineages identified during this study.

APPENDIX D

TABLE OF DIVERSITY STATISTICS

Appendix C is contained in a separate Microsoft Excel file and includes statistical paramenters for Chapters III, IV, and V.

VITA

Name: Brandi Kiel Reese

Address: Department of Oceanography
Texas A&M University
3146 TAMU
College Station, Texas 77843-3146

Email Address: brandi@ocean.tamu.edu

Education: B.S., Geology, Southern Methodist University, 2001
M.S., Soil and Water Sciences, University of California, Riverside, 2007
Ph.D., Chemical Oceanography, Texas A&M University, 2011

Professional Experience:
Graduate Assistant Researcher, Texas A&M University (2007-2011)
Graduate Student Researcher, University of California, Riverside (2005-2007)
Project Manager, AEI Consulting, Hermosa Beach, CA (2002-2007)

Publications:

Reese, B.K., Mills, H.J., Dowd, S.E. and Morse, J.W. 2011. Benthic biogeochemistry of microbial iron and sulfate reduction in the Gulf of Mexico hypoxic zone. Geomicrobiology (in press).

Reese, B.K., Finneran, D.W., Mills, H.J., Zhu, M.-X., Morse, J.W. 2011. Examination and refinement of the determination of aqueous hydrogen sulfide by the methylene blue method. Aquatic Geochemistry 17(4):567-582.

Reese, B.K. and Anderson, M.A. 2009. Dimethyl sulfide production in a hypersaline eutrophic lake, Salton Sea, California. Limnology and Oceanography 54: 250–261.

Reese, B.K., Anderson, M.A., and Amrhein, C. 2008. Hydrogen sulfide production and volatilization in a polymictic eutrophic lake, Salton Sea, California. *Science of the* Total Environment 406:205-218.

Parker, D.R., Seyfferth, A.L., and **Reese, B.K.** 2008. Synoptic survey of perchlorate in groundwater: A synoptic survey of "pristine" sites in the coterminuous United States. Environmental Science and Technology 42:1465-1471.

Fellowships and Awards: Philanthropic Educational Organization Fellowship (2010-2011); Texas A&M University Diversity Fellowship Award (2007-2010); ACS Graduate Student Award in Environmental Chemistry (2010); Buck Weirus Spirit Award (2010); Lighthouse Research and Development Fellowship Achievement Award (2009-2010)